SOLAR DOMESTIC HOT WATER HEATER PERFORMANCE: EFFECT OF CHANGING ANNUAL LOAD AND AVERAGE USE PROFILE

MOHIT SINGH-CHHABRA

B.E., University of Pune, 2005

A thesis submitted to the

Faculty of the Graduate School of the

University of Colorado in partial fulfillment

of the requirement for the degree of

Master of Science

Department of Civil Engineering

2014

This thesis entitled:

Solar Domestic Hot Water Heater Performance: Effect of Changing Annual Load and Average Use Profile

written by Mohit Singh-Chhabra

has been approved for the Department of Civil Engineering

Dr. Michael Brandemuehl (Committee Chair)

Dr. Moncef Krarti

Dr. John Zhai

Date: 4/6/2015

The final copy of this thesis has been examined by the signatories, and we

Find that both the content and the form meet acceptable presentation standards

Of scholarly work in the above mentioned discipline.

Abstract

Singh-Chhabra, Mohit (M.S, Civil Engineering)

Solar Domestic Hot Water Heater Performance: Effect of Changing Annual Load and Average Use.

Thesis directed by Professor Michael Brandemuehl

The objective of this research is to understand, using computer simulation, the effects of changing domestic hot water load and usage patterns on the system performance of active and passive solar domestic hot water (SDHW) systems. Annual hot water load, mains water temperature, daily hot water load profile shape, and daily hot water load were the parameters varied to simulate variations in load and usage patterns that we expect would occur in a household. The effect of changing these parameters was quantified by studying change in annual solar fraction and annual system efficiency.

Active and passive SDHW system construction was first defined. The system components of both active and passive system solar hot water systems simulated were determined by market research. The components were sized adequately using accepted component sizing guidelines. Daily hot water draw profiles developed at NREL (National Renewable Energy Laboratory) were used as the base draw profiles. The base profile has

morning and evening hump and a daily hot water load of 60 gallons on weekdays and 75 gallons on weekends. The annual simulations were conducted in TRNSYS using a five minute time-step.

Active (glycol) systems show greatest variation in simulated performance due to large changes in annual load. Passive (ICS) systems display high sensitivity to hot water profile shape. This difference between the two systems is due to the presence of a well-insulated solar storage tank in the glycol system.

The glycol system shows less variation in performance due to variation in draw profile than the ICS system due to the presence of an appropriately sized and insulated solar storage tank in the glycol system. The solar storage tank helps glycol systems meet the demand for hot water during hours of low sunlight (early morning and late evening). ICS systems show higher sensitivity to profile shape as they cannot meet hot water load during morning and evening times; this morning and evening hot water load is met by the auxiliary heating tank.

CONTENTS

TABLES

FIGURES

1 Thesis Aim and Problem Statement

Domestic water heating is responsible for about 18% of all residential energy consumed in the United States (U.S. Energy Information Administration (U.S. E.I.A), 2009). This translates to 1.8 quads (quadrillion Btu's) of energy use every year. This is almost equal to the total energy consumption of the state of Wisconsin (U.S E.I.A, 2010). Currently 13% of the nation's electricity is generated through renewable energy sources (U.S. E.I.A, 2012).

Soaring gas and electricity prices, as well as concern for the environment, are driving the search for alternative methods to meet our energy needs. Solar energy can be used to meet domestic hot water needs in two ways. One method is to use photovoltaic panels to produce electricity, which in turn can be used for heating water and other purposes; the second method is to use solar energy to directly heat water.

In many climates, a Solar Domestic Hot Water (SDHW) system can meet a high percentage (50 to 85%) of domestic hot water needs (J.Burch, 2005). A simple SDHW system consists of a solar collector, a storage tank, back up heater, a pump (optional) and necessary plumbing equipment.

SDHW systems have been used for more than a century. However, a clear understanding of the working of hot water systems was not developed until the 1940s (Winter, 2005). Better understanding of these systems led to the development of tools such as the f-Chart (University of Wisconsin, 1975) that help estimate savings potential from SDHW systems. Though commonly used methods of estimating SDHW potential provide good results, they have some limitations. Most present day methods assume that SDHW systems are sized appropriately and have a fixed/ invariant draw profile (Winter, 2005). Research has shown that system performance could

change significantly due to change in day-to-day hot water loads and hot water profile shape (W.E.Buckles and S.A.Klein (Solar Energy Laboratory, 1980). Studies on the development of SDHW systems state that quantifying the effect the aforementioned variables have on SDHW performance is the next step in better understanding SDHW systems (Winter, 2005).

The objective of this research is to evaluate, using computer simulation, the effects of domestic hot water load and usage patterns on the system performance of active and passive solar water heating systems. The following parameters were varied to simulate variations in load and usage patterns that we expect would occur in a household:

- **Annual Hot Water Load** – The annual load on the system is varied by a factor of two (increased and decreased) relative to typical household consumption. While the variations in load could occur due to changes or uncertainty in hot water usage, the analysis also reflects the effect of over and under sizing of systems.
- **Mains Water Temperature** – Though mains water temperature has a direct correlation with energy required to heat water, there is uncertainty in how mains water temperature exactly varies (Christensen, 2007). Assuming that mains water temperature varies according to ambient annual temperature, the magnitude of mains water temperature is varied by a fixed amount to ascertain its effect on SDHW system performance.
- **Daily Load Profile Shape -** The effect of hot water draw profile shape on the performance of a SDHW system is analyzed by simulating SDHW systems with three distinct daily draw profiles.

- **Variation in Day-to-Day Hot Water Use** – Daily draw volume is assumed to vary while keeping annual hot water load constant to account for irregular daily usage patterns that would occur in most homes.

These parameters collectively represent the variations we would expect to see in hot water use in a household. All of these parameters were studied individually and in combination for both ICS and glycol systems to ascertain which of these factors significantly affect SDHW system performance. All these parameters are described in detail in Sections 3 and 4 of this thesis.

The effect of these parameters is quantified by studying change in annual solar fraction[1] and annual system efficiency[2]. Specifically, the percentage change in annual solar fraction and annual system efficiency for each case is analyzed. Along with studying annual results, a typical summer and winter day were studied using simulation results at fifteen minute intervals. This enabled us to identify exactly why system performance changed in each case.

[1] Annual solar Fraction is defined as fraction of total purchased energy to heat water that is replaced by solar energy in one year. Further Explanation in Section 4.5

[2] Annual system efficiency is defined as the fraction of total energy incident on the collector that is converted to useful energy to heat water in one year. Further Explanation in Section 4.5

2 Literature Review

Though SDHW systems, in various forms, have been available in the market for centuries, there has been little understanding of the working of these systems until recently (Winter, 2005). SDHW systems gained popularity during the 1970s in the USA due to the increased interest in renewable energy following projections of oil shortage. However, this popularity could not be sustained[3] as the industry suffered due to a lack of knowledge of the operation of SDHW systems (Arizona Solar Center, 2001). Recently however, better understanding of the working of SDHW systems is being attained through systematic research efforts by established institutions like the Department of Energy (DOE) and National Renewable Energy Laboratory (NREL). This research and subsequent understanding of SDHW systems is helping the Solar Hot Water industry produce better products and subsequently popularize SDHW systems. The rest of this section has been further divided into the following subsections:

- **SDHW Systems –** This section highlights research done on the benefits of SDHW systems in the USA.
- **Usage Patterns** – Different draw profiles that are frequently used are studied and their effect on the performance of SDHW systems is analyzed.
- **Load Variation** – The effect of change in load on SDHW systems, both on a day to day basis and an annual basis are studied.

[3] Federal and state tax credits for solar energy were initiated under President Carter in the '1970s, and were eliminated under President Ronald Reagan in 1985. This dealt a blow to the solar industry. (Arizona Solar Center, 2001).

2.1 SDHW Systems

As the popularity of SDHW systems increases, the need to accurately quantify the savings potential from the installation of these systems also arises. DOE studied the potential for energy savings through the use of SDHW systems ((NREL), 2007) This study showed that with available resources, SDHW systems can potentially save 457 trillion BTU in natural gas end-use, 53 trillion BTU in oil and LPD end-use and 42.9 billion kWh in electricity end-use. These savings could result in a reduction of 2 to 3 % of CO_2 emmisions in the residential and commercial sector.

Further research done on active SDHW systems has been able to show location dependant savings potential in the residential sector. Figure 1 shows the solar fractions of a typical active SDHW system installed on rooftops in different parts of the USA in the residential sector. Each contour color represents a different solar fraction, while dots on the map represent different weather stations. The dots represent the weather stations (200) that the simulations were conducted in.

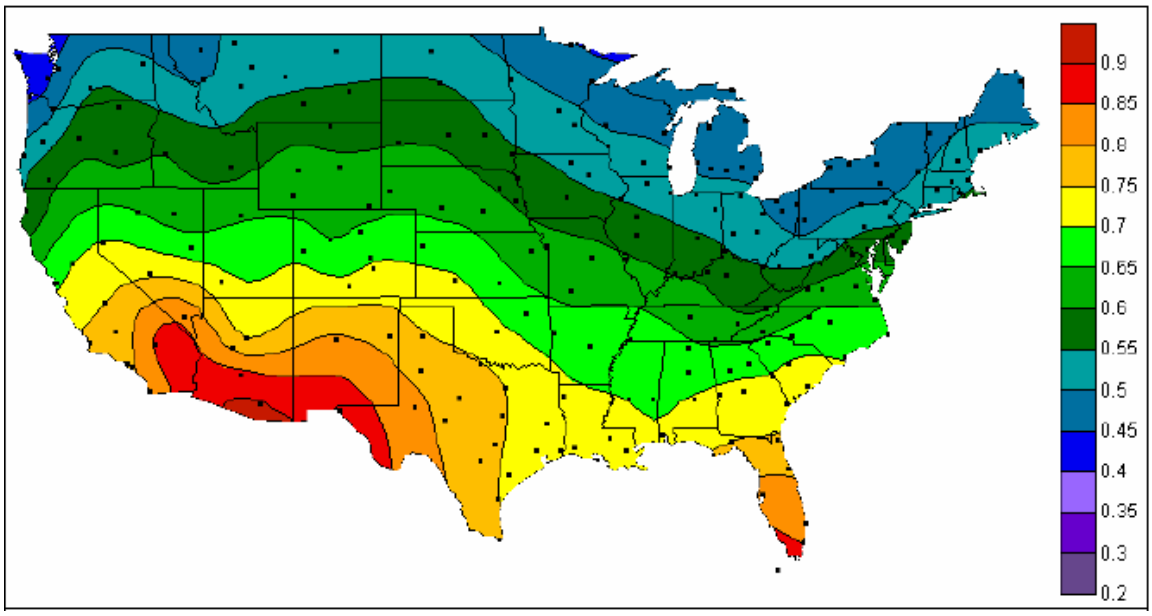

Figure 1Solar Fraction of a Base Residential SDHW System in different Parts of the USA (J.Burch, 2005)

As seen in Figure 1, solar fraction across the country varies between 0.4 and 0.85, the majority of weather stations showed a solar fraction between 0.5 and 0.7. Another contour map produced in the same study showcased the effect of using cheaper glycol systems. Lower cost system simulations showed that the majority of the USA would have solar fractions between 0.45 and 0.65.

ICS systems are one of the simplest constructions of SDHW systems available in the market. They are also called breadbox or batch systems. These systems do not have a separate storage tank or a pump. Instead, hot water is stored in the collector itself and this system relies on natural convection for water flow. Due to the absence of a pump or a dedicated solar storage tank, these systems are cheaper than glycol systems. Also these systems have low maintenance costs as they do not have any moving parts.

ICS systems have two main drawbacks. Firstly, they lose almost all of the energy gained during the course of the day through the collector glazing (Jeff W. Thornton, 2000)), as hot water is stored in the collector. Hence they usually provide lower solar fractions than glycol systems with similar properties (Parker, 2009). Secondly they often suffer from pipe freezing and bursting. This happens as pipes carrying water are often exposed to ambient weatehr conditions. If the temperature falls below freezing often, the chances of pipe freezing and bursting are high. Research has been done on ICS systems, locations where they are feasible.

Traditionally, installation of ICS systems was based on hueristic practices, was limited to places where pipe freezing was not thought to be a problem. Chances of pipe freezing were based on past experience and not on scientific evidence (Salasovich, 2001). Shown in Figure 2 are maps of the united states showing probability of at least one freeze occuring in 20 years. It is important to note that probability of freezing is highly dependant on pipe configuration and hot water draw.

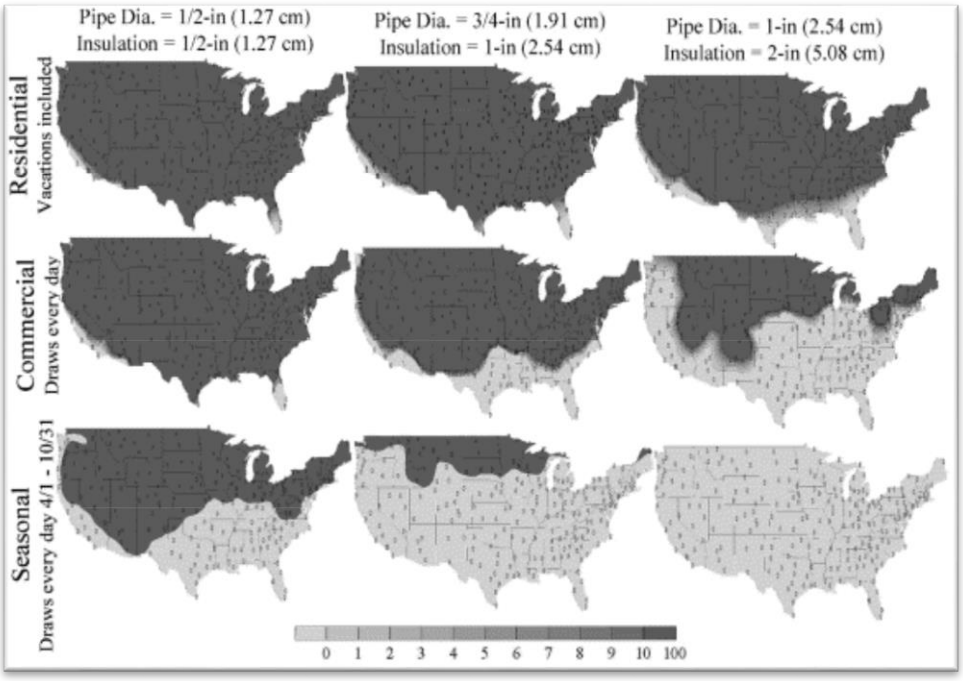

Figure 2 Probability of At Least One Freeze in 20 Years (Salasovich, 2001)

It is important to note that the numbers discussed above are energy savings potential and not guaranteed savings. Savings are dependent on location as well as individual characteristics of the system ((NREL), 2007). While estimating savings potential, assumptions are made regarding the system characteristics. For example, the Florida Solar Energy Center (FSEC) gives a full list of assumptions made while evaluating potential of SDHW systems in Florida. Assumptions made are regarding hot water load, hot water load profile, water mains temperature, collector orientation and air temperature around the storage tanks. Of these, hot water load and draw profile are determined from nationwide studies by FSEC ((FSEC), A Review of Hot Water Draw Profiles Used in Performance Analysis of Residential Domestic Hot Water Systems, 2004). As discussed later on in this section, changes in these assumptions can have a significant impact on savings potential.

2.2 Usage Patterns

Research has determined that wide variations in the daily draw pattern can reduce system thermal performance, especially when the draw frequently exceeds the storage tank capacity (W.E.Buckles and S.A.Klein (Solar Energy Laboratory, 1980). For purposes of simulating domestic hot water loads, various studies have been conducted to ascertain a typical domestic hot water profile. Some of the prominent daily draw profiles are presented below:

- *The ASHRAE 90.2 draw-profile*: This profile is part of a national consensus standard with concurrence of industry stakeholders ((FSEC), 2004)
- *The SRCC recommended draw-profile:* SRCC's hot water draw profiles areadapted from 1995 ASHRAE Applications Handbook, Chapter 45 and 'A Domestic Hot Water Use Database' (Stogsdill, 1990) ((FSEC), 2004).
- *Becker draw-profile:* The Becker draw profile is based on measurements from 142 homes in the Hood River Oregon area, data from 74 homes in Florida and 24 homes in North Carolina (Stogsdill, 1990).
- *Perlman draw-profile*: This profile is based on a data set of Canadian residences, the residences used had two aduts, two children, a clotheswasher, and a dishwasher (Perlman, 1985).
- *Bouchelle draw-profile*: Is based on hot water demand profiles for a large 204-home sample study in central Florida (D.S. Parker, 2000).

A research conducted by the Florida Solar Energy Center (FSEC) compared these different draw profiles with each other ((FSEC), 2004). Shown in Figure 3 is a comparison of these aforementioned hot water draw profiles.

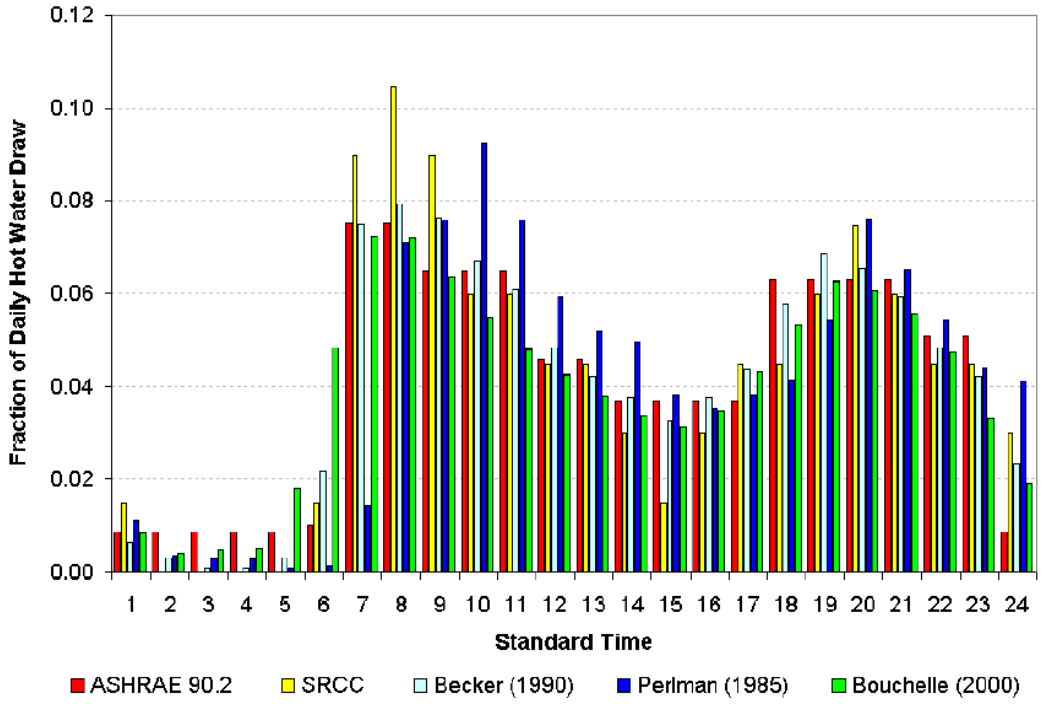

Figure 3 Histogram of Daily Hot Water Draws Normalized By Total Daily Draw

In Figure 3, the SRCC and Perlman profiles stand out as they are significantly different from each other. The rest of the profiles are relatively similar. What is common between these profiles is that all of them show a morning and an evening peak at 8 AM and 8 PM respectively.

The most defensible of these profiles are the ASHRAE 90.2 and the Becker profiles. The Becker profile is based on the largest compilation of US-based hot water data. The ASHRAE profile is part of a national consensus standard with concurrence of industry stakeholders ((FSEC), 2004).

The effect of varying daily hot water draw profile, while keeping total daily draw constant has been studied previously by W.E Buckles and Klein (W.E.Buckles and S.A.Klein (Solar Energy Laboratory, 1980)). The study used six different draw profiles that have been

shown in Figure 4. All of these profiles use a constant daily draw volume of 300 l/day on two glycol systems, a one tank and a two tank system.

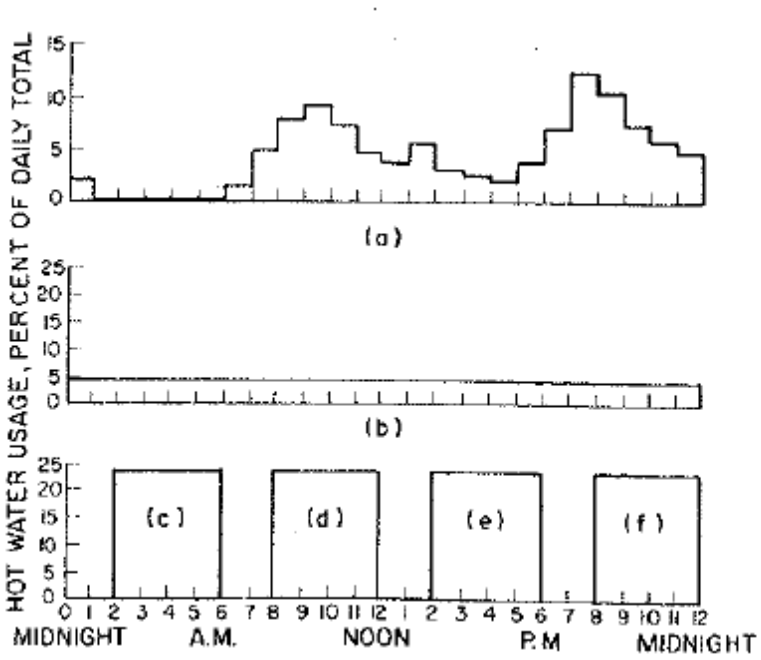

Figure 4 Draw Profiles Simulated to Study Dependence of Profile on SDHW System Performance (W.E.Buckles and S.A.Klein (Solar Energy Laboratory, 1980)

Profile (a) is a typical load distribution profile prepared from data collected in a RAND Corp. survey of residential hot water heating (J.J.Mutch, 1974). To vary demand from day to day, the draw profile was changed by adding an additional zero flow-hour between 1 AM and 6 AM. Hence this profile has a 25 hour time period instead of a 24 hour time period. Profile (b) has a constant draw volume for each hour of the day, while profiles (c) through (f) have total daily hot water draw concentrated in different 4 hour bins throughout the day. All simulations were performed using Madison, WI, as the location.

The solar fraction for the base profile (RAND) was found to be 0.66. Profile (a) and Profile (b) shows a small change in solar fraction (Decreased from 0.66 to 0.65 in each case).

This is as SDHW systems with reasonable storage capacity are insensitive to small day to day draw variations. This effect was further studied by varying the daily draw in an extreme manner (while keeping total hot water draw for a week constant). The solar fraction was found to vary significantly- from 0.63 to 0.57.

For profiles (c) through (f), the results showed a significant change in solar fraction. Solar fraction for early morning draws was found to drop to 0.60 (c), while for a predominantly afternoon draw (e) the solar fraction was seen to be as high as 0.67.

2.3 Load

Solar Domestic Hot Water Systems are sized with a consideration of the annual hot water load requirement. Hence the size of the system relative to the annual load has a significant effect on the performance of a system. Guidelines and rule of thumb exist for sizing collectors and system components according to the load requirement. DOE/NREL (NREL, 1996) and FSEC (FSEC, 2006) both have released formal documents describing guidelines to design a functional SDHW system. These guidelines help a user correctly choose and size a SDHW system based on user needs and application

Annual solar fraction usually increases as either the load on the system reduces while keeping system size constant or the system size increases keeping load constant. This increase in solar fraction shows a trend of diminishing marginal returns, with very large systems meeting more than 95 % of the systems loads (Beckman, 2006). Figure 5 shows how solar fraction varies in different locations for both glazed and unglazed collectors. We see that there is variation in solar fraction as we change collector size (J.Burch and J.Salasovich (NREL), 2005).

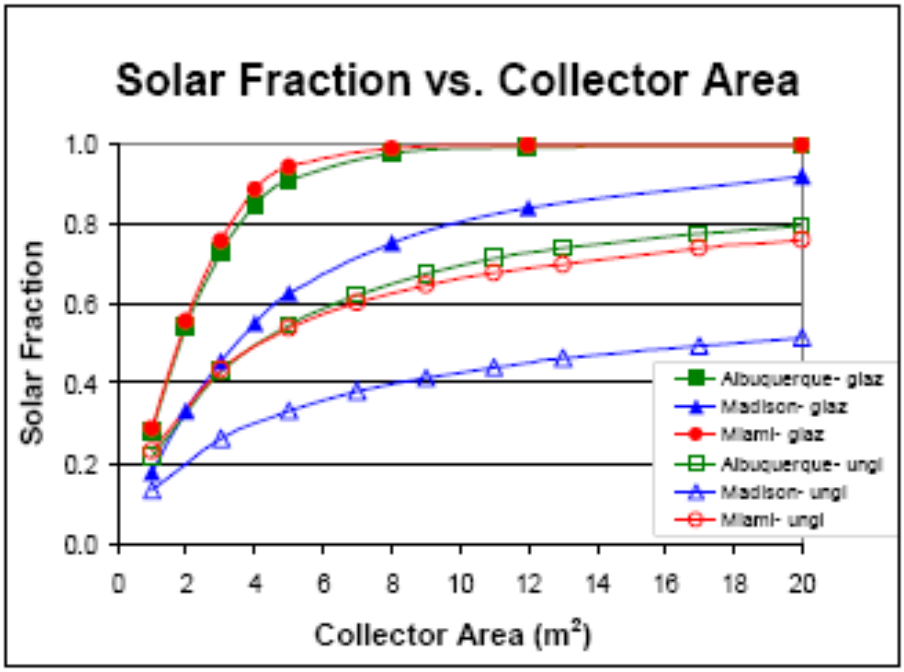

Figure 5 Variation of Solar Fraction with Collector Area in Madison, Albuquerque and Miami (J.Burch and J.Salasovich (NREL), 2005).

The above study changes collector area while keeping draw volume (and hence load on the system) constant. This has a similar effect as keeping collector area constant while changing draw volume.

System load can also be changed by changing the temperature delta that a system is required to meet. This temperature delta is the difference between the set point temperature and the mains temperature. Mains temperature is the temperature of the water at the mains inlet to a household. NREL has proposed an algorithm that calculates the mains temperature over a year based on location (Christensen, 2006). In this study, mains temperature data for about 15 sites throughout the U.S. were fit with a sinusoidal form. The equation developed was,

$$T_{mains} = (T_{amb.,avg} + \Delta T_{offset}) + Ratio^{*} (\Delta T_{amb\ max}/2)^{*}\sin (0.986\ ^{*}[Day\ \#\ -\ 15^{o} - \varphi_{lag}] -\ 90^{o})$$

Where:

T_{mains} = mains (supply) temperature to domestic hot water tank

$T_{amb,avg}$ = annual average ambient air temperature

$\Delta T_{amb,max}$ = maximum difference between monthly average ambient temperatures (e.g., $T_{amb,avg,july} - T_{amb,avg,january}$)

0.986 = degrees/day (=360/365)

Day # = Julian day of the year (1to365)

ΔT_{offset} = 6.0 °F

Ratio = $0.4 + 0.01 (T_{amb,avg} - 44)$

φ_{lag} = $35 - 1.0 (T_{amb,avg} - 44)$

Figure 6 shows how collector efficiency is affected as mains water temperature change. There is a direct relationship between system efficiency of a SDHW system and the mains water temperature. With an increase in mains water temperature, we would expect to see a decrease in system efficiency.

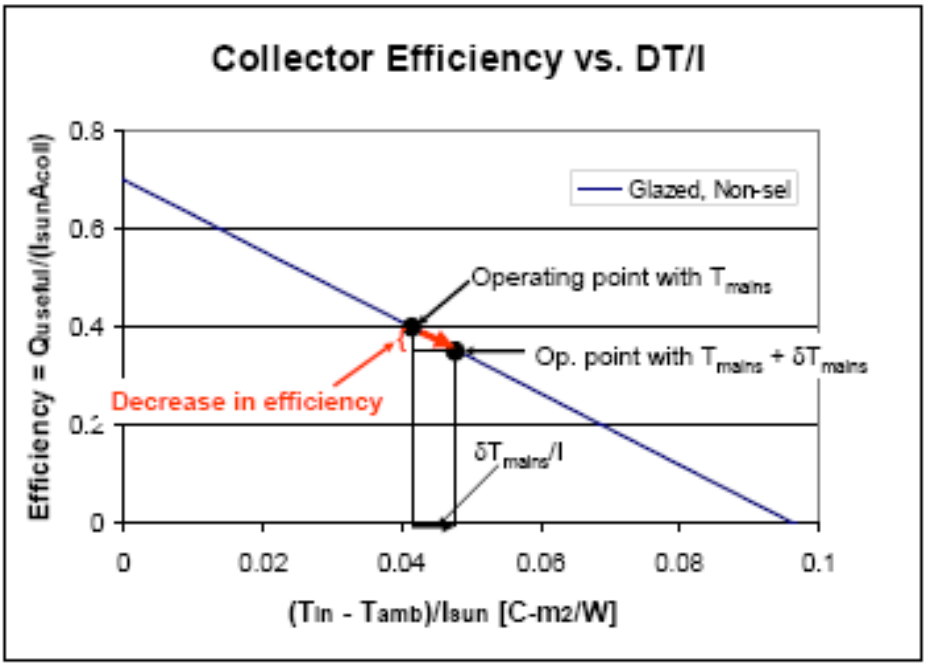

Figure 6 Effect of Change in Mains Temperature on Collector Efficiency (Christensen, 2006).

3 System Description

3.1 Introduction to Glycol and ICS Systems

This section describes the working, and the components of both solar hot water systems simulated, and the research carried out to ascertain the properties of these systems. Before describing the various components of the systems modeled in great detail, it is important to understand the basic principles behind the working of the two SDHW systems in question. The diagrams of the glycol and ICS systems shown here (Figure 7 and Figure 8) and their description match that of the systems modeled. The description of each component of these systems is presented later on in this section.

3.1.1 Glycol System

The Glycol system consists of two loops, a solar-side loop (the collector, heat transfer fluid, solar storage tank, and associated piping) and a load-side loop (the water heating/ auxiliary tank and associated piping). The solar loop of a glycol system uses a pump that moves propylene glycol through the collector and a heat exchanger. There is a second pump that takes water from the solar storage tank and moves it through the heat exchanger and back to the solar storage tank. Hence this heat exchanger is used to transfer energy from the working fluid (glycol) to the load side fluid (water).

The load side loop consists of the auxiliary tank (water heating tank), which is connected to the solar storage tank via piping. When hot water is drawn, it is drawn from this (auxiliary) tank. This tank has two heating elements that insure that water is always around the desired temperature (Around 130 degrees F). The water drawn from this tank is replaced by the water stored in the solar storage tank. The water drawn from the solar storage tank is replaced by mains water. The solar storage tank is an energy storage device that provides the auxiliary heater with

preheated water that is usually much higher than the mains water temperature. Figure 7 is a diagram of the system described in this paragraph and the system used for simulation.

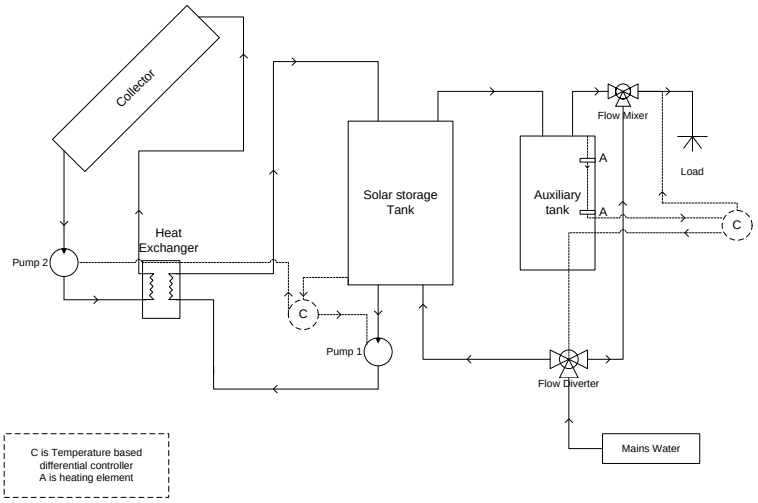

Figure 7 Diagram of Glycol System Modeled

There are two controllers and two three way valves in the above diagram. They perform the following functions,

- The controller on the solar loop turns the two pumps on and off when necessary.
- The controller on the load side loop is used to insure that the water delivered to the load is at the specified set-point. This is done by measuring the temperature in the auxiliary tank (near the delivery node) and mains water temperature to determine a ratio which is used while mixing mains water with water coming out of the auxiliary tank.
- The flow diverter in the load side loop supplies the flow mixer with mains water if temperature of water coming out of the auxiliary tank is higher than the specified set-point. The amount of water diverted is specified by the controller.

- The flow mixer mixes water coming out of the auxiliary tank with mains water if necessary. The output from the flow mixer is the water that is delivered to the load.

3.1.2 ICS System

The ICS system combines the collector and the solar storage tank into an "integrated collector and storage" mechanism (Hence the name, ICS). In this system the solar loop consists of the collector and associated piping, the load side loop consists of an auxiliary tank and associated piping. There are no pumps in this system; it relies on convection and pressure difference between the load and the mains water for flow.

The working of the load side loop is similar to the glycol system described above. The main working component of the solar loop is the collector. This collector is connected to mains water and auxiliary storage tank via piping. The working fluid in this system is the same as the fluid that is delivered to load (Water). There are two instances when water from the collector is transferred to the auxiliary tank,

- When there is a draw, water from the auxiliary tank is replaced by water stored in the collectors.
- Flow takes place due to natural convection, i.e. if temperature of water in the collector is high enough to create flow between tank and collector.

The water drawn from the solar storage tank is replaced by mains water. Figure 8 shows a schematic diagram of the system described here

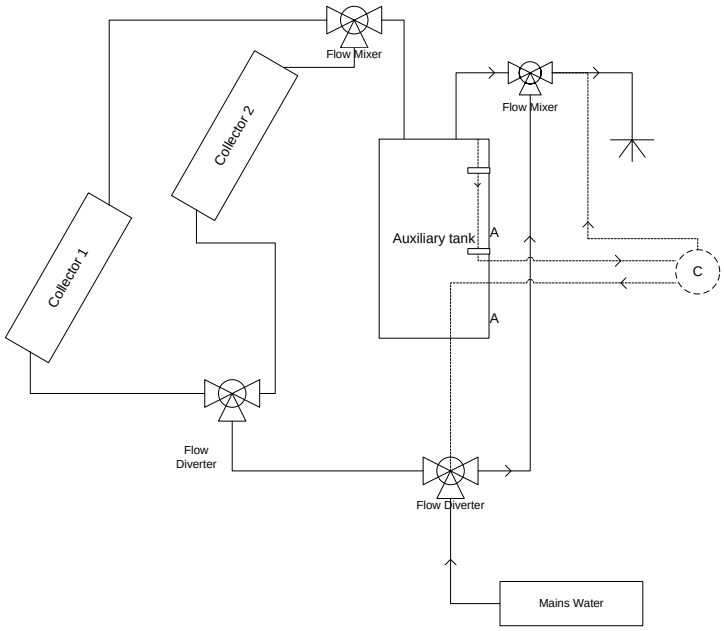

Figure 8 Diagram of ICS System Modeled

Along with the integrated collector and the auxiliary tank, there are 4 three way valves and one controller in the above diagram. They perform the following functions,

- There is a flow diverter and a flow mixer on the solar loop. These are only installed if more than one collector is present; they connect two or more collectors in *parallel*[4].
- The flow diverter in the load side loop supplies the flow mixer with mains water if temperature of water coming out of the auxiliary tank is higher than the specified set-point. The amount of water it diverts is specified by the controller.
- The controller on the load side loop is used to insure that the water delivered to the load is at the specified set-point. This is done by measuring the temperature in

[4] The reason for connecting more than once collector is stated later in this section.

the auxiliary tank and mains water temperature to determine the mixing ratio of mains temperature and hot water temperature to deliver water at the specified temperature.

- The flow mixer mixes water coming out of the auxiliary tank with mains water at the ratio specified by the load side controller (as explained above) if necessary. The output from the flow mixer is the water that is delivered to the load.

3.2 System Components

The components used in the construction of base case Glycol and ICS system as well as the parameters used to define them are described in this section.

3.2.1 Flat Plate Collector for Glycol System

The main parameters used to define a collector were researched and appropriate values for these parameters were ascertained. The main collector parameters researched were,

- Collector Size.
- Thermal properties of the collector.
- Flow rate of the working fluid through the collector.
- Orientation of the collector.
- Collector tilt angle.

Though the collector size is dependent on hot water load, the size is also constrained by collector sizes available in the market. Commonly available sizes are in steps of 1 and 2 square meters (Beckman, 2006). According to DOE, NREL's SDHW consumer's guide, *"Contractors usually follow a guideline of about 20 square feet (2 square meters) of collector area for each of*

the first two family members. For every additional person, add 8 square feet (0.7 square meters) if you live in the Sun Belt area of the United States, or 12 to 14 square feet (1.1 to 1.3 square meters) if you live in the northern United States" [5].

For the purpose of this study a collector area of 4 square meters was selected as it matches the average DOE researched collector sizing (average of sunbelt and northern United States contractor practices) for a four person household (the annual hot water load in this study represents a four person household). This 4 square meter collector size can be constructed using commonly available flat plate collectors. The solar storage tank size was determined using the chosen collector size of 4 square meters (this is explained in Section 3.2.4)

To ascertain the thermal properties (FrTa and FrUl) of the collector, SRCC (Solar Rating & Certification Corporation) collector rating data was studied for flat plate collectors (SRCC, 2009). Data for certified collectors was organized first by coating type and then by its thermal properties. A scatter diagram was plotted with FrUl on the Y axis and FrTa on the x axis, as shown in Figure 9.

[5] "A Consumer's Guide: Heat Your Water with the Sun"- U.S. DOE. Available at: http://www.nrel.gov/docs/fy04osti/34279.pdf

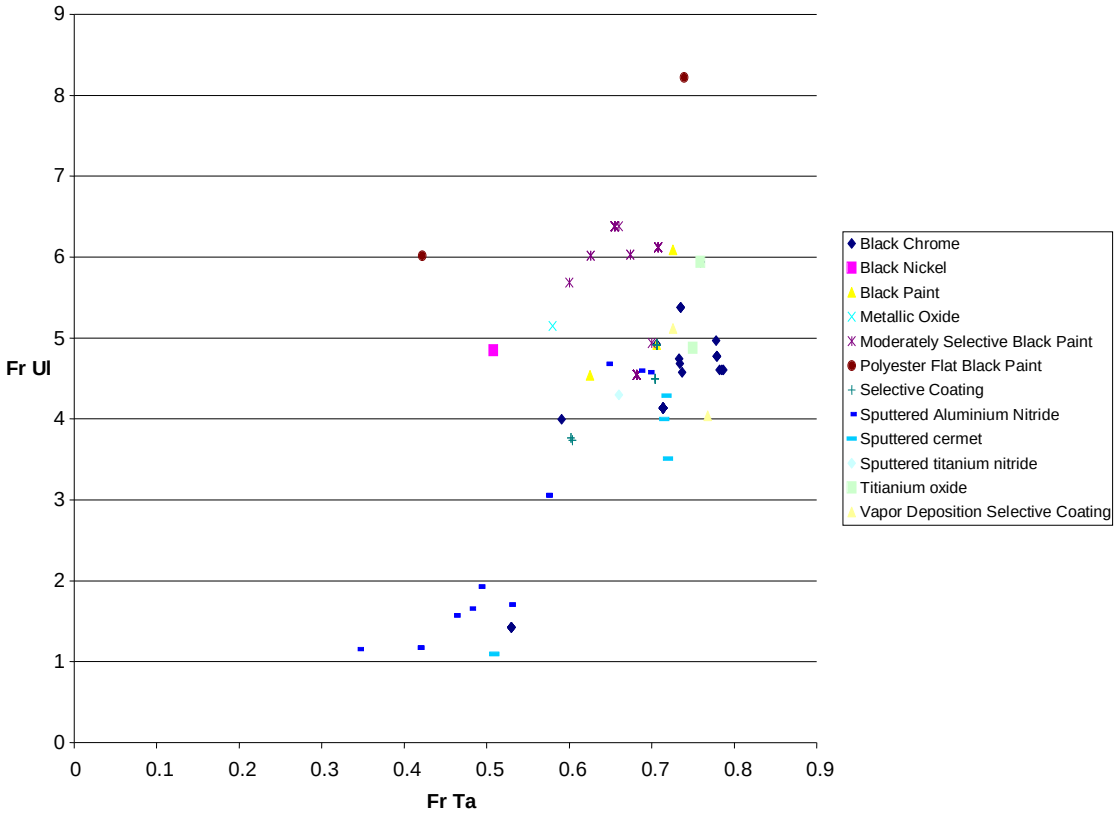

Figure 9 Thermal Properties of Collectors

After plotting this collector data, typical properties of collector were identified[6]. FrUl of 4.6 and an FrTa of 0.74 were chosen as properties of a typical collector.

3.2.2 Collector Flow Rate

Recent research has shown that it is advantageous to use a lower flow rate (between 0.002 and 0.007 kg/m^2 Sec) as it promotes stratification in the tank and results in decrease of first

[6] This was done by studying Figure 5, with consultation from Professor, Michael Brandemuehl.

cost and operation cost due to the need for a smaller pump (Beckman, 2006). The collector flow rate assumed here is 0.004 kg/ m^2 Sec.

3.2.3 Integrated Collector with Storage

Product research was done to determine the properties of the collector in the ICS system. The various parameters that were researched were,

- Collector size
- Thermal properties of the collector.
- Glazing properties of the collector.
- Collector storage volume.

The size of the collector was assumed to be the same as the size of the collector for the glycol system- 4 square meters. An average value of 0.83 was chosen for Tau-Alpha (Transmittance * Absorptance) based on research on commercially available collectors (Thermal Conversion Technologies).

To determine the collector storage capacity, research was done on SRCC rated ICS collectors and their storage capacities (SRCC, 2009). These are presented in Table 1.

Manufacturer	Collector Model	Collector Area (sq. m)	Storage Volume (liters)	Storage Cap/Unit Area (Liters/sq. m)
Thermal Conversion	PT-20-CN	1.00	67.20	67.20
Thermal Conversion	PT-30-CN	2.04	116.70	57.21
Thermal Conversion	PT-40-CN	2.77	156.70	56.57
Thermal Conversion	PT-50-CN	2.77	186.20	67.22
Sun earth Inc.	CP – 20	1.29	75.60	58.52
Sun earth Inc.	CP – 30	1.97	120.96	61.39
Sun earth Inc.	CP – 40	2.29	151.20	66.13

Table 1 ICS Collectors and their Storage Capacities

The average storage capacity per unit area (liters/sq.m) was found to be 62.04. The typical back and side insulation were found to be R 16 and R 12 respectively. Research was done on the arrangement of ICS collectors (Sun Earth Inc. was contacted) and it was found that ICS collectors are recommended to be installed in parallel for maximizing efficiency.

3.2.4 Solar Storage Tank

The size, insulation value, number of nodes, tank environment temperature, and position of ports were determined for a solar storage tank in order to accurately model it.

Annual system performance remains relatively insensitive to storage capacity once storage capacity is more than 50 liters per square meter of collector (Beckman, 2006). The f-chart tool uses a standard capacity of 75 liters/sq. m, this study assumed the same standard capacity as f-chart. Using a 4 sq. m collector, we get a storage size of 300 liters (Beckman, 2006). The insulation value of storage and auxiliary tanks used for this simulation was assumed to be R 14 (Brandemuehl, 2007- Private Interview).

Water tanks operate with significant degrees of stratification. To take stratification into account, tank models have been developed with hot water in the top half of the tank and cold water in the bottom half of the tank. Studies have shown that stratification in tanks has a significant effect on the performance of a solar hot water system. The tank modeled here is modeled as a multi-node tank to take into account the effect of stratification in the storage tanks. For domestic solar hot water tanks, in a study by Kleinbach et al (1993), it was shown that at least 10 nodes are necessary to accurately predict measured performance after comparing modeled data to measured data. In another study by Oberndoofer et al. (1999) modeled a number of different systems using from 1 to 100 tank nodes and concluded that no more than 10 nodes

are necessary for accurate annual predictions. Taking these factors into account it was decided that both storage and auxiliary tanks will be modeled as stratified tanks with 10 nodes each.

The tank environment temperature is the temperature of the space the tanks (Solar storage and auxiliary) are present at. Hence, this is the temperature to which the tanks lose heat. In the glycol model, both tanks are assumed to be indoors (Basement). Hence the temperature they are kept at is assumed to be 20 degrees Celsius.

The solar storage tank has 2 inlet and 2 outlet ports, these were specifically placed to encourage stratification. The inlet port for the solar loop is in the top node of the tank, while the outlet node for the solar loop is in the bottom node of the tank. There is an additional inlet port in the bottom of the tank, from where the mains water enters. Hot water from the solar storage tank leaves from the top node of the storage tank and into the auxiliary tank. As the cold water inlet and outlet ports are in the bottom node of the tank, and the hot water inlet and outlet nodes are in the top, stratification is encouraged.

3.2.5 Auxiliary Tank

The auxiliary tank was assumed to have a capacity of 40 gallons, two electric heating elements with a heating capacity of 4.5 kW each. The auxiliary tank was sized for a nuclear family of 3 -4 (Lowe's, 2009) and the corresponding auxiliary element heating rate was chosen from a list of water heaters (Whirlpool, 2009). The inlet and outlet ports in the auxiliary tank are on the top node to encourage stratification.

Operation of the two heating elements is controlled via temperature sensor. There is a temperature sensor at the outlet port, which switches on whenever the temperature at that port drops below the setpoint temperature (51.67 C). This triggers the first heating element, if the

temperature at the outlet port falls 3 degrees C below the setpoint, the second heating element switches on as well.

3.2.6 Pipes

Both indoor and outdoor pipes were modeled in the simulation. Four pipes were simulated, these are-

- Indoor pipe to the collector.
- Outdoor pipe to the collector.
- Outdoor pipe from the collector.
- Indoor pipe from the collector.

In the ICS system, the pipes form a loop between the auxiliary tank and the collector. In the Glycol system these pipes form a loop between the collector and the heat exchanger (which is indoors).

The pipe diameter is assumed to be ¾ inches, and pipes are assumed to have an insulation value of R-3[7]. The total pipe length is assumed to be 25 feet long each way, with 15 feet being indoors and 10 feet being outdoors. These values were chosen assuming location of collector on the roof, tanks in the basement.

[7] Pipe properties were chosen after studying codes and standards for different states from the website ww.dsireusa.org

3.2.7 Pumps

As stated previously, pumps are present only in the glycol system. A pump was chosen using the recommendations given in the RETScreen (RETScreen, 2009) manual. Shown below is a chart that shows recommended pump power as a function of the collector aperture area.

Collector Aperture Area (square meters)	Solar Pump (W)
2 to 6	20 to 45
6 to 12	85
12 to 35	185
35 to 60	205

Table 2 Solar Pump Power as a Function of Collector Area

For the given collector (4 meters) a 30 Watt pump was chosen. This will result in a flow of 0.08 kg/sec.

3.2.8 Working Fluid

The working fluid for the glycol system is propylene glycol. Research was done to ascertain the properties of this working fluid. The specific heat and specific gravity of the antifreeze in this model are 3.59 kJ/ kg K and is 1.06 respectively. The working fluid for the ICS system is water with a specific heat 4.18 kJ/kg ^{O}C.

3.3 System Sizing and Effects of System Sizing

The glycol system was sized by first sizing the collector appropriately for the load, which represents a family of four, and then sizing the hot water tank. For a family of four, the collector was sized at 4 square meters, and the solar storage tank was sized at 300 liters. The details of sizing these are presented in Sections 3.2.1 and 3.2.4 respectively. The size of the ICS system collector was 4 square meters as well, sized using the same logic as the glycol system.

The size of system has a significant impact on the useful energy, and hence the *Sf* of the system. As the size of the system is increased keeping load constant, the *Sf* of a system increases as well. The increase of the *Sf* is in the form of a curve of diminishing returns, where the rate of increase of *Sf* decreases with increase in system size. Hence, for a well sized solar system, the magnitude of change in *Sf* due to increasing the system size by a factor of two is smaller than the magnitude of change in *Sf* due to the decrease in size by a factor of two. An identical effect will be observed if the load on the system is decreased while keeping the system size constant. Section 2.3 of the literature review discusses this effect and the previous research on this topic.

4 Methods of Analysis

4.1 Introduction to TRNSYS

System performance for all scenarios is modeled using TRNSYS, an hourly transient simulation program that was developed at the University of Wisconsin – Madison (W.E.Buckles and S.A.Klein (Solar Energy Laboratory, 1980). TRNSYS is an energy simulation tool under continuous development by the Solar Energy Laboratory (SEL) at the University of Wisconsin – Madison, The Centre Scientifique et Technique du Bâtiment (CSTB) in Sophia Antipolis, France, Transsolar Energietechnik GmBH in Stuttgart, Germany and Thermal Energy Systems Specialists (TESS) in Madison, Wisconsin. TRNSYS is modular in nature, which makes it flexible and allows the user to incorporate mathematical models that better represent designs unique to the system.

A five minute time step was used for all simulations. The time step was chosen to match the time step of the hot water draw profile used in the simulation. Another advantage of using

TRNSYS was the availability of a wide variety of system components present in its libraries including and different types of collectors, storage tanks and controllers among other features

4.2 System Components – Modeling Details

Presented in Table 3 are the TRNSYS components used to model the ICS and glycol systems for this research.

Component Name	Glycol System	ICS System	Notes
Weather Data	Type 15 -2 Data Reader and Weather Processor		-
Flat Plate Collector	Type 1 Flat Plate Solar Collector	NA	Slope of collector set to the latitude of the location. Azimuth Angle = 0^{O}
Heat Exchanger	Type 91 Constant Effectiveness HX	NA	-
Integrated Collector with Storage	NA	Type 550 Tubular ICS Collector	Slope of collector set to the latitude of the location. Azimuth Angle = 0^{O}
Solar Storage Tank	Type 4a Stratified Storage Tank	NA	Tank has 10 nodes equally spaced Heating elements in Type 4a turned off
Glycol Pump	Type 3	NA	-
Solar Storage Pump	Type 3	NA	-
Auxiliary Tank	Type 4 Auxiliary Storage Tank (Electric Elements)		2 heating elements Tank has 10 equally spaced nodes
Pipes	Type 31		-

Table 3 TRNSYS Components used to Model Glycol and ICS Systems

4.3 Hot Water Draw Profiles

In this research, a hot water draw profile is used to simulate hot water draw of typical households. This hot water draw profile is constructed by determining hot water demand in gallons per minute (gpm) at different times of the day. This draw profile is constructed using

three types of loads; shower loads, dishwasher loads and clothes washer loads. These loads have either a 0.5, 1.5 or a 2.5 gpm flow rate. The 2.5 gpm loads are due to clothes washers.

4.3.1 Nuclear Family (Base) Profile

This profile approximates the hot water use for a stay-at-home family. The highest draw flow rate is 1.5 gpm and the highest duration of draw is fifteen minutes. There are two separate profiles to represent a weekday and a weekend. Figure 10 and Figure 11 show a typical weekday and weekend draw profile for a Nuclear family. The weekday draw is 60 gallons; weekend draw is 75 gallons. The weekday and weekend profiles differ from each other as the weekday profile typically has all loads below 2.5 gpm. This is as it is assumed that there are no clothes washer loads (2.5 gpm) on the weekdays. This profile will be referred to as the Base Profile for rest of this research.

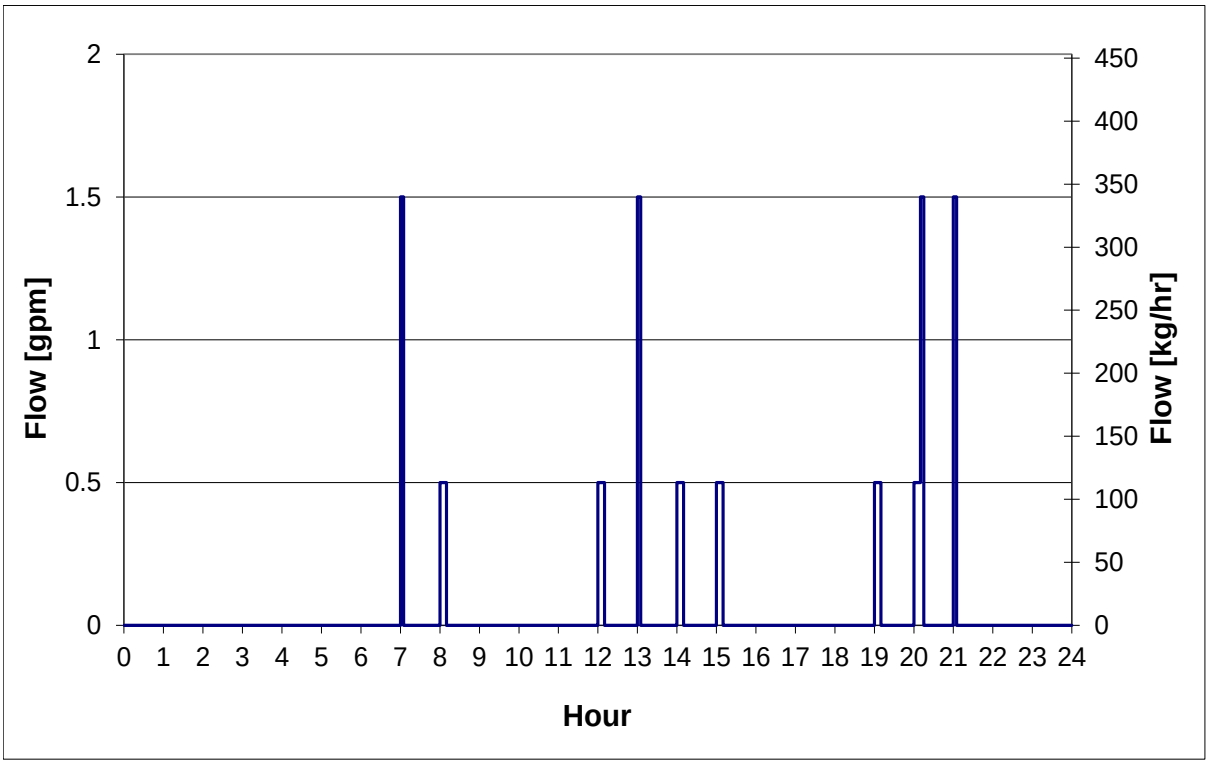

Figure 10 Base (Nuclear Family) Profile - Weekday

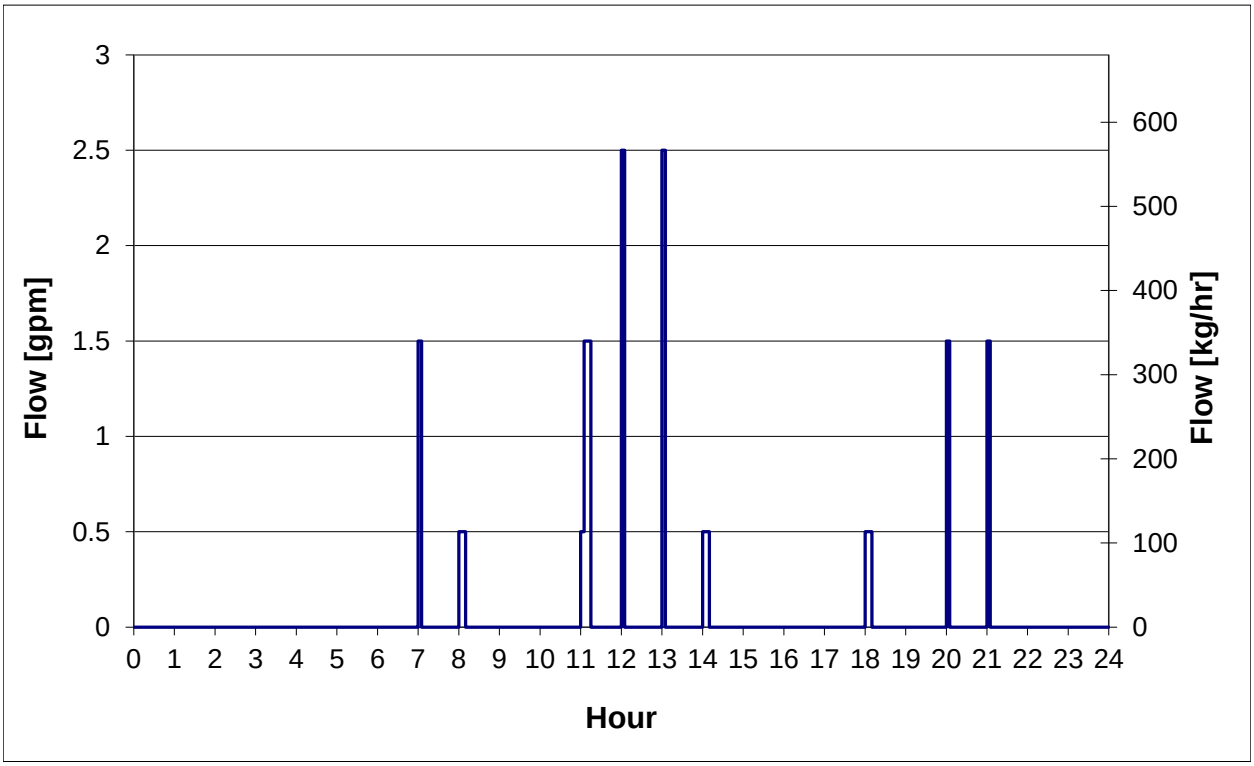

Figure 11 Base (Nuclear Family) Profile - Weekend

4.3.2 Yuppie (Evening) Profile

The Yuppie (Evening) profile has no draws during the middle of the weekday as it is designed for a working household. This profile is characterized by a high percentage of daily draw (more than 50 %) before 9 AM during weekdays. Hence as seen in Figure 12, there are no draws between nine in the morning and six in the evening (working hours during a weekday). The weekend draw profile (Figure 13) does not have a draw before 9 AM. It has loads with high flow rate (2.5 gpm) in the afternoons that correspond to clothes washer loads. The total daily draw is 60 Gallons for a weekday and 67.5 gallons for a weekend. The weekend draw was adjusted to match the total weekend draw for a Base Profile. There were two options to do so; (1) to introduce a new 7.5 gallon draw in the profile, and (2) to adjust the each draw in the profile

with a multiplier (75/67.5). To retain the shape of the Yuppie profile, the multiplier was chosen. As we are adding 7.5 gallons to a day, by spreading it over all the draws in a weekend day, we retain the Yuppie Profile Shape while introducing a minimal load (~1 gallon) per draw. This profile will be referred to as the Evening Profile for the rest of this research.

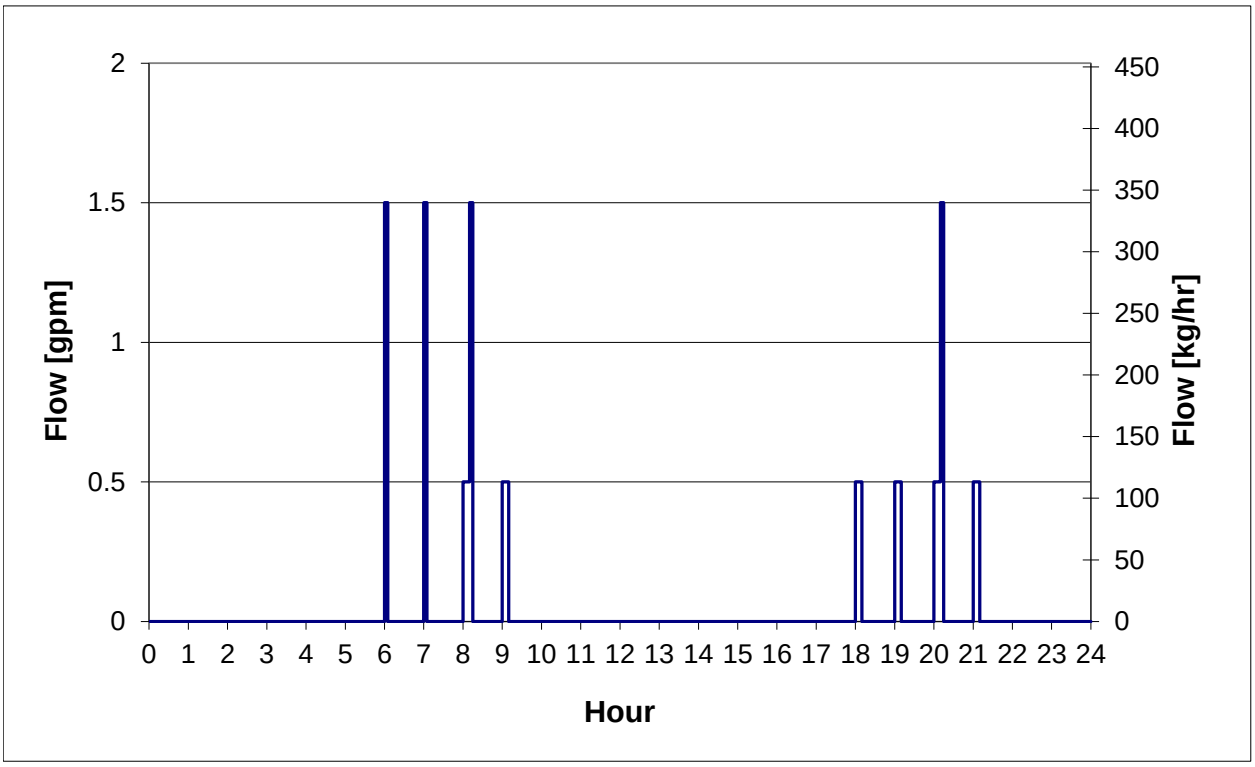

Figure 12 Yuppie (Evening) Profile - Weekday

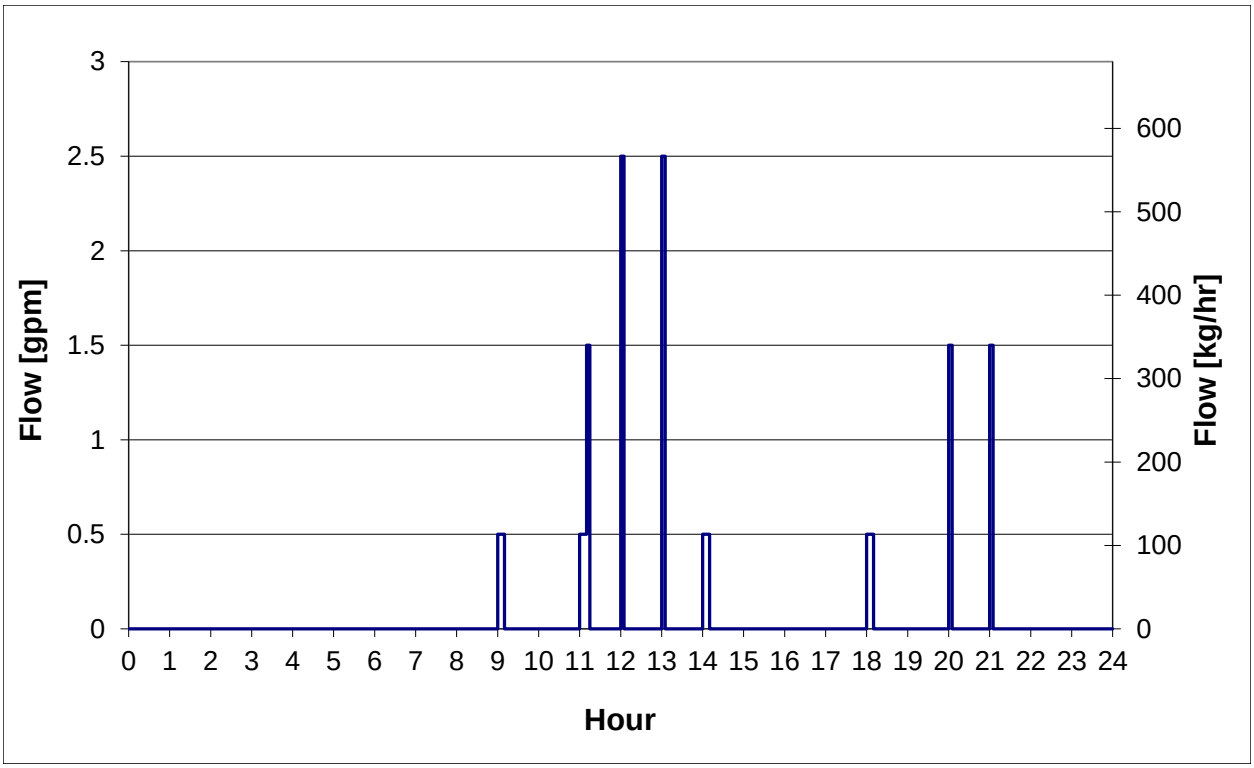

Figure 13 Yuppie (Evening) Profile - Weekend

4.3.3 Morning Profile

The morning profile was developed for the purpose of this study. This was done to show the effect a Nuclear family with a high morning draw (higher than Yuppie) has on system performance. This was done by moving two draws form the evening (1.5 gpm for 5 minutes) to the morning. The new morning draws are at 1.5 gpm, at 6 AM (7.5 gallons @ 1.5 gpm) , 7 AM (5 gallons @ 0.5 gpm) and at 8 AM (7.5 gallons @ 1.5 gpm). The profile for the weekend was kept the same.[8]

[8] This was done after discussions with Michael J Brandemuehl.

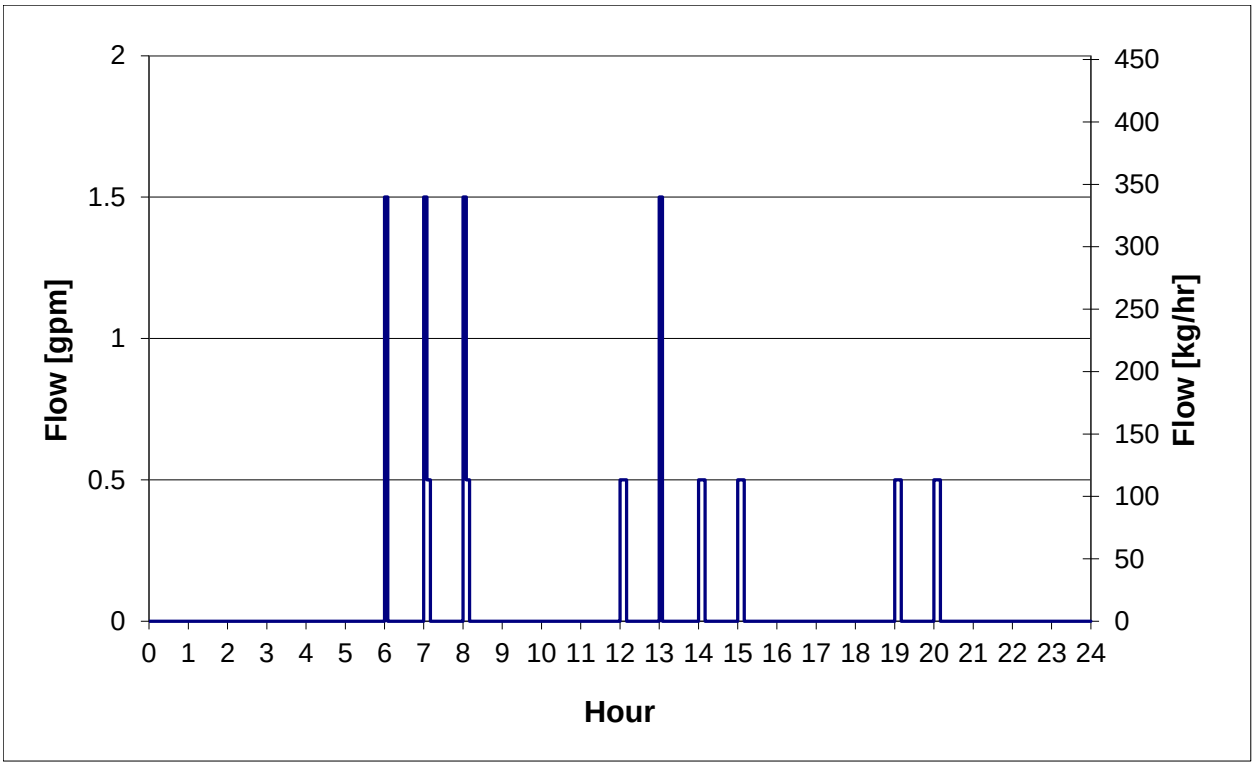

Figure 14 Morning Profile – Weekday

4.3.4 Extreme Profile

This profile contained the daily hot water load in one hour, between 5 AM and 6 AM. The weekday and weekend total daily loads were kept the same as the Nuclear profile. The flow rate during the one hour of flow was kept consistent at 60 gallons per hour for weekdays and 75 gallons per hour for weekends.

4.3.5 Hourly Profile

This profile was constructed to compare the 5-minute profiles to an hourly profile with equal integrated water draws. Hence, the total annual, daily and hourly loads are the same as the Nuclear profile. The flow rate and flow duration of the Hourly profile were adjusted to create an hourly profile with equal integrated water draws. This draw profile is presented in Figures 15 and 16.

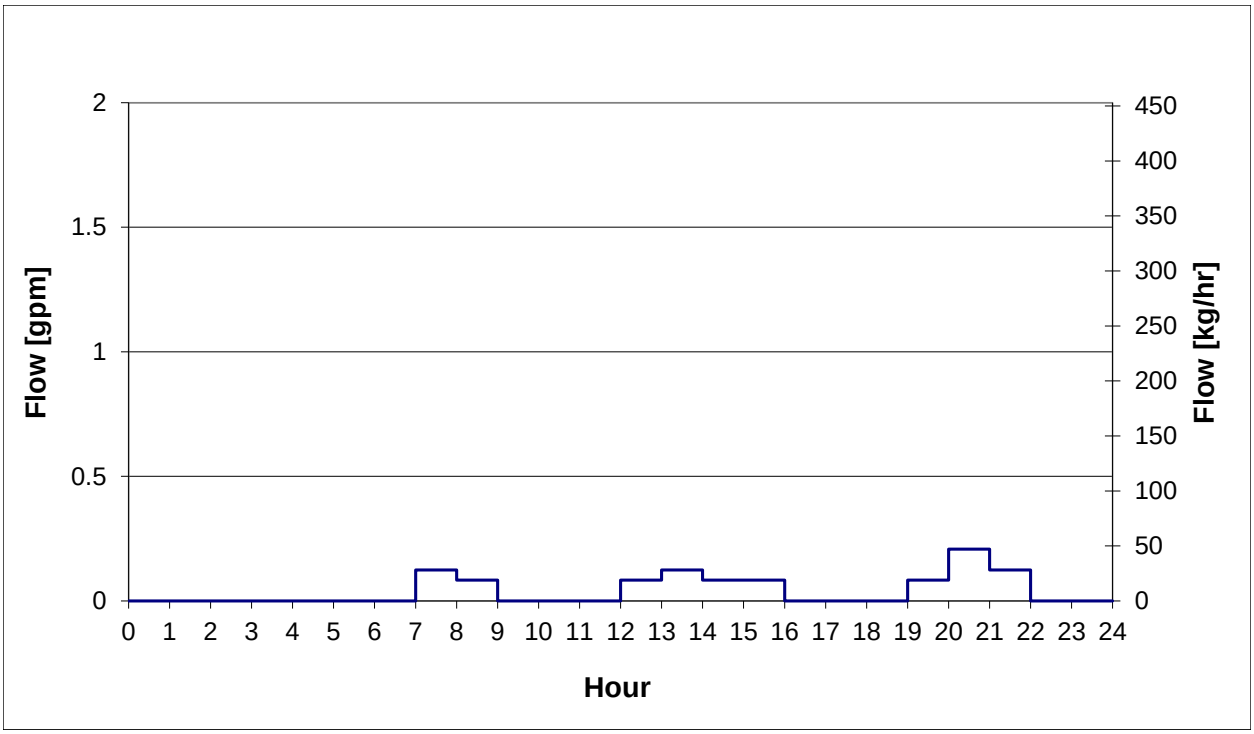

Figure 15 Hourly Profile- Weekday

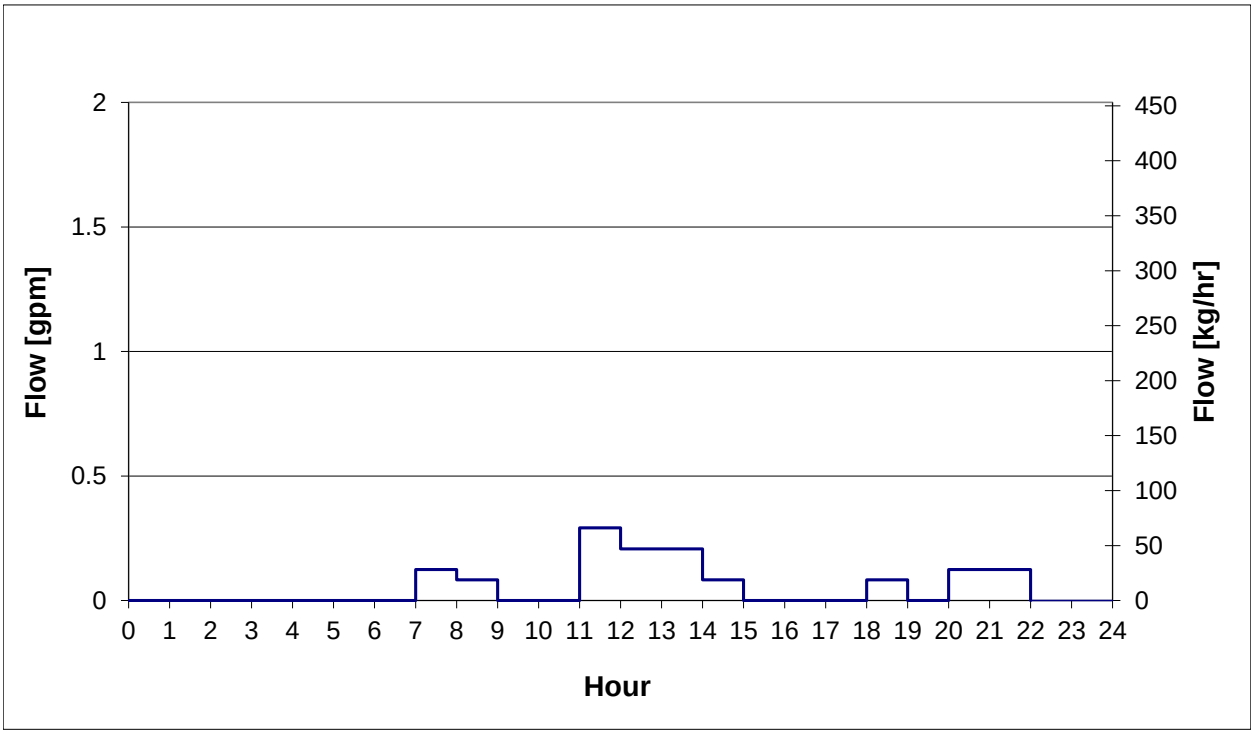

Figure 16 Hourly Profile - Weekend

4.4 Load Variations to Base Profile

This section describes the variations made to the load on the solar hot water system to study the effect of change in performance of an active and a passive solar hot water system due to load variations, the variations made to annual load are:

- Increasing the load by a factor of two.
- Decreasing the load by a factor of two.
- Introducing a random day to day variation in the load while keeping the annual load constant.
- Decreasing Mains Water temperature.

4.4.1 Increasing the Load by a Factor of Two

To study how system performance changes when the load on the SDHW system is greater than rated load, an extreme case in which the load on the system is twice the rated load was considered. The analysis is analogous to a scenario where the system size is reduced by a factor of two. The load was increased by two different methods, increasing the flow rate of each draw and increasing the duration of the draw. The effect on system performance by changing the flow rate by a factor of two and the duration of the draw by a factor of two was found to be similar (See Section 5.1.1 and 5.1.2). Hence for all the simulation runs, only the flow rate was varied.

4.4.2 Decreasing the Load by a Factor of Two

The effect of over-sizing a SDHW system or using less hot water than a SDHW system is rated for was studied. This effect was studied in a similar manner to the effect of increasing the load. The flow rate of each draw was reduced by a factor of two. Hence, the total hot water load on the system was changed to be 50 % of the base load.

4.4.3 Introducing Random Day-to Day Variations in Load (While Keeping Annual Load Constant)

A random variation in draw volume was introduced for each day of the year. This was done in the following manner,

- The annual load on the system was kept constant.
- A unique multiplier was introduced for each day of the year. This multiplier was used to change daily draw volume by changing flow rate of each draw of the day,
- This multiplier was constrained such that it varied between 0 and 2.
- The mean of all 365 multipliers (1 for each day) was 1, standard deviation was 0.4.

This is illustrated in Figure 17 and Figure 18. Figure 17 shows the value of each random multiplier used in a year, while Figure 18 shows the frequency of different random multipliers used in a year. The frequency is charted by sorting the multipliers into a bin of 0.1.

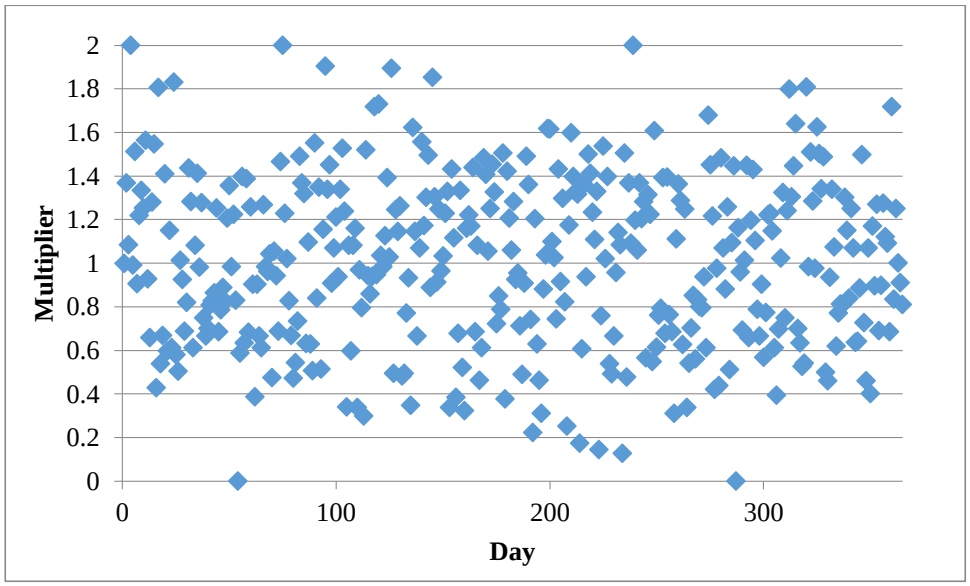

Figure 17 Scatter Plot Showing Random Multiplier for each Day of the Year

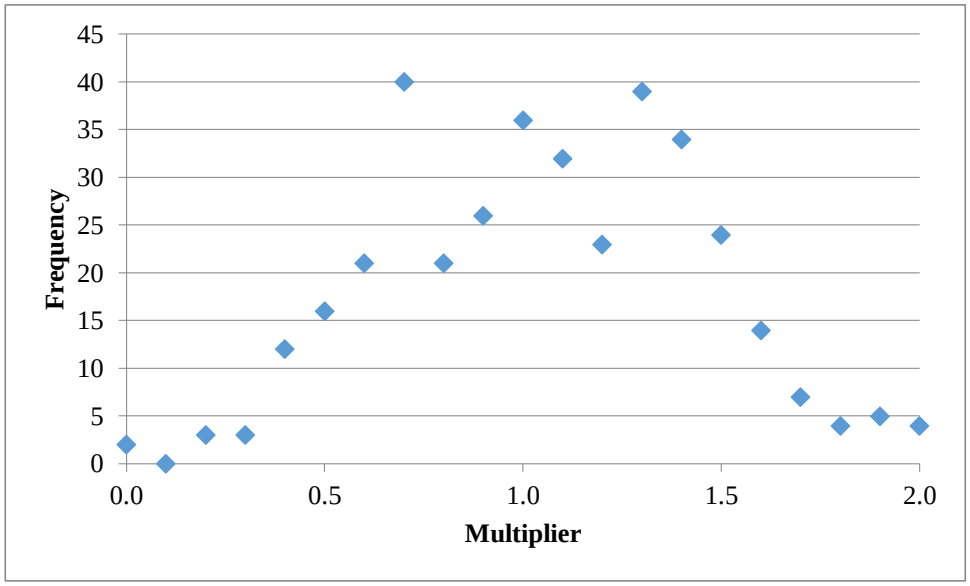

Figure 18 Frequency of all Daily Multipliers in One Year

4.4.4 Changing Mains Temperature

The mains temperature algorithm defined in Section 2 was used in all simulations. The mains temperature was changed by reducing it by 3° C at each time-step. Shown in Figure 19 is a

comparison of the two mains water temperature profiles for Boulder, CO. T_{Mains} represents TRNSYS calculated mains temperature described in section 2; T_{Mains}`` is the modified mains temperature.

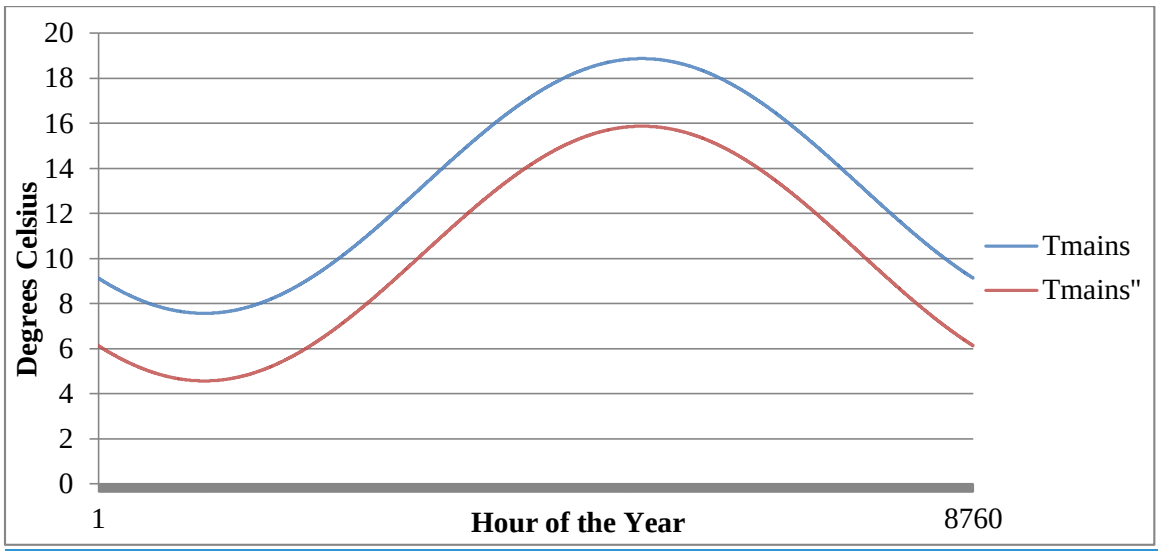

Figure 19 Comparison of the Two Mains Water Temperature Algorithm Used

4.5 Metrics Used to Study Results

The results for all simulations were studied using Annual system efficiency and Annual solar fraction Annual system efficiency is defined as the fraction of total energy incident on the collector that is converted to useful energy to heat water in one year. Research has found that system efficiency is a product of the system and the load on the system, this system efficiency does not change much with location (Barker, 2007).

Annual solar Fraction is defined as fraction of total purchased energy to heat water that is replaced by solar energy in one year. The solar fraction for a system is dependent on system location. For locations with higher incident radiation, solar fraction of SDHW systems are higher than for locations with lower incident radiation. Although the system efficiency and solar

fraction are not mathematically related, for a given location, the higher the system efficiency, the higher the solar fraction for a system.

5 Results

Results of all simulations performed are presented here. The results were obtained by simulating the base system described in Section 3; variations were made to this base system by using all draw profiles explained in Section 4.

The results were studied using annual solar fractions and system efficiencies. These have been presented in graphical form. This was supplemented by studying the working of the system for a typical summer and winter day using hourly data. Hourly data helped understand the drivers of change in system performance for different scenarios simulated.

These simulations were performed for ten representative cities in the USA. As we are not attempting to study trends with respect to climate for our various cases, ten representative cities were chosen and the effect of each parameter on glycol systems was studied in detail. The ten representative cities were chosen as,

- Each of these cities represents a potential big market in its region.
- Collectively they represent a wide range of climates that is found in the USA.
- These ten cities are shown in the map below.

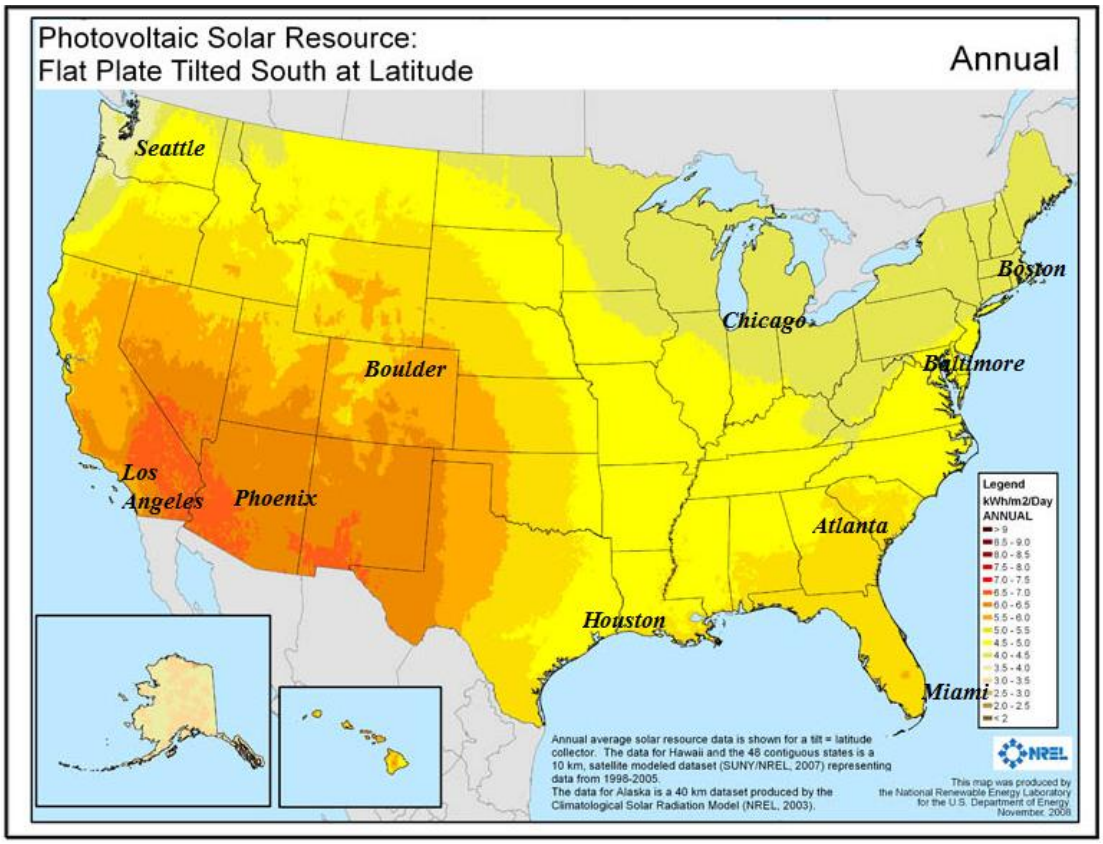

Figure 20 Map showing the representative cities that SDHW systems were simulated in (NREL, 2008)[9].

Due to possibility of pipe freeze, an ICS system cannot be modeled for all these nine cities, hence of these nine cities 5 were deemed safe to model for ICS system installation (Salasovich, 2001). These cities are Los Angeles, Phoenix, Houston, Miami, and Atlanta.

In the following sub sections simulation results for both the ICS and the glycol systems are studied in detail, for cities in which installation of both ICS and glycol systems is possible,

[9] City locations are approximate.

these two systems and their results are compared with respect to the changes made to the base system.

5.1 Glycol System Results

In this section, results of all the simulations on the glycol system are presented and explained. Before explaining the effect of different load profiles on the glycol system, the working of the base glycol system with a nuclear family profile is explained. The base system is studied using five minute data for a typical summer (June 15) and a typical winter day (December 15) for Boulder, CO. Figure 21,Figure 22 present the ambient temperature (T_{amb}), incident solar radiation ($Q_{Incident}$) on the collector and the hot water draw pattern (HWDraw) on these two days.

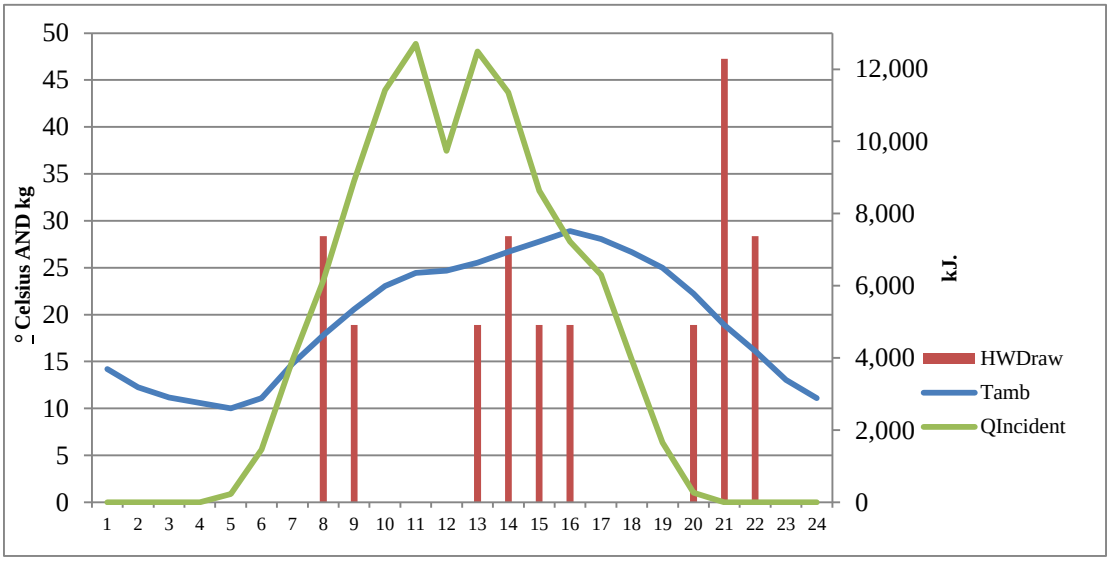

Figure 21 Typical Summer Day Weather, Boulder CO

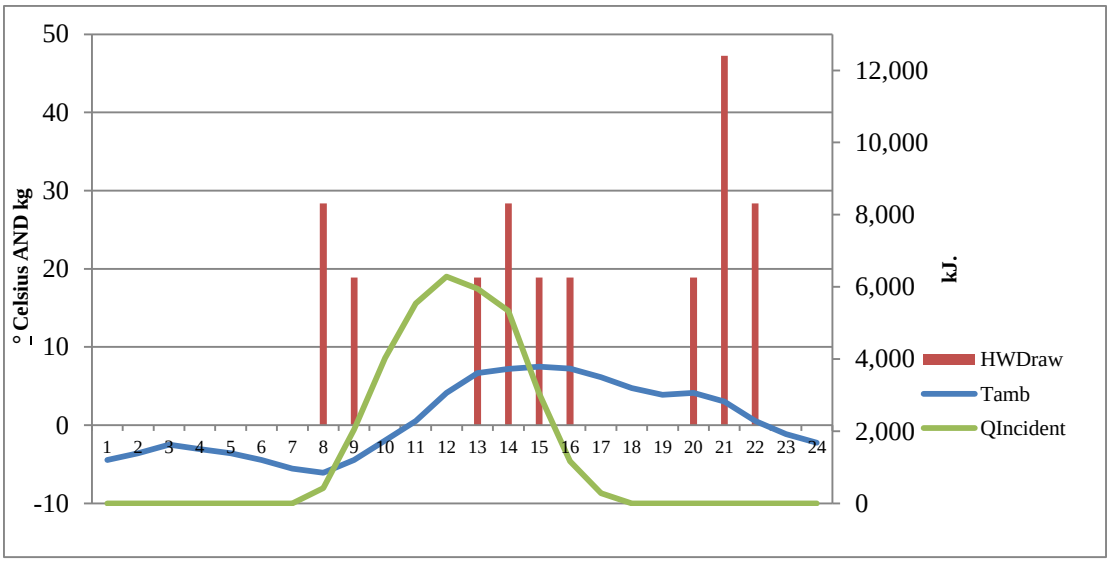

Figure 22 Typical Winter Day Weather, Boulder CO

On the summer day, incident solar radiation starts around 5 AM, peaks at noon and ends around 8 PM. Incident solar radiation starts before the first hot water draw of the day and exists for all except the last three hot water draws of the day. The ambient temperature peaks at 30^{O}C (4 PM) and has a minimum value of 10^{O}C (5 AM).

On the winter day, incident solar radiation doesn't start until 8 AM, peaks at noon and ends at around 5 PM. The peak value of the solar radiation (~6,000 J) is less than half of that of the peak value at a typical summer day (> 12,000 J). No incident solar radiation exists for all hot water draws before 9 AM and after 3 PM. The ambient temperature peaks around 8^{O}C and has a minimum value of approximately -5^{O}C.

To study the performance of the active system for these days, the three parameters system studied during the course of a day are,

1. HW_{Draw}, this is the rate of hot water draw in gallons per minute.

2. Q_{Aux}, this is the amount of energy given to the system through the auxiliary heating tank, in KJ.
3. $T_{soltank}$, this is the average temperature of the solar tank. The solar tank temperature is an indicator of system performance. The solar tank temperature influences the efficiency of the solar collector and the amount of energy required by the auxiliary heating elements. The system collects energy only when the temperature of the bottom node of the solar tank is lower than the temperature of the fluid coming out of the collector. Also, a sufficiently high solar tank temperature ensures that fluid entering the auxiliary tank is at a high temperature, which in turn reduces use of auxiliary heating elements.

Shown in *Daily System Performance: *Sf* = 100%, *n* = 32%

Figure 24 and * Daily system performance: *Sf*= 23%, *n* = 26%

Figure 23 are hourly data for the aforementioned variables for a typical winter day (December, 15) and a typical summer day (June, 15). Both are weekdays.

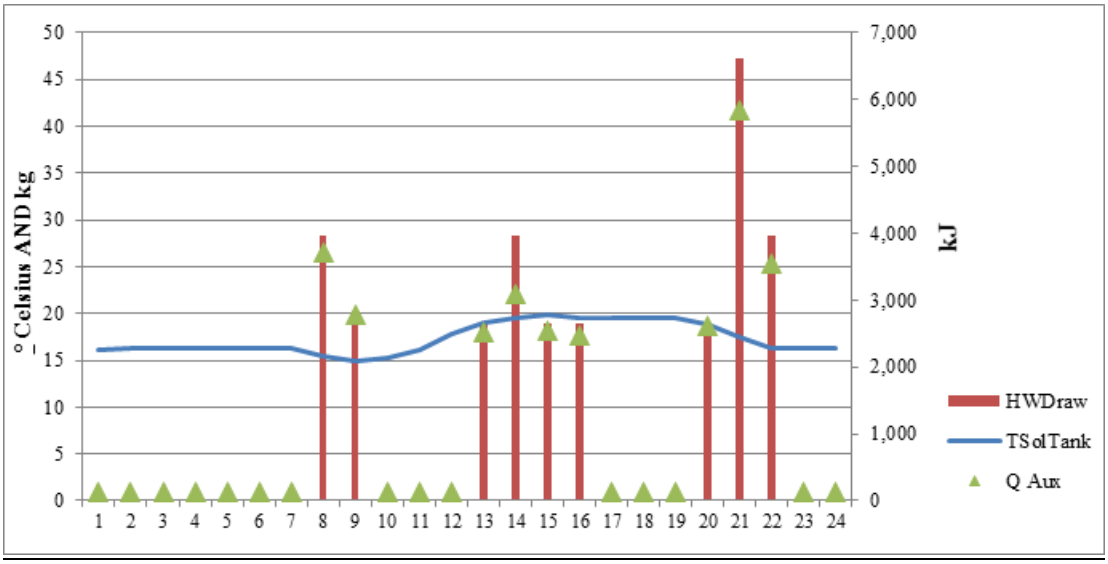

* Daily system performance: *Sf*= 23%, *n* = 26%

Figure 23 System Performance in a Typical Winter Day in Boulder*

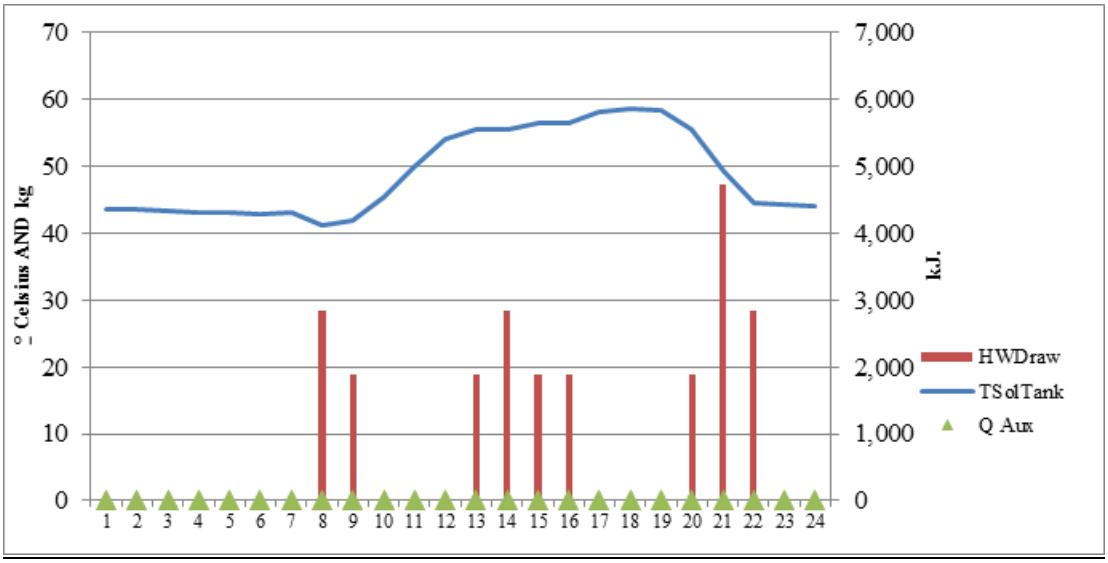

*Daily System Performance: *Sf* = 100%, *n* = 32%

Figure 24 System Performance in a Typical Summer Day in Boulder

The average temperature of the solar tank ($T_{soltank}$) is much lower in the winter than summer due to higher solar radiation in the summer. The temperature ranges between approximately 15°C and 20°C in the winter, compared to the summer where it ranges between 41 and 59°C. Higher mains water temperatures (not shown in the chart) in the summer also mean reduced load on the system. Hence, Q_{Aux} is not needed in the summer; the system provides enough energy to meet the hot water load.

In the winter, auxiliary heaters are required almost as soon as there is a draw. The amount of auxiliary heat required (Q_{Aux}) is correlated with HW_{Draw}; at times of high HW_{Draw}, Q_{Aux} is also higher.

The *Sf* (solar fraction) of the system is a function of the location and its climate; Phoenix and Miami have a high ambient temperature, and high incident radiation. They also have the highest *Sf*. The *Sf* and *n* (system efficiencies for all ten locations that were simulated are shown in Figure 25. It should be noted that the cities have been arranged in order of increasing solar fraction. This presentation trend has been retained throughout this section.

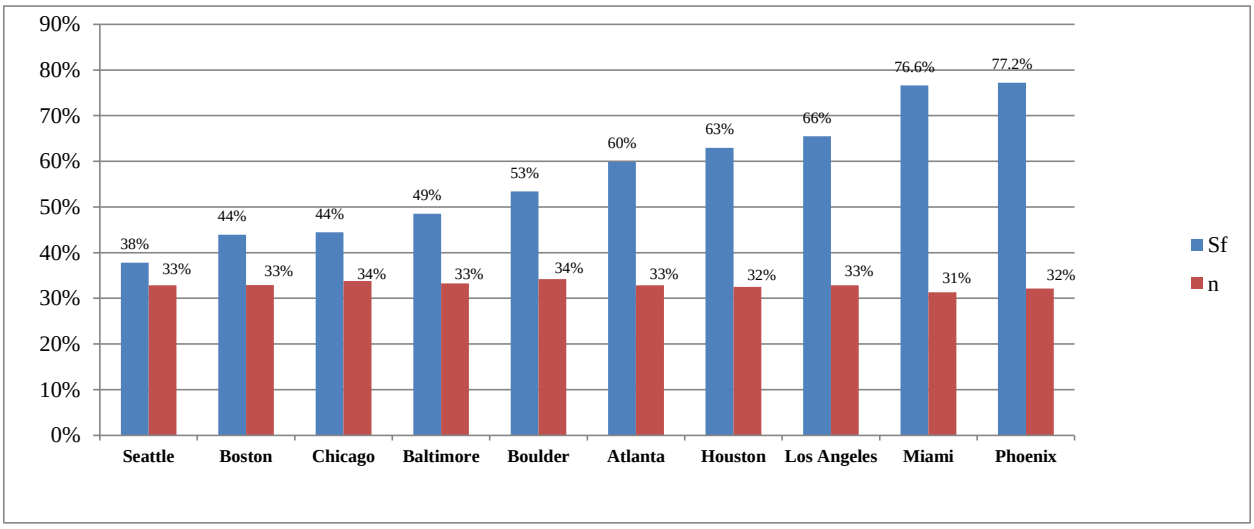

Figure 25Solar Fraction and System Efficiencies For All Locations Simulated.

The system efficiencies do not change with location. This is as system efficiency is a function of the system and independent of the location a system is in as previous research indicates (Barker, 2007).

5.1.1 Effect of Increasing the Load by Doubling Flow Rate (Scenario 2x)

The annual load on the system was doubled by increasing the flow-rate of each draw by a factor of two (Scenario 2x); and by increasing the time of each draw (Scenario 2x-1) by a factor

of two. Both of these cases were examined separately to understand the difference in system performance in both of these scenarios. Results for these scenarios, and all scenarios presented in this research, are presented as a percentage change from the base case.

$$\%Change = (ScenarioValue - BaseValue) / BaseValue$$

"Base Values" are the *Sf, n* of the Glycol System with Nuclear family load profile and the "Scenario Value" are the *Sf, n* of the Glycol system with twice the load as the Nuclear family profile. Here, a positive value indicates an increase in *Sf* or *n*, whereas a negative value indicates a decrease in the value of these variables. Figure 26shows how solar fraction and system efficiency change in Scenario 2x.

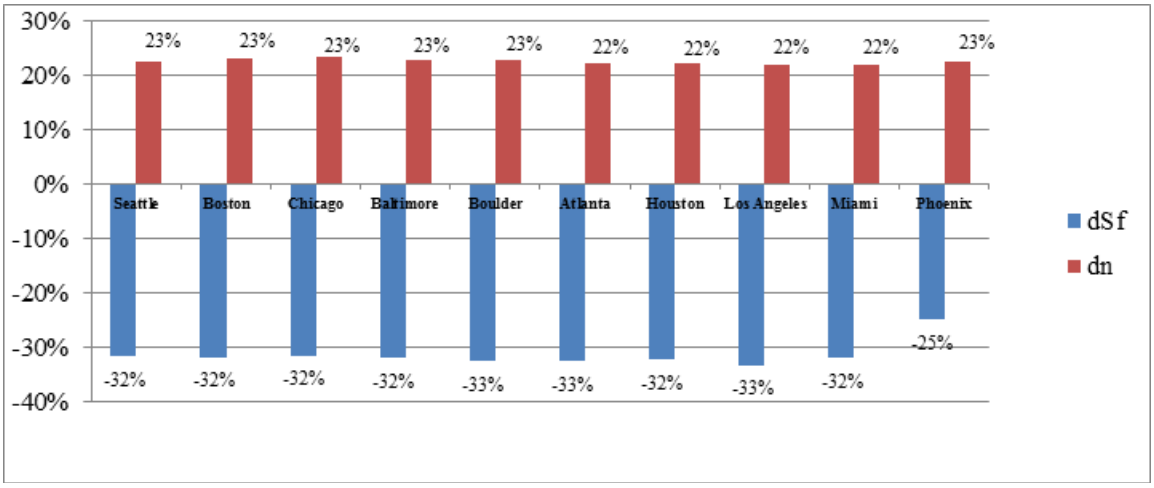

Figure 26 Change in System Performance Under Scenario 2x.

We see in the chart above, that -

- *n* increases by of 22 - 23 % in all cases.
- *Sf* decreases by an average of 33 % for all cases except Phoenix, which shows a decrease of 25 %.

Figure 27 illustrates working of the Glycol system with Base and Scenario 2x for a winter day (December, 15) in Boulder, CO. As the load on the system increases, $T_{SolTank}$ decreases. This is as twice the rated HW_{Draw} is drawn from the solar tank at each draw. This decrease in $T_{SolTank}$ leads the system to convert more of the incident solar radiation into useful energy. The increase in useful energy is not enough to offset the increase in system load. Hence, the auxiliary heating elements are required to produce more Q_{Aux}.

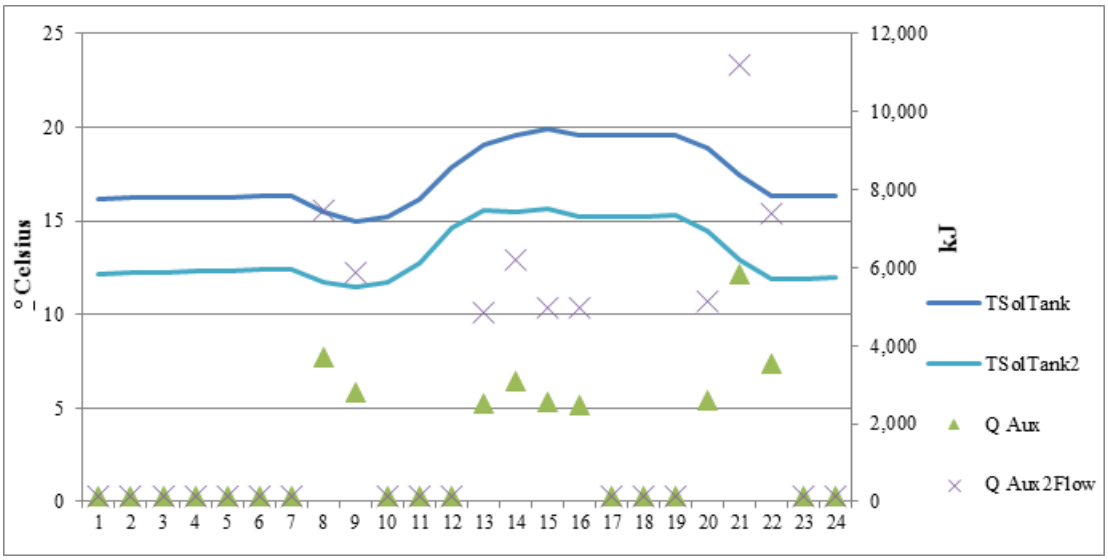

*Daily System Performance, Scenario 2x: *Sf* = 15%, *n* = 32%; Base Scenario *Sf* = 23%, *n* = 26%

Figure 27 Comparison between Performance of glycol System with Base and Twice the Load

5.1.2 Effect of Increasing Load by Doubling Draw Duration (Scenario 2x-1)

To observe the difference in system behavior due to a Scenario 2x-1 versus Scenario 2x, the system was simulated in all locations by increasing the duration of each draw by a factor of two. The change in system performance due to Scenario 2x as compared to Scenario 2x-1 is presented in Figure 28. All changes are with respect to Scenario 2x.

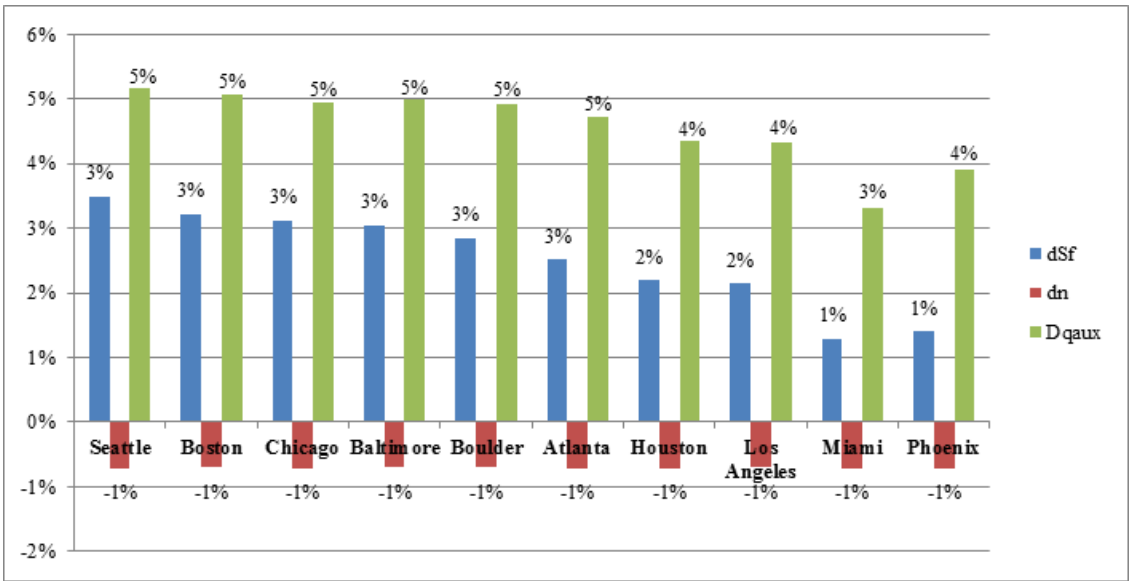

Figure 28 Comparison of Increasing Flow Rate and Flow Duration by a Factor of Two

The two systems perform almost identically, with system efficiency changing by less than a percent the solar fraction changing by less than 3.5 % in all cases. The only parameter of the system that changes significantly is the Q_{Aux} (3 to 5 %). These values are higher for an increase in draw duration.

This can be explained as follows; the auxiliary tank model has 10 nodes, a total volume of 40 gallons. The third node has a temperature-measuring device, which insures that the top 3 nodes of the tank stay at the set point temperature (T_{set} = 51.67 degrees). Due to stratification, temperatures below the third node are below the set point. When the daily consumption is doubled, in Scenario 2x, there are certain time steps when the hot water draw is greater than the volume of the water in the first 3 nodes of the tank. Hence, some water that is below the set-point is also delivered and some potential energy that would have been provided by the auxiliary heating elements is lost. In the case of Scenario 2x-1, this does not happen as often, as the total draw is divided amongst more time-steps. Therefore, the average temperature delivered to the

load in the case of Scenario 2x-1 is higher. This is what contributes to the slight difference in total annual load, solar fraction and auxiliary energy use in the two cases.

*Daily System Performance for both scenarios: *Sf* = 15%, *n* = 32%

Figure 29 presents how a glycol system performs on a typical winter day (December 15th – Boulder, Colorado) in Scenario 2x and Scenario2x-1. A winter day was chosen as the load on the system is greatest at this time of the year; any difference in system performance between the two scenarios would be apparent on this day.

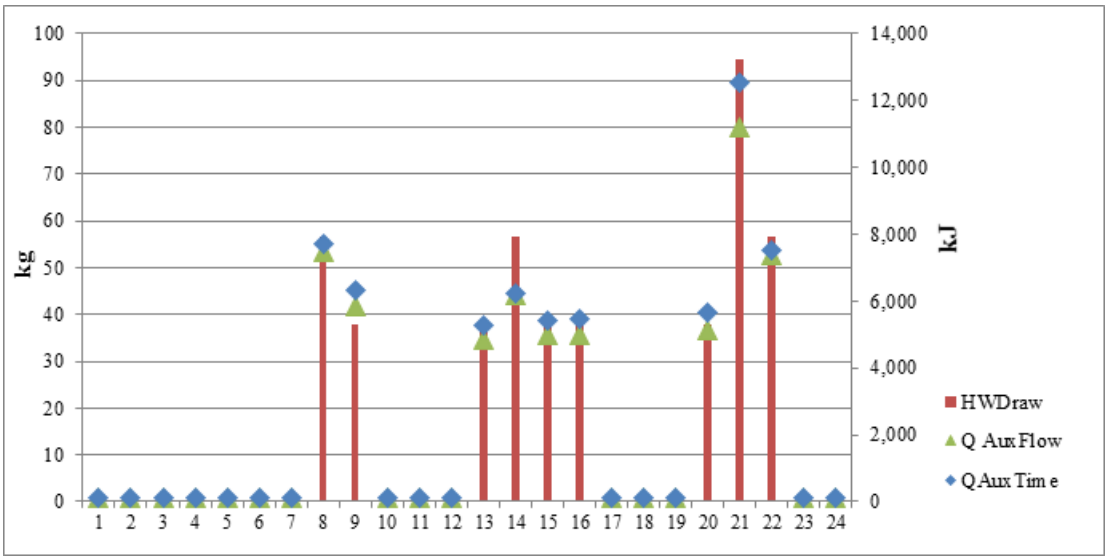

*Daily System Performance for both scenarios: *Sf* = 15%, *n* = 32%

Figure 29 Comparison between Increasing Flow Rate and Flow Duration by a Factor of 2 on December, 15 (Boulder, CO)

The system performs identically in the two scenarios with the exception of a large night time draw (2100 hours). As explained above, this incident of hot water draw is larger than the volume of the hot water contained in the top three nodes in the tank, resulting in some water not being instantaneously heated upon draw. This is why the system consumes approximately 4 % less energy on an average for Scenario 2x, as compared to Scenario 2x-1.

5.1.3 Effect of Reducing Load by Halving Annual Hot Water Draw (Scenario 0.5x)

To study the effect of decreasing the annual load on the system, the flow rate of each draw was decreased by a factor of two (Scenario 0.5x). In this scenario, solar fraction increases while system efficiency decreases. Figure 30 presents the results for this scenario.

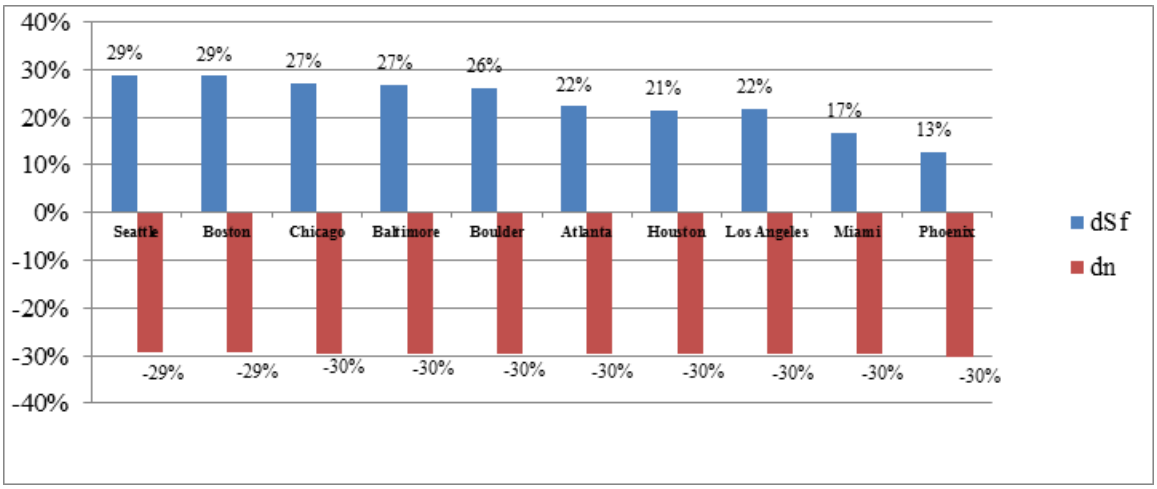

Figure 30 Effect of Halving Draw Flow Rate. (Scenario 0.5x)

On reducing annual load by a factor of two, we notice that:

- *n* decreases by 30 % of all locations.
- *Sf* increases for all locations; this percentage increase in solar fraction is greatest for location with lowest base *Sf* (Seattle). Location with highest base *Sf* shows least percentage increase in *Sf* (Phoenix).

The useful energy produced by the Glycol system is directly correlated to the draw. The system works less and produces less useful energy when the annual hot water draw is reduced. This happens esp. if the solar storage tank is appropriately sized.

*Daily System Performance, Scenario 2x: *Sf* = 29%, *n* = 19%; Base Scenario *Sf* = 23%, *n* = 26%

Figure 31 illustrates working of the Glycol system for Base and Scenario 0.5x for a winter day (December, 15) in Boulder, CO.

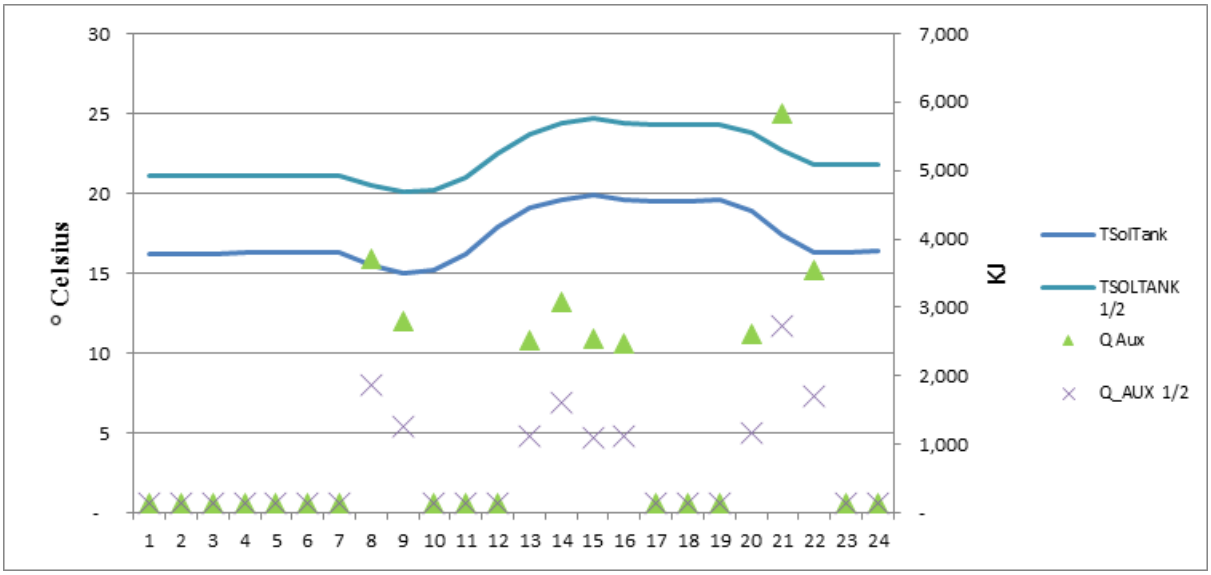

*Daily System Performance, Scenario 2x: *Sf* = 29%, *n* = 19%; Base Scenario *Sf* = 23%, *n* = 26%

Figure 31 Comparison between Performance of Glycol System with Base and Half the Load (Scenario 0.5x)

As the load on the system decreases, the average temperature of the solar tank increases, as half the rated hot water is drawn from the solar tank at each draw. This increase in solar tank leads the system to convert less of the incident solar radiation into useful energy. As the system is working to meet half of its rated load, it has a higher *Sf* than the base case, even though *n* decreases, less useful energy is converted by the system.

5.1.4 Effect of Changing Draw Profile to a Morning Centric Profile (Scenario M)

The effect of changing the hot water draw profile to a Morning Centric profile (Scenario M) is presented in this section. The base system was simulated using the morning centric profile,

which has the same annual load as the base profile, but a greater proportion of load in the morning[10]. The results of Scenario M are shown in Figure 32.

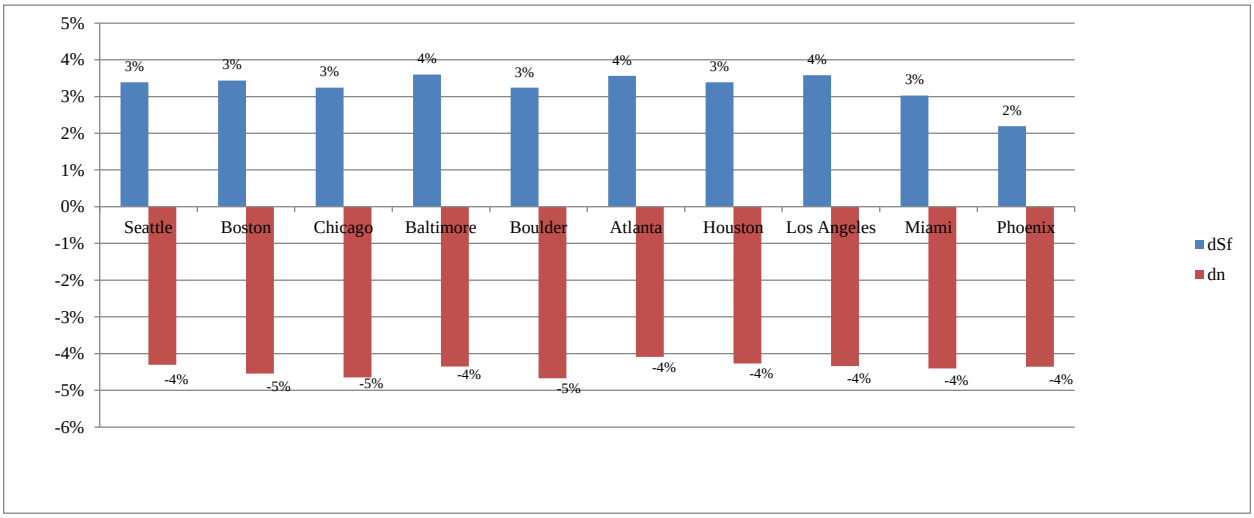

Figure 32 Effect of Changing Draw Profile to Morning Centric Profile (Scenario M)

Changing draw profile to a morning centric profile has the following effects on annual *n* and *Sf*:

- *Sf* increases slightly for all locations, by approximately 4 %, except for Phoenix where the percentage decrease is 2%.
- *n* decreases for all locations by an average of 2 %.

These trends can be explained by studying hourly data for a typical winter day. Presented in Figure 33 is a comparison of the working of the glycol system with a base and Scenario M. This figure presents the working on a typical winter day (December 15) in Boulder, CO.

[10] Details of the Morning Centric profile are provided in Section 4.3

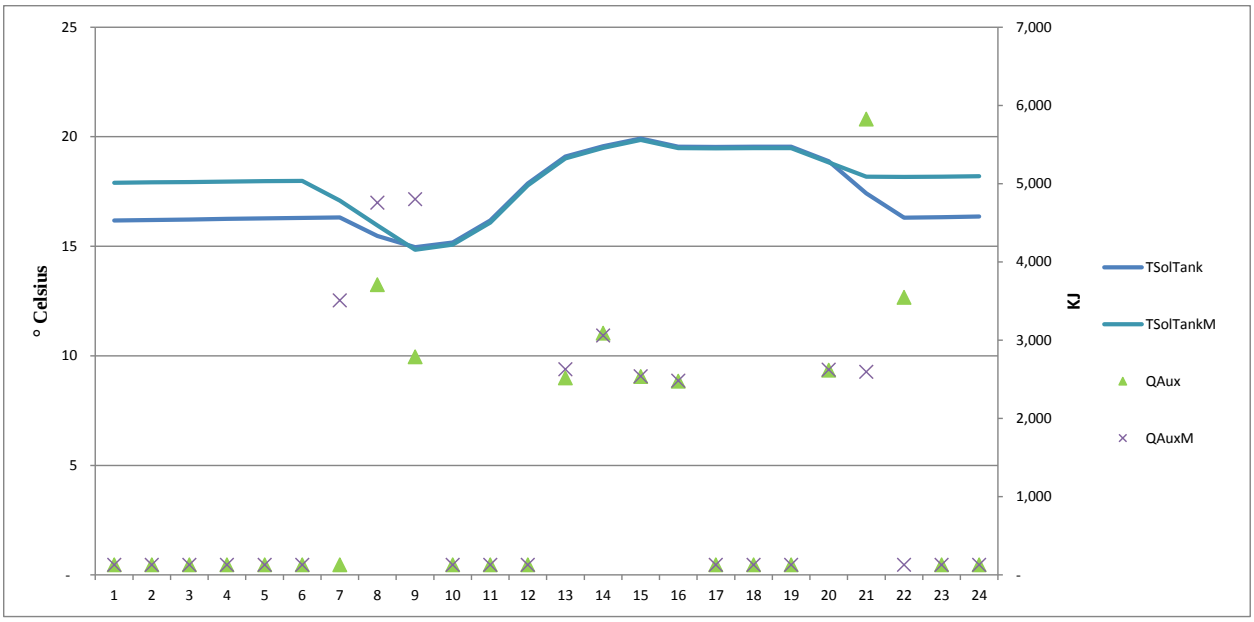

*Daily System Performance, Scenario 2x: *Sf* = 18%, *n* = 30%; Base Scenario *Sf* = 23%, *n* = 26%

Figure 33 Comparison between Performance of Glycol System with Base and Morning Profile (Scenario M)

$T_{SolTank}$ is higher for Scenario M, average of 18 ^{O}C compared to 17.3 ^{O}C, for December 15. Due to the additional morning loads, Q_{Aux} is higher in the morning for Scenario M. $T_{SolTank}$ is the same for both Scenarios between 9 AM and 9 PM; as Scenario M has lower evening load, the system has to spend less Q_{Aux} in the evening and it has a higher $T_{SolTank}$ after 9 PM. This higher $T_{SolTank}$ gets stored through the next morning and helps offset the additional morning load. The increase in Q_{Aux} in the morning is not enough to offset the decrease in evening load. Hence the system has a lower *Sf* in Scenario M.

5.1.5 Effect of Changing Draw Profile to an Evening Profile (Scenario E)

The Evening[11] profile has the same annual load, but more morning load than the Base profile and less morning load than the Morning Centric profile, and more evening load than both Base and Morning Profiles. The results of this Scenario Y are presented in Figure 34.

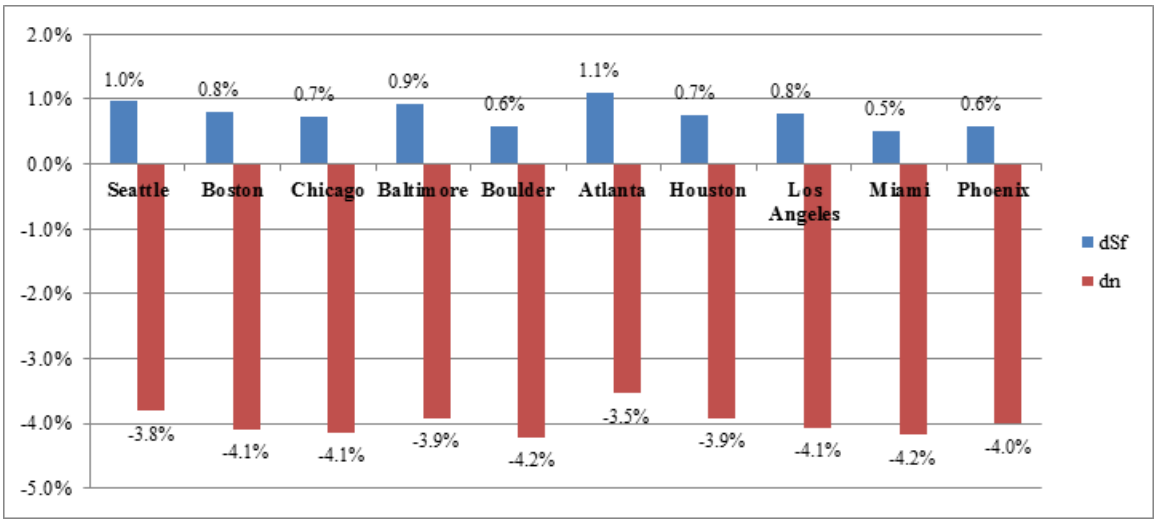

Figure 34 Effect of Changing Draw Profile to a Evening Profile, Scenario E

Scenario E has the following effects on annual *n* and *Sf*:

- *Sf* increases slightly for all locations, by approximately 0.5 – 1 %.
- *n* decreases for all locations by an average of 4 %.

These trends can be explained by studying hourly data for a typical winter day. Presented in *Daily System Performance, Scenario 2x: *Sf* = 22%, *n* = 26%; Base Scenario *Sf* = 23%, *n* = 26%

[11] Details of the Evening profile are presented in Section 4.3

Figure 35 is a comparison of the working of the glycol system with the base Scenario and Scenario E. This figure presents the working on a typical winter day (December 15) in Boulder, CO.

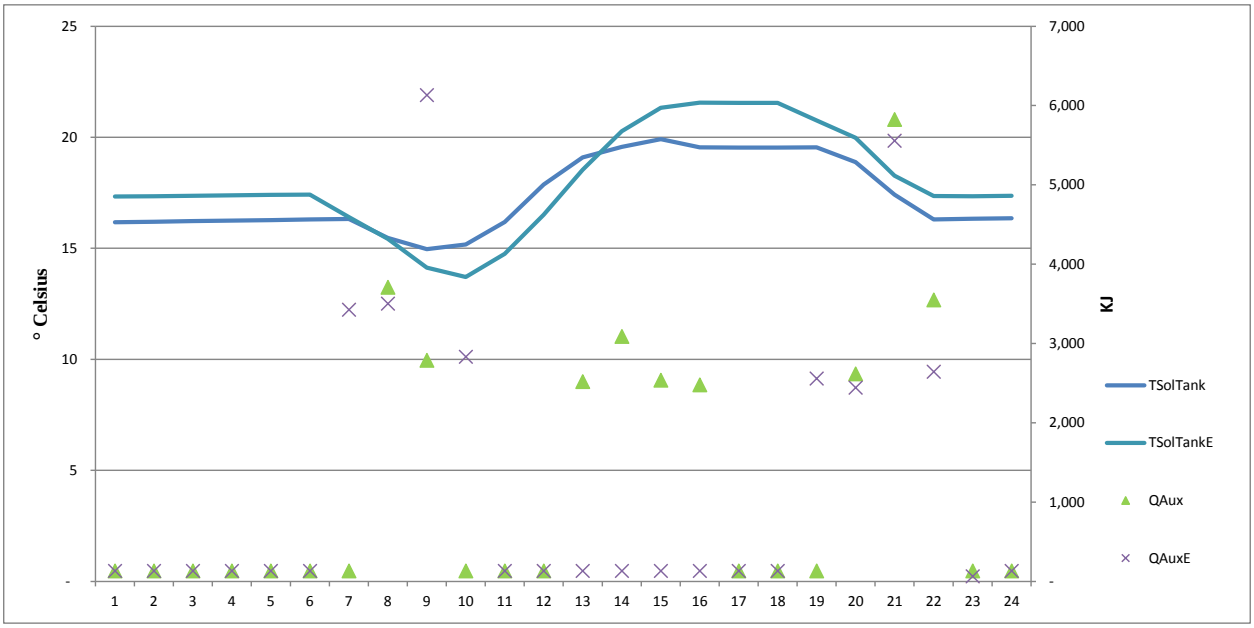

*Daily System Performance, Scenario 2x: *Sf* = 22%, *n* = 26%; Base Scenario *Sf* = 23%, *n* = 26%

Figure 35 Comparison between the Performance of a Glycol System with Nuclear and Evening Profile

The glycol system cannot meet the increased morning load with solar energy alone. The system uses approximately twice the auxiliary energy (Q_{Aux}) for the Scenario E in the morning (1 AM through 9 AM). This extra morning load also results in a larger draw from the solar storage tank; this causes the $T_{solTank}$ to decrease. This lower $T_{solTank}$ causes the system to become more efficient, by driving the system to collect more energy. By 1 P.M, $T_{solTank}$ for the Scenario E is greater than $T_{solTank}$ for the Base Scenario. Due to the decreased load for the afternoon in Scenario E, $T_{solTank}$ for Scenario E is higher than $T_{solTank}$ for the Base Scenario for the rest of the day. The average $T_{solTank}$ for this day is 18°C for the Scenario E and 17.3°C for the Base. The total Q_{AUX} is approximately 31,100 kJ for the Base and Scenario E. This increased $T_{SolTank}$ leads

to the system collecting less useful energy and being less efficient. The ability of the system to store energy to offset some of the increased loads leads to *Sf* staying almost constant.

5.1.6 Effect of Reducing Mains Temperature (Scenario T_M)

The glycol system was simulated using the nuclear profile; the mains temperature was decreased by 3 °C at all hours of the year (Scenario T_M). Scenario T_M has an increased annual load on the system. This increase in load is different than the increase in load due to Scenario 2x. This is as the total hot water draw is kept constant, but the amount of energy needed from the system is increased. The results of this scenario are presented in Figure 36.

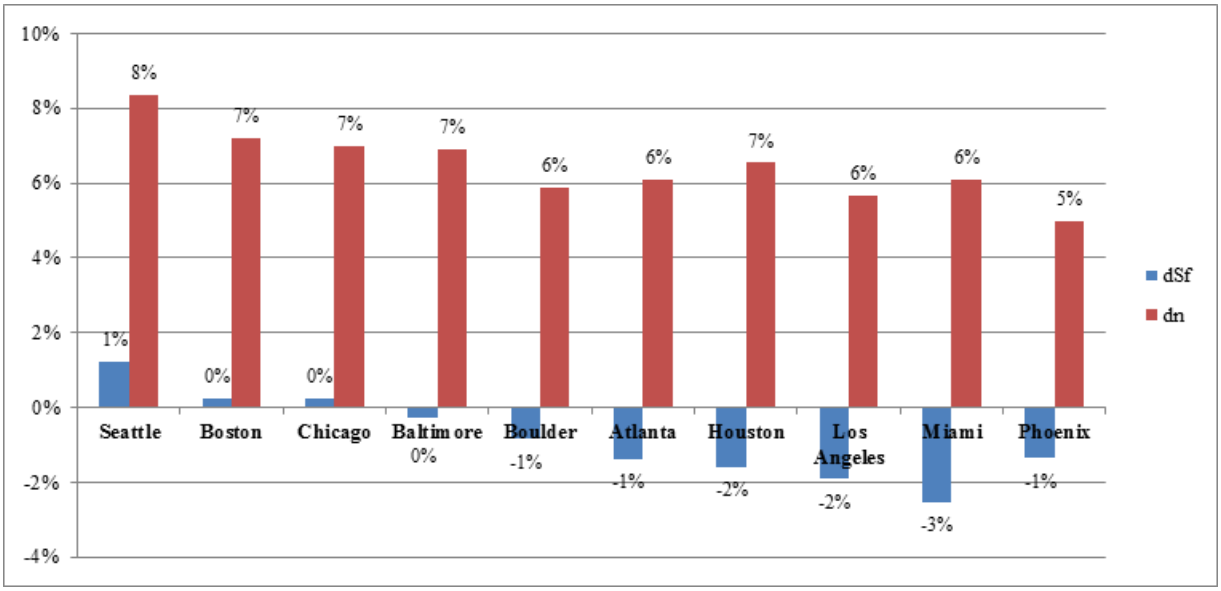

Figure 36 Effect of Reducing Mains Temperature (Scenario T_M)

We see the following changes in Scenario T_M:

- *n* (System Efficiency*)* increases for all locations by an average of 7 %.
- *Sf* (Solar Fraction) remains almost unchanged. The *Sf* is impacted most for Miami, it reduces by 3 %.

This trend can be explained by studying hourly data for a typical winter day (December,15th) in Boulder, CO, presented in

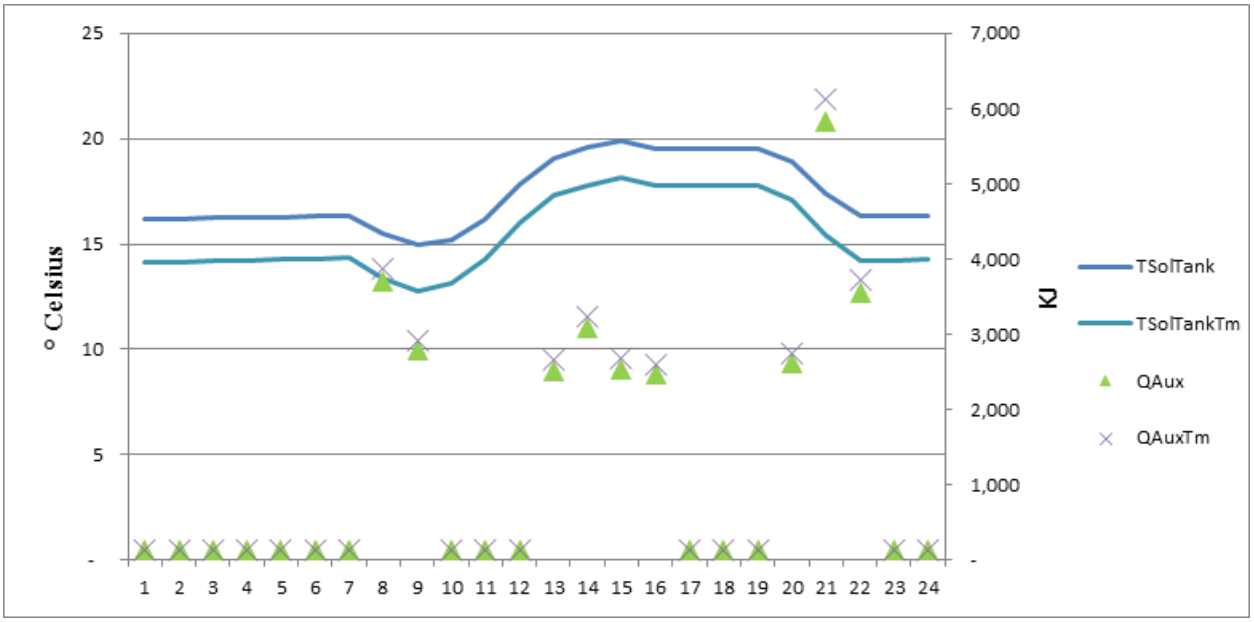

*Daily System Performance, Scenario 2x: *Sf* = 24%, *n* = 30%; Base Scenario *Sf* = 23%, *n* = 26%

Figure 37 Comparison between Glycol System with Nuclear Profile and Base Profile with Reduced Mains Temperature

The temperature of the solar tank is two degrees lower for Scenario T_M. The reduced $T_{SolTank}$ drives the system to collect more solar energy and hence become more efficient. Average $T_{SolTank}$ is 17.3 °C for the base case and 15.4° C for Scenario T_M. Even though, mains temperature was reduced by 3° C, the difference in $T_{SolTank}$ between the two scenarios is 1.9° C, this is due to the systems increased efficiency. Q_{Aux} is 5 % higher on this day for Scenario T_M. This increase in Q_{Aux} causes the *Sf* to stay relatively constant even though system efficiency is improved.

The trend for change in system performance due to Scenario T_M was analyzed for different set of annual total loads (Half load, base load and twice the load). Figure 38 and Figure 39 present the results of these simulations.

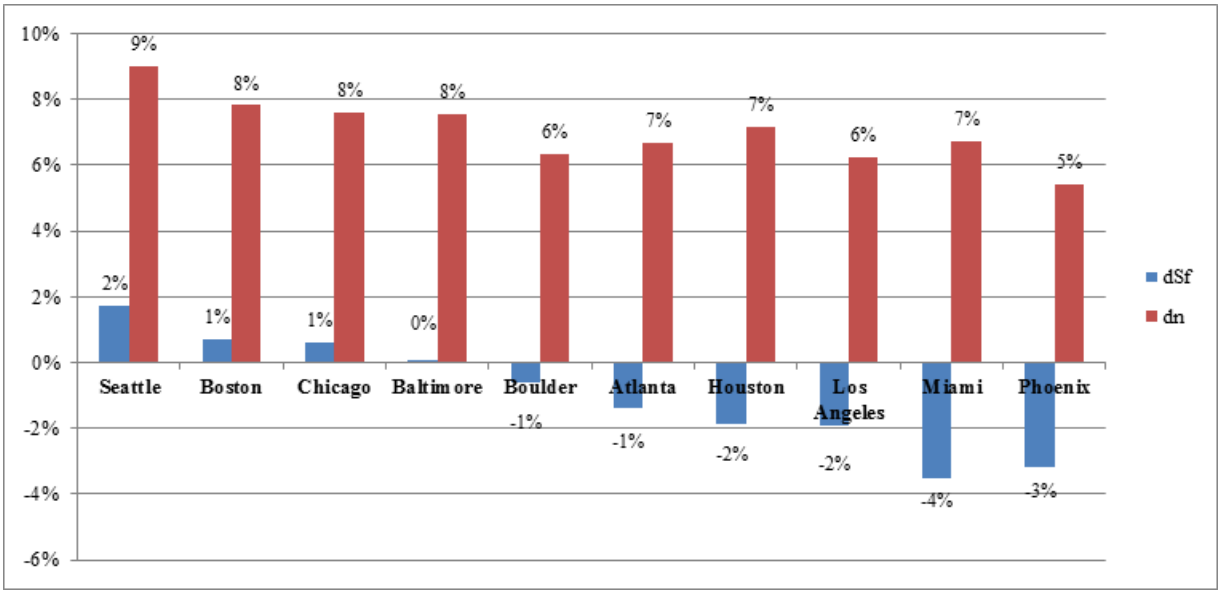

Figure 38 Effect of Reducing Mains Temperature when Glycol System is Simulated with Twice the Load, Scenario TM 2x

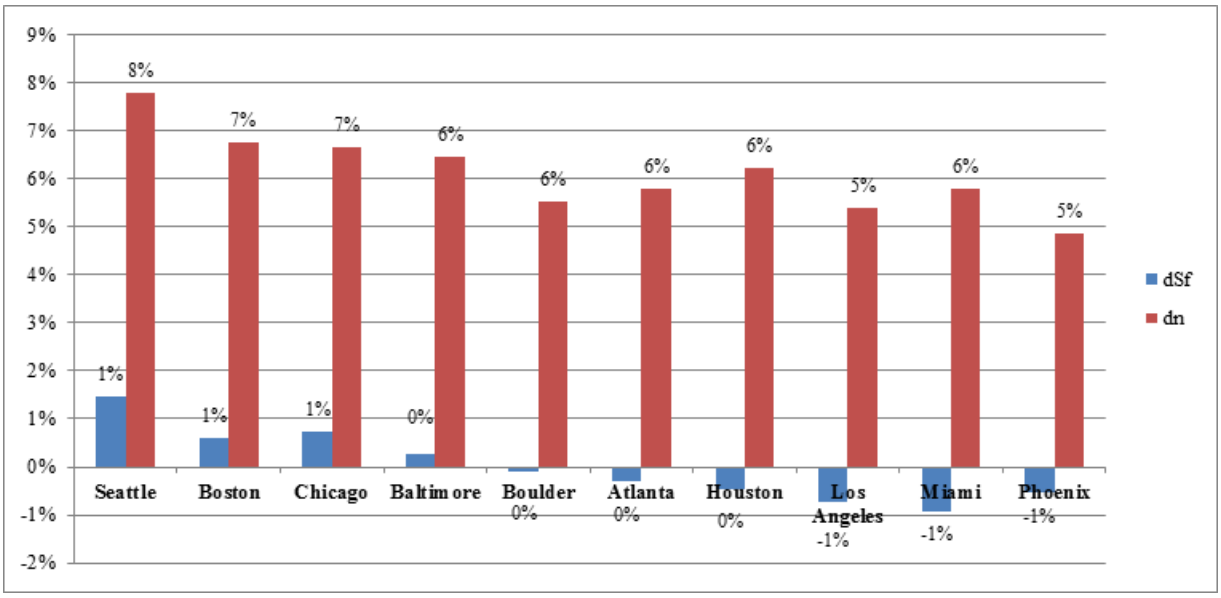

Figure 39 Effect of Reducing Mains Temperature when Glycol System is Simulated with Half the Load Scenario TM 0.5x

The change is system performance when mains temperature is reduced for different load levels is very similar to the change in performance from the base load case to Scenario T_M. In each case, *Sf* stays relatively constant, while *n* increases.

5.1.7 Effect of Day to Day Variation in Load (Scenario V)

The glycol system was simulated by varying the day to day hot water load on a Nuclear profile[12] (Scenario V). These results are presented in Figure 40.

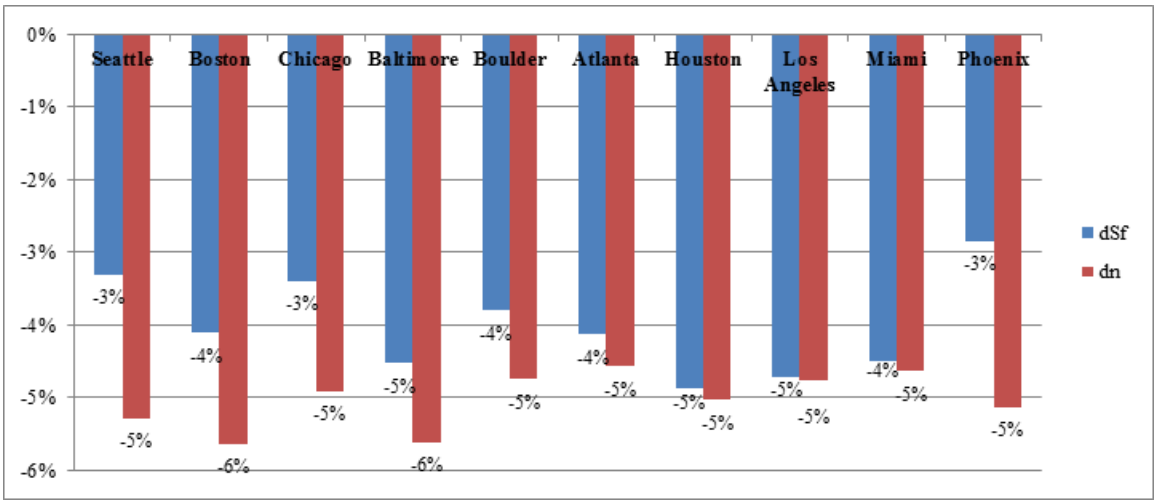

Figure 40 Effect of Introducing Day to Day Variations in Load on the Glycol System, Scenario V

We observe the following changes when we switch to Scenario V:

- *Sf* decreases for all locations by approximately 5 %
- *n* decreases for all locations by 3 to 5 %.

This decrease in *Sf* and *n* can be explained by understanding system performance under different levels of load. This is presented by the system efficiency curve, which plots system

[12] This is explained in detail in Section 4.3

efficiency as a function of load on the system. For a glazed flat plate collector, the system efficiency decrease is greater with a unit decrease in load than with a unit increase in load. This can be explained through Figure 41 which presents a comparison of change in *Sf* when the annual load is doubled and when annual load is halved.

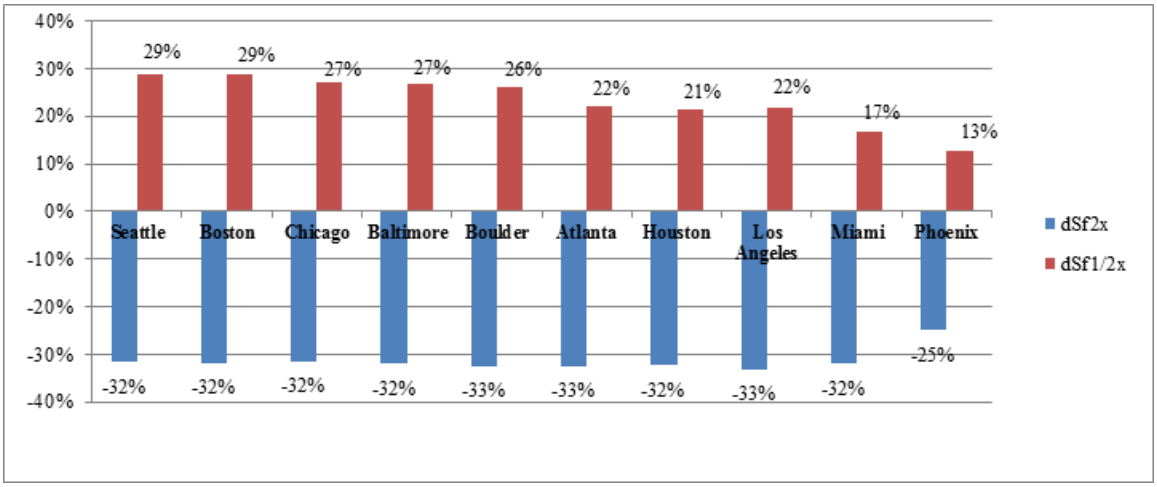

Figure 41 Comparison of Change in Sf between System Simulated with Twice and Half Load

A comparison of change in efficiency between the system running at twice and half the annual load is presented in Figure 41.

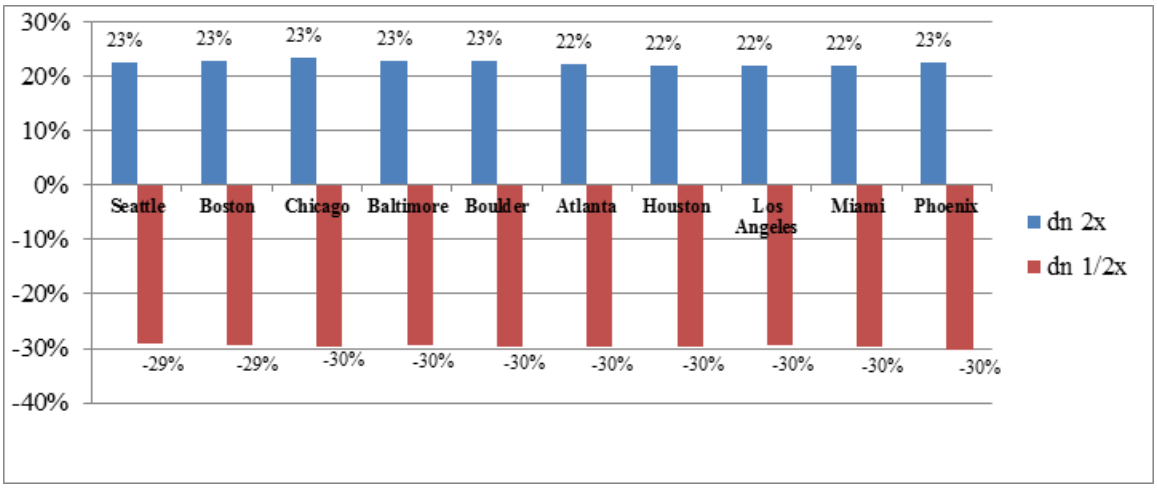

Figure 42 Comparison of Change in *n* between System Simulated with Twice and Half Load

Decrease in *n* is always greater when the system is running at half load than the increase in system efficiency when the system is running at twice the load. The increase in *Sf* when the load is halved is less than the decrease in *Sf* when the load is doubled.

In Scenario V, the system can be thought of running at a reduced load for half the year and an increased load for the other half. Hence the trend in *dSf* and *dn* are a combination of the trends we see at the two different load levels. This can be summarized as:

- Decrease in *dSf* is greater when the load is doubled than the increase when load is halved. Hence when variation in draw is introduced, we see an overall decrease in *Sf*
- Decrease in *n* is greater when the load is halved, than the increase in *n* when the load is doubled. Hence, we see an overall decrease in *n* when day to day variation is introduced.

5.1.8 Effect of Day to Day Variation in Load on Different Load Profiles

Scenario V was simulated with different draw profiles, Morning and Yuppie. The results of these Scenario are presented in Figure 43 and Figure 44.

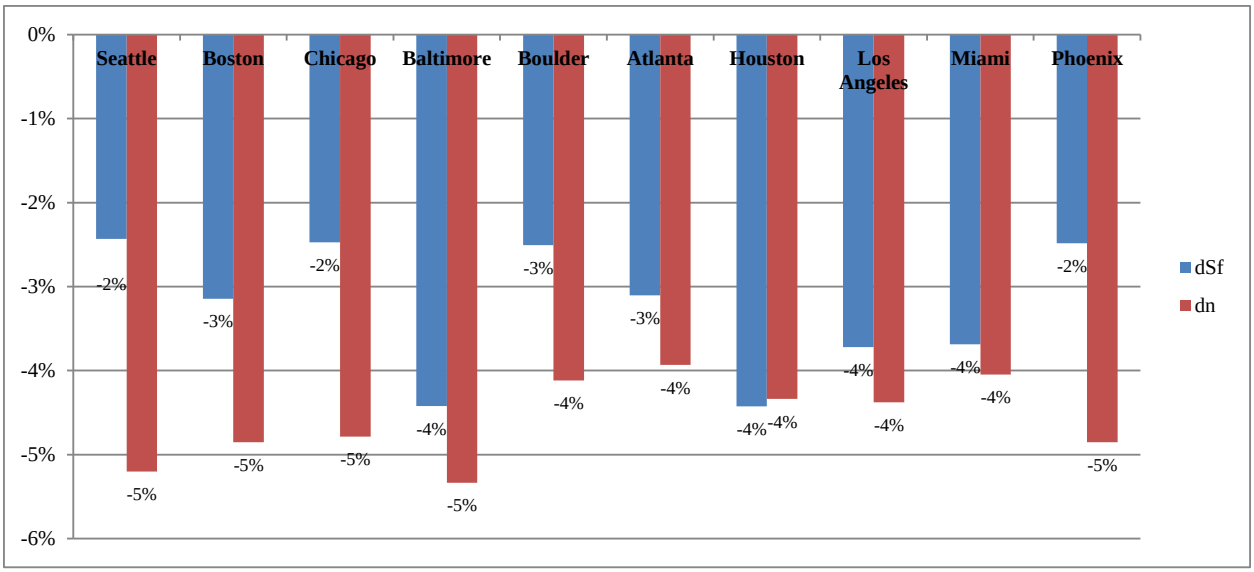

Figure 43 Simulating Scenario V with a Morning Profile

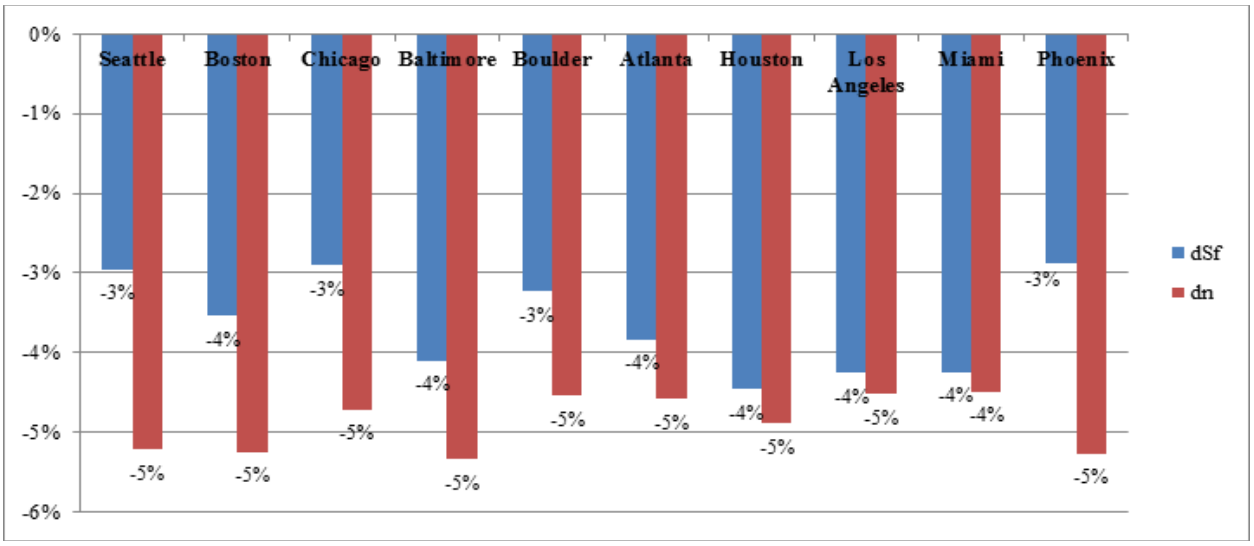

Figure 44 Simulating Scenario V with an Evening Profile

The change is system performance when Scenario V is simulated for different load profiles is very similar to the change in performance from the base load case to Scenario V. In each case, *Sf* and *n* decrease by 2 – 5%.

5.1.9 Effect of Using Extreme Profile (Scenario X)

The Extreme[13] profile has the same daily and annual load as the Nuclear profile, all of the load is concentrated in one morning hour (5 AM to 6 AM). The results of this Scenario X are presented in Figure 45.

[13] Details of the Extreme profile are presented in Section 4.3

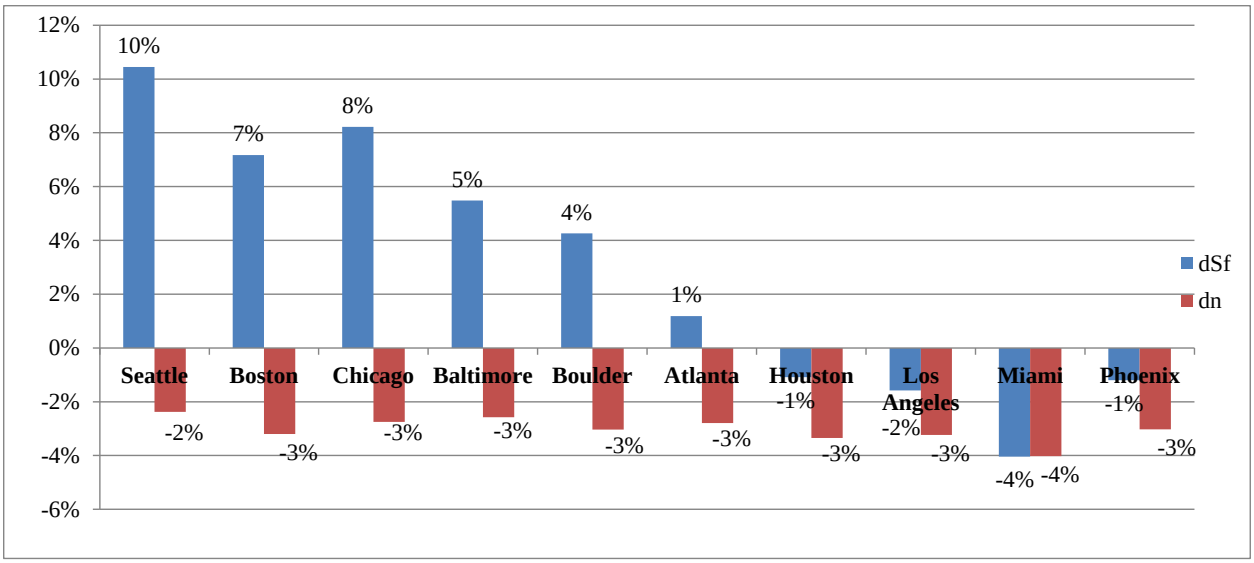

Figure 45 Effect of Changing Draw Profile to Extreme Profile (Scenario X)

Scenario X has the following effects on annual *n* and *Sf*:

- *Sf* increases for colder locations, maximum increase is 10% (Seattle). *Sf* shows a slight decrease for warmer locations, maximum decrease of 4% (Miami).
- *n* decreases for all locations by an average of 3 %.

The solar tank temperature shows an increase in all locations for Scenario X. This leads to a decrease in the ability of the system to gain useful solar energy, thus the system efficiency decreases for all locations.

The system consumes less auxiliary energy in Scenario X in colder climates than base scenario even though *n* decreases. The amount of time the heating elements[14] in the auxiliary

[14] There are two heating elements in the auxiliary tank; one at the top of the tank, one at the mid-point of the height of the tank. In the colder climates, each hot water draw leads to the

tank are on is greater for Base Scenario than Scenario X. Concentrating the daily hot water load in one hour reduces the total time the heating elements are required to be on in colder climates. Hence, less auxiliary heating energy is used and we see an increase in *Sf* even though *n* decreases as well.

In warmer climates, much fewer hot water draws in Base Scenario (none is summer) have auxiliary heating energy associated with them. Here, a decrease in *n* means a decrease in useful energy gain and a decrease in *Sf* due to increase in auxiliary energy required.

The Scenario X system working details for a winter day (December 15th) in Boulder, CO is presented in Figure 46 along with a comparison of the Base Scenario.

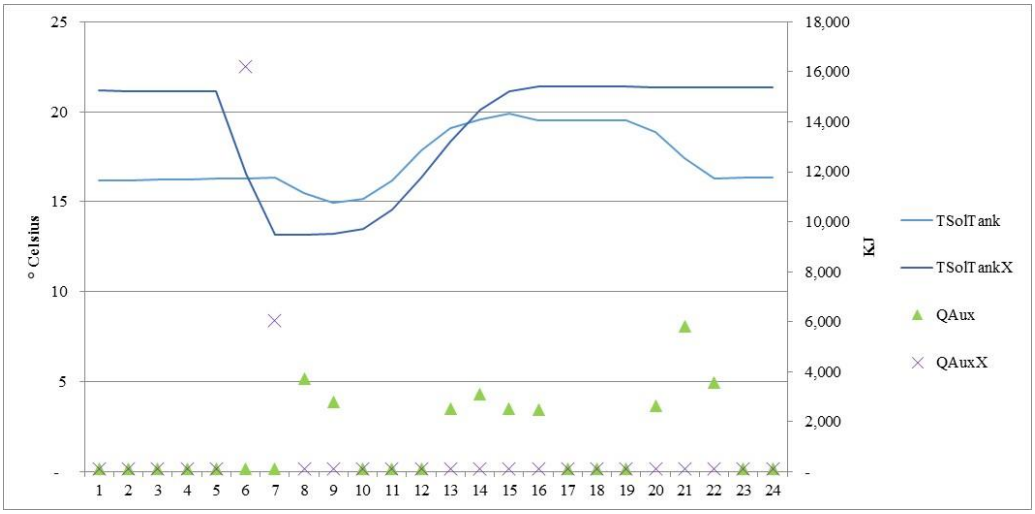

*Daily System Performance, Scenario X: *Sf* = 26%, *n* = 25%; Base Scenario *Sf* = 23%, *n* = 26%

Figure 46 Comparison between Glycol System with Nuclear Profile and Scenario X (Boulder, CO)

auxiliary heating element being turned on, it stays on until the temperature inside the auxiliary tank reaches the hot water set-point. Hence the system stays on even after the draw is completed.

$T_{SolTankX}$ is stable at around 21^{O}C except the hour of the hot water draw and around six hours following the extreme draw; useful energy is gained during these six hours until the system maxes out on the amount of useful energy it can gain during the day. All auxiliary energy is used during the hour of hot water draw. $Q_{Aux\ X}$ is 25 kJ, Q_{Aux} is 31 kJ through the course of the day even though the useful energy gained by the two systems is approximately the same. This is due to the fact that auxiliary energy use is optimized when all the required auxiliary energy is used at one time as opposed to the auxiliary heaters working at every hot water event during the course of the day which leads to auxiliary heaters being turned on at every instance of hot water draw.

The draw profile would affect glycol system performance significantly if the system (collector size and solar storage tank capacity) was not appropriately sized to meet the daily load.

5.1.10 Effect of Using Hourly Profile (Scenario H)

The Hourly[15] profile has the same daily and annual load as the Nuclear profile, but the draw duration are hourly instead of being in steps of five minutes. The results of this Scenario H are presented in Figure 47.

[15] Details of the Hourly profile are presented in Section 4.3

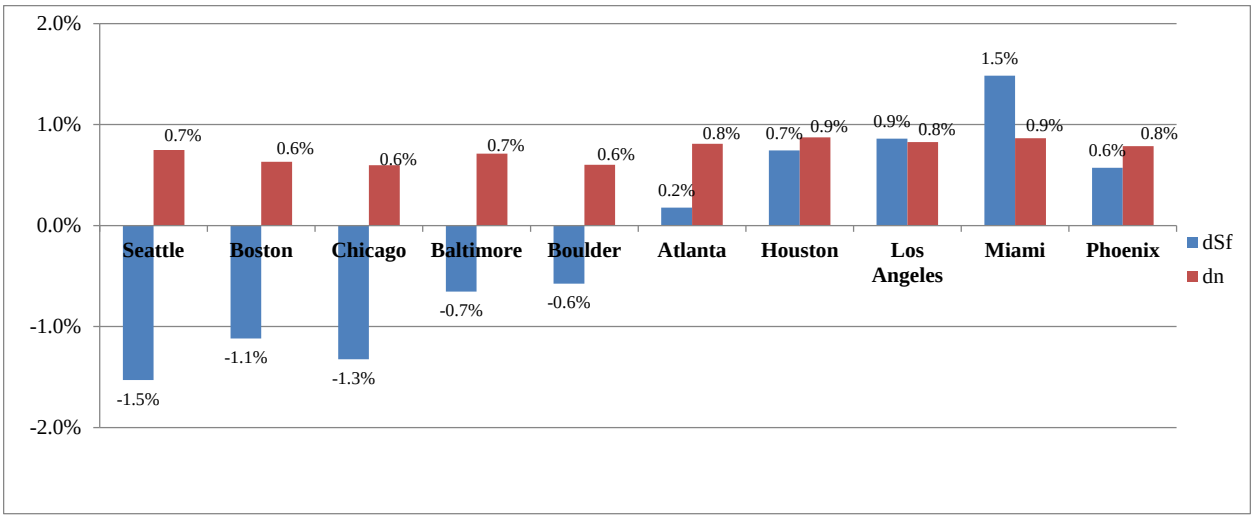

Figure 47 Effect of Changing Draw Profile to Hourly Profile (Scenario H)

The system performs almost identically when simulated with both draw profiles. This is due to a well sized storage tank present in glycol system. The hourly data for a typical winter day (December 15th) in Boulder, CO also shows almost no difference in system performance for the two profiles.

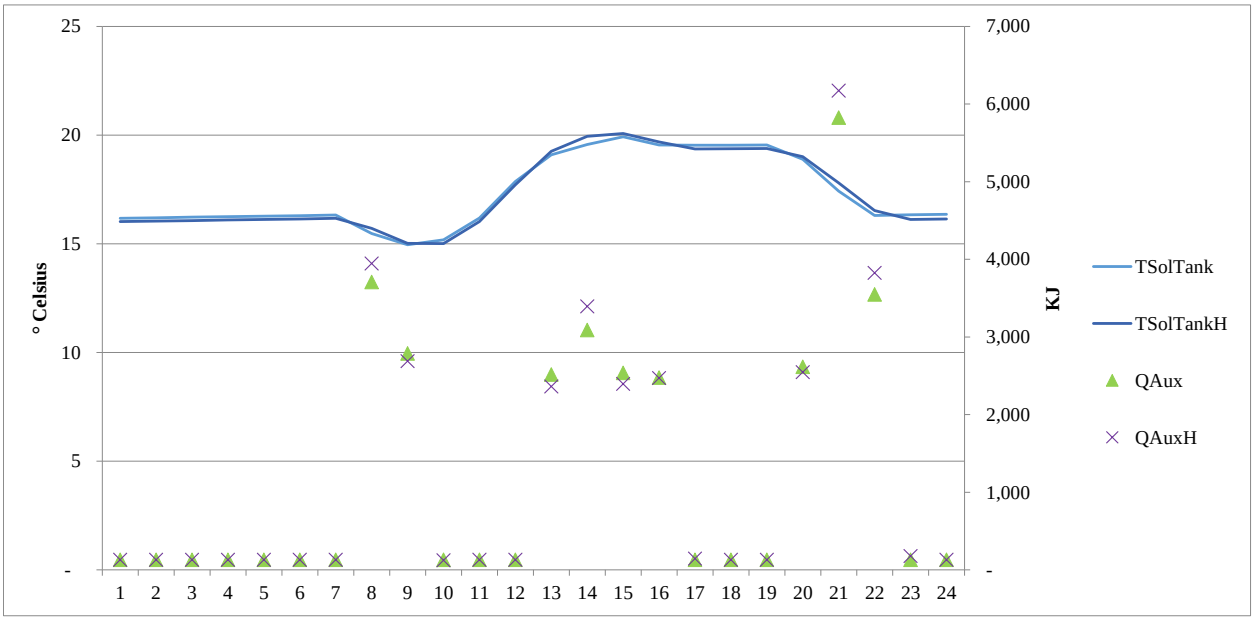

*Daily System Performance, Scenario 2x: *Sf* = 22%, *n* = 27%; Base Scenario *Sf* = 23%, *n* = 26%

Figure 48 Comparison between Glycol System with Nuclear Profile and Scenario H (Boulder, CO)

5.2 ICS System Results

In this section, results of all the simulations on the ICS system are presented and explained. Before explaining the effect of different load profiles on the ICS system, the working of the base ICS system with a nuclear family profile is explained. The base system is studied using five minute data for a typical summer and a typical winter day for Los Angeles, CA. Figure 49Figure 50 present the ambient temperature (T_{amb}), incident solar radiation ($Q_{Incident}$) on the collector and the hot water draw pattern (HWDraw) on these two days.

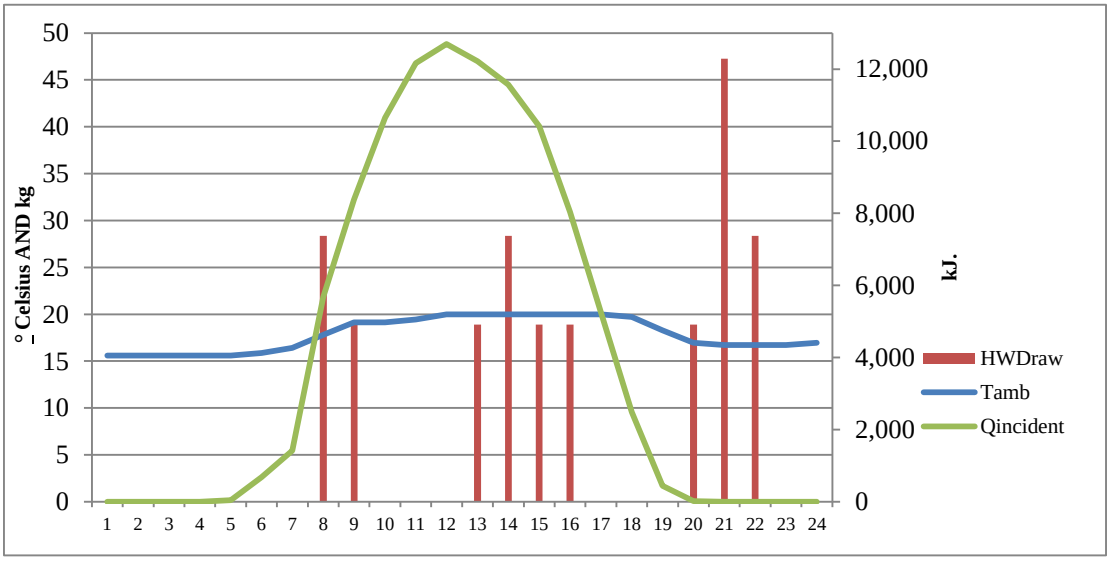

Figure 49 Typical Summer Day Weather, Los Angeles CA

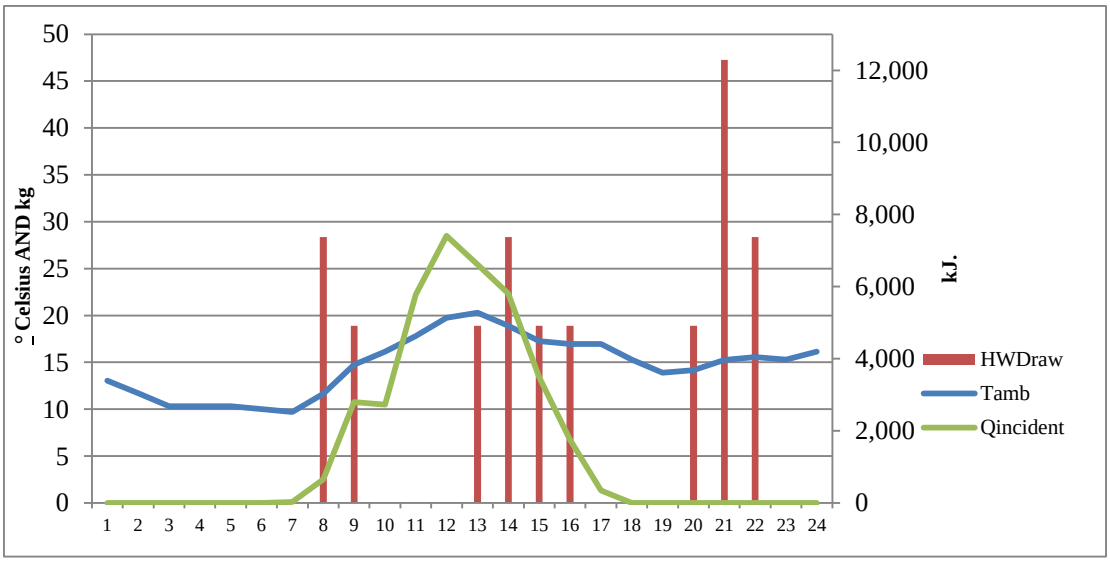

Figure 50 Typical Winter Day Weather, Los Angeles CA

On the summer day, incident solar radiation starts around 5 AM, peaks at noon and ends around 8 PM. Incident solar radiation starts before the first hot water draw of the day and exists for all except the last three hot water draws of the day. The ambient temperature peaks at 20^{O}C (4 PM) and has a minimum value of 15^{O}C (5 AM).

On the winter day, incident solar radiation doesn't start until 8 AM, peaks at noon and ends at around 6 PM. The peak value of the solar radiation (~8,000 J) is significantly less than the peak value at a typical summer day (> 12,000 J). Minimal incident solar radiation exists for all hot water draws before 9 AM and after 6 PM. The ambient temperature peaks around 20^{O}C and has a minimum value of approximately 10^{O}C.

The three parameters of the system studied during the course of a day are,

1. HW_{Draw}, this is the rate of hot water draw in gallons per minute.
2. Q_{Aux}, this is the amount of energy given to the system through the auxiliary heating tank, in KJ.

3. $T_{soltank}$, this is the average temperature of the solar tank. The solar tank temperature is an indicator of system performance. The solar tank temperature influences the efficiency of the solar collector and the amount of energy required by the auxiliary heating elements. The system collects energy only when the temperature of the bottom node of the solar tank is lower than the temperature of the fluid coming out of the collector. Also, a sufficiently high solar tank temperature ensures that fluid entering the auxiliary tank is at a high temperature, which in turn reduces use of auxiliary heating elements.

Shown below is hourly data for the aforementioned variables for a typical winter day (December, 15) and a typical summer day (June, 15). Both are weekdays.

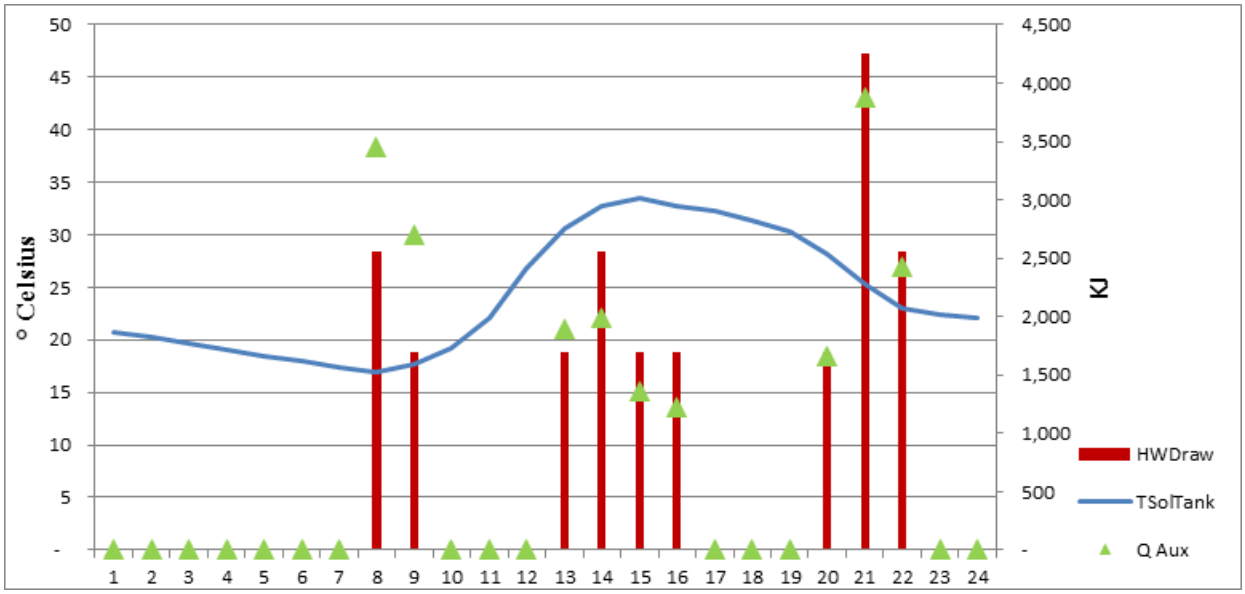

* Daily system performance: *Sf*= 33%, *n* = 27%

Figure 51 System Performance in a Typical Winter Day in Los Angeles

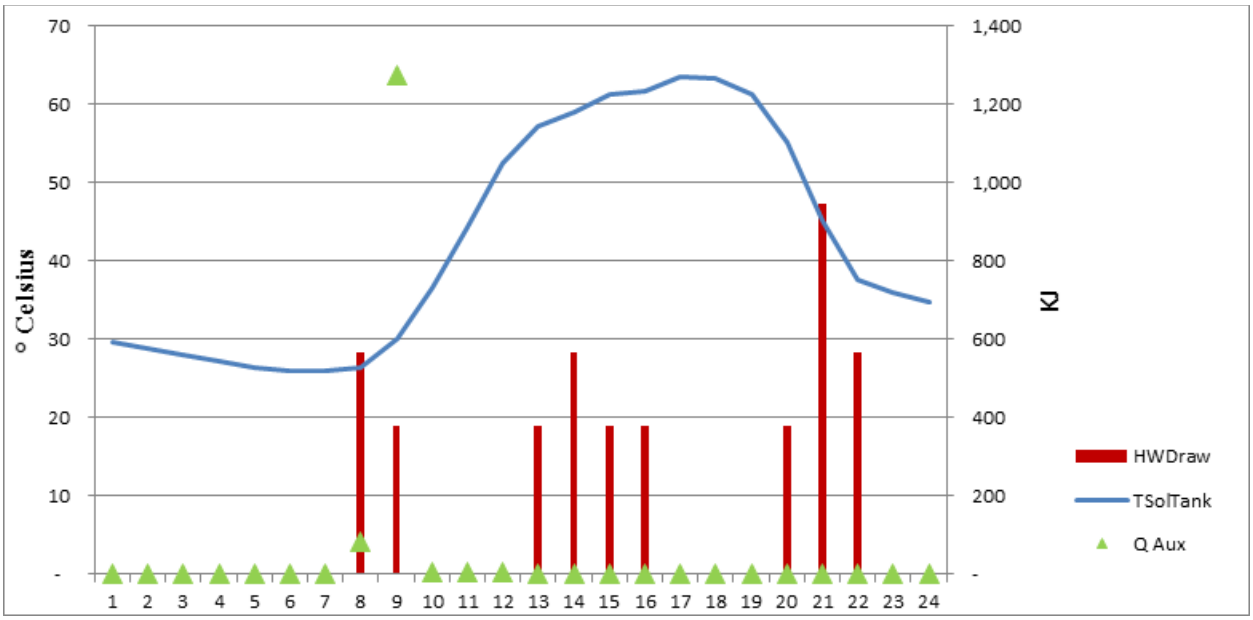

* Daily system performance: *Sf*= 96%, *n* = 35%

Figure 52 System Performance in a Typical Summer Day in Los Angeles

The average temperature of the solar tank ($T_{soltank}$) is much lower in the winter than summer due to higher solar radiation in the summer. The temperature ranges between approximately 17°C and 34°C in the winter, compared to the summer where it ranges between 26 and 63°C. Higher mains water temperatures (not shown in the chart) in the summer also mean reduced load on the system. Hence, Q_{Aux} is only needed to meet one instance of a morning load in the summer; the system provides enough energy to meet the hot water load.

In the winter, auxiliary heaters are required almost as soon as there is a draw. The amount of auxiliary heat required (Q_{Aux}) is correlated with HW_{Draw}; at times of high HW_{Draw}, Q_{Aux} is also higher.

The *Sf* (solar fraction) of the system is a function of the location and its climate; Phoenix and Miami have a high ambient temperature, and high incident radiation. They also have the highest *Sf*. The *Sf* and *n* (system efficiencies) for all five locations that were simulated are shown

in Figure 53. It should be noted that the cities have been arranged in order of increasing solar fraction. This presentation trend has been retained throughout this section.

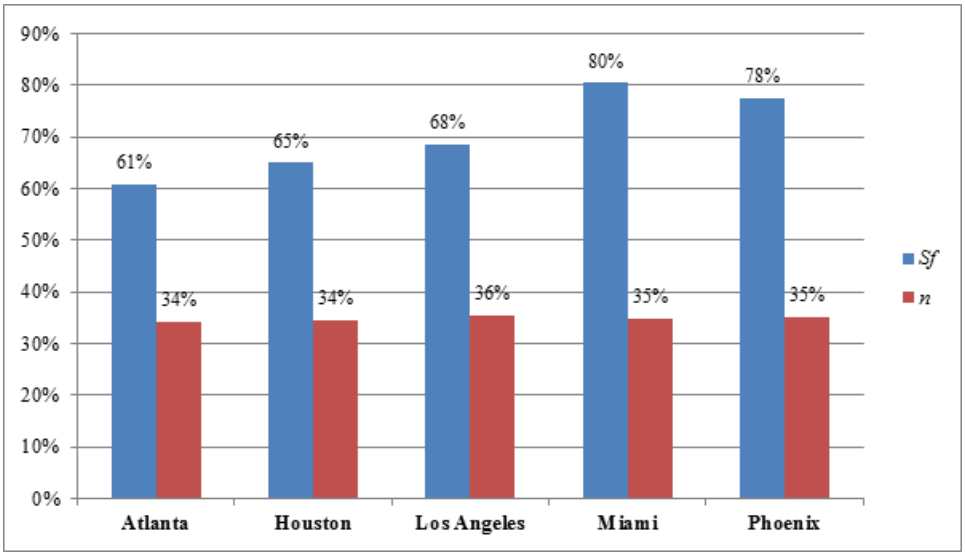

Figure 53 Solar Fraction and System Efficiencies For All Locations Simulated.

The system efficiencies do not change with location. This is as system efficiency is a function of the system and independent of the location a system is in as previous research indicates (Barker, 2007).

5.2.1 Effect of Increasing the Load by Doubling the Flow Rate (Scenario 2x)

The annual load on the system was doubled by increasing the flow-rate of each draw by a factor of two (Scenario 2x); and by increasing the time of each draw (Scenario 2x-1) by a factor of two. Both of these cases were examined separately to understand the difference in system performance in both of these scenarios. Figure 54 presents how solar fraction and system efficiency change in Scenario 2x.

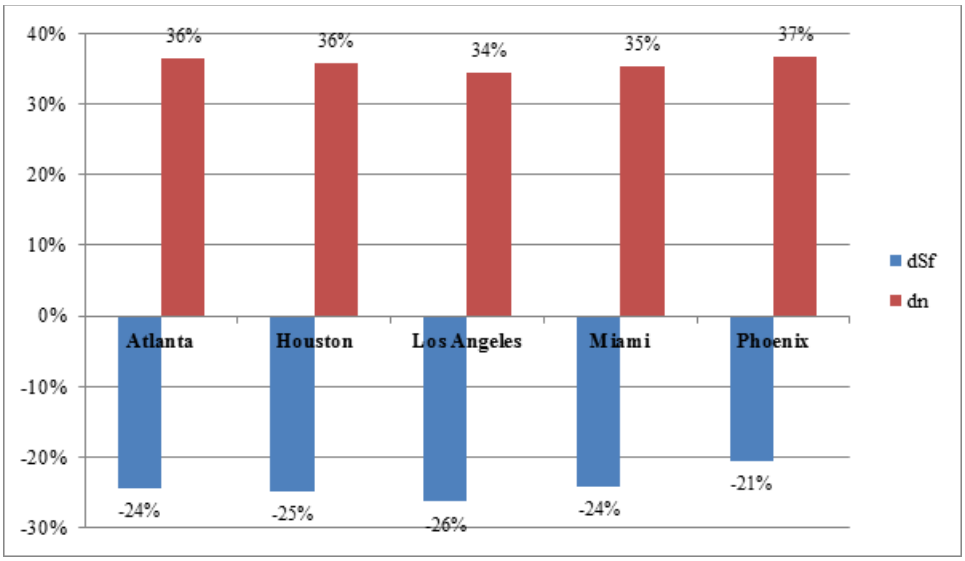

Figure 54 Change in System Performance Under Scenario 2x.

We see in the chart above, that -

- *n* increases by of 34 - 37 % in all cases.
- *Sf* decreases by an average of 25 % for all cases except Phoenix, which shows a decrease of 21 %. This is as Phoenix has much higher solar radiation than the other locations.

Figure 55 illustrates working of the ICS system with Base and Scenario 2x for a winter day (December, 15) in Los Angeles, CA. As the load on the system increases, $T_{SolTank}$ decreases. This is as twice the rated HW_{Draw} is drawn from the solar tank at each draw. This decrease in $T_{SolTank}$ leads the system to convert more of the incident solar radiation into useful energy. The increase in useful energy is not enough to offset the increase in system load; the auxiliary heating elements are required to produce more Q_{Aux}. Hence, we see an increase in *n* and a decrease in *Sf* for all locations.

Note, between 8 A.M and noon, $T_{SolTank}$ in both cases is identical after the morning loads, which likely use up all useful energy gathered until then. During this four hour period, the two systems collect the same amount of useful energy.

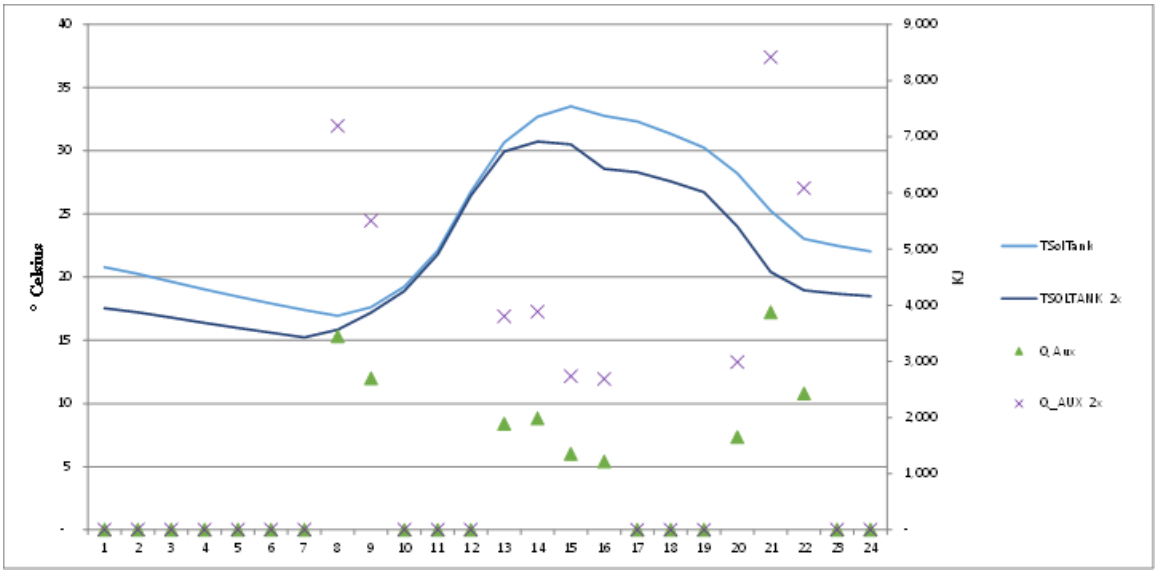

*Daily System Performance, Scenario 2x: *Sf* = 24%, *n* = 38%; Base Scenario *Sf* = 33%, *n* = 27%

Figure 55 Comparison between Performance of ICS System with Base and Scenario 2x

5.2.2 Effect of Reducing Load by Halving Annual Hot Water Draw (Scenario 0.5x)

To study the effect of decreasing the annual load on the system, the flow rate of each draw was decreased by a factor of two (Scenario 0.5x). In this scenario, solar fraction increases slightly while system efficiency decreases by a much greater amount. Figure 56 presents the results for this scenario.

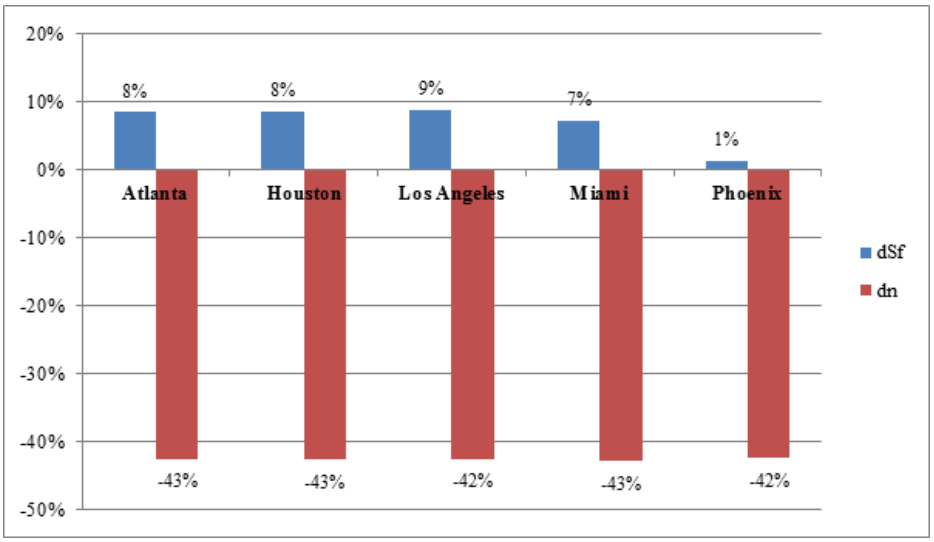

Figure 56 Effect of Halving Draw Flow Rate on ICS System (Scenario 0.5x)

On reducing annual load by a factor of two, we notice that:

- *n* decreases by approximately 42% of all locations.
- *Sf* increases for all slightly locations; this percentage increase in solar fraction is greatest (8%) for location with lowest base *Sf* (Atlanta). Location with high base *Sf* shows least percentage increase in *Sf* (Phoenix) (1%).

The useful energy produced by the ICS system is directly correlated to the draw. The system works less and produces less useful energy when the annual hot water draw is reduced. Hence on reducing the total annual draw, the system becomes less efficient (by about 43%); and has a similar (but slightly higher) annual *Sf* as base case.

*Daily System Performance, Scenario 2x: *Sf* = 35%, *n* = 15%; Base Scenario *Sf* = 33%, *n* = 27%

Figure 57 illustrates working of the ICS system for Base and Scenario 0.5x for a winter day (December, 15) in Los Angeles, CA.

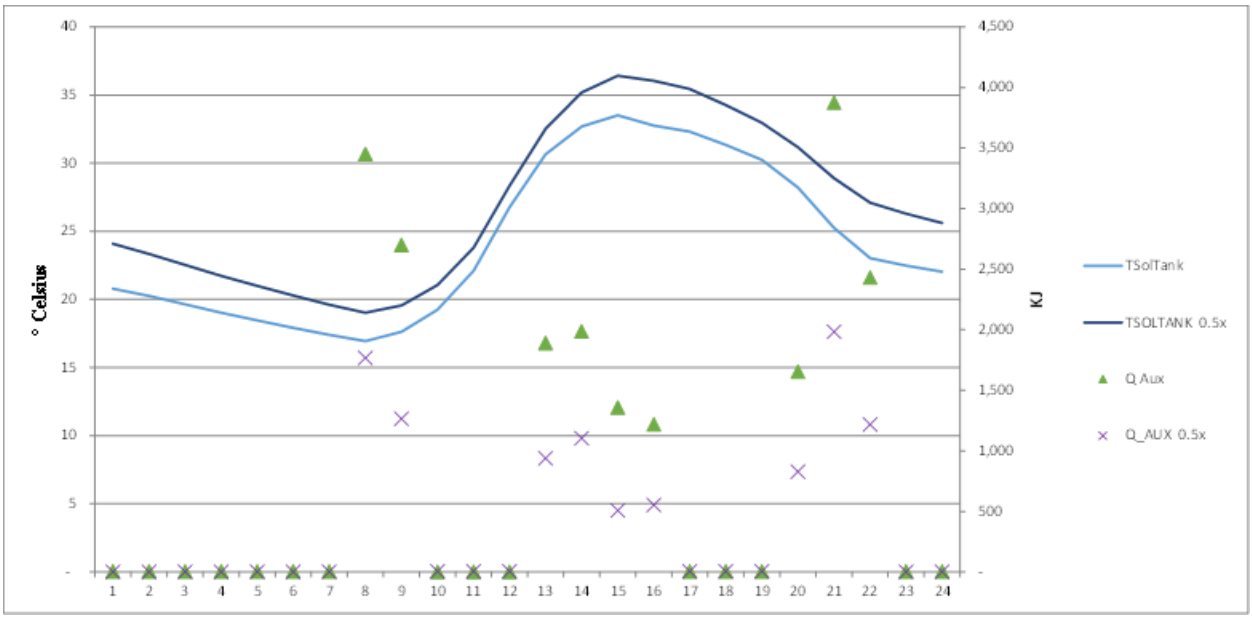

*Daily System Performance, Scenario 2x: *Sf* = 35%, *n* = 15%; Base Scenario *Sf* = 33%, *n* = 27%

Figure 57 Comparison between Performance of ICS System with Base and Half the Load

As the load on the system decreases, the average temperature of the solar tank increases, but by only 2.5 ^{O}C; even though half the rated hot water is drawn from the solar tank at each draw. This increase in solar tank leads the system to convert less of the incident solar radiation into useful energy and hence the amount of energy stored in the solar storage tank is less for Scenario 0.5x. As the system is working to meet half of its rated load, it has a slightly higher *Sf* than the base case, even though *n* decreases, less useful energy is converted by the system.

5.2.3 Effect of Changing Draw Profile to a Morning Centric Profile (Scenario M)

The effect of changing the hot water draw profile to a Morning Centric profile (Scenario M) is presented in this section. The base system was simulated using the morning centric profile,

which has the same annual load as the base profile, but a greater proportion of load in the morning[16].

Figure 58 presents the change in *n* and *Sf* for all simulated locations for Scenario M.

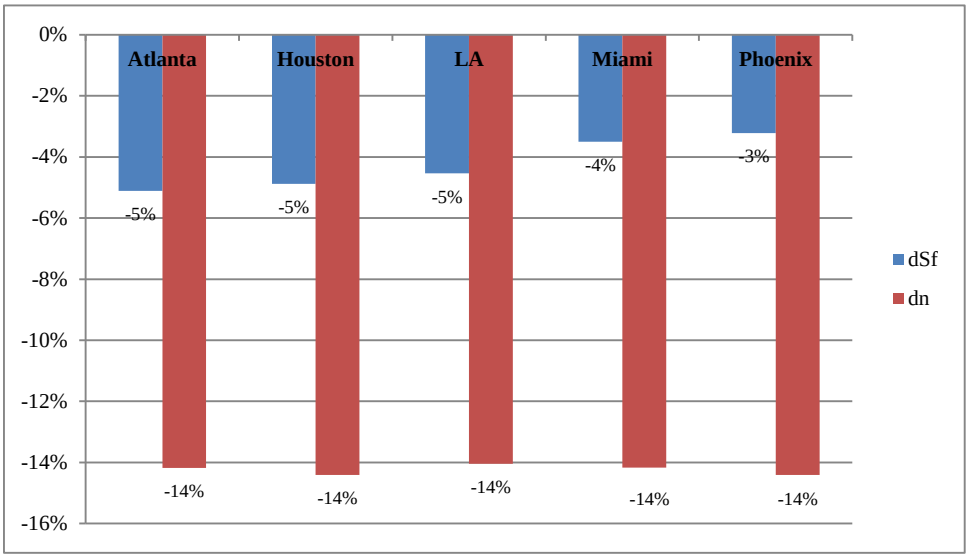

Figure 58 Effect of Changing the Draw Profile to Morning Centric Profile (Scenario M)

Scenario M has the following effects on annual *n* and *Sf*:

- *Sf* decreases for all locations, by approximately 3 – 5 %.
- *n* decreases for all locations by an average of 14 %.

These trends can be explained by studying hourly data for a typical winter day. Presented in *Daily System Performance, Scenario 2x: *Sf* = 27%, *n* = 22%; Base Scenario *Sf* = 33%, *n* = 27%

Figure 59 is a comparison of the working of the ICS system with a base and Scenario M. This figure presents the working on a typical winter day (December 15) in Los Angeles, CA.

[16] Details of the Morning Centric profile are provided in Section 4.3.

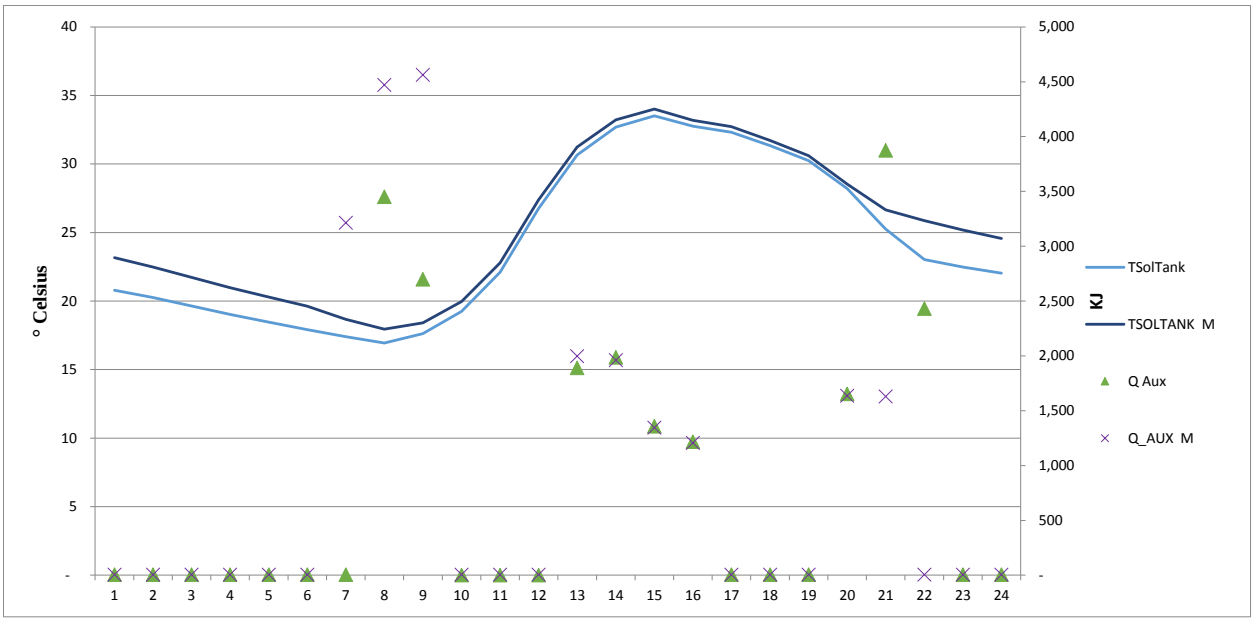

*Daily System Performance, Scenario 2x: *Sf* = 27%, *n* = 22%; Base Scenario *Sf* = 33%, *n* = 27%

Figure 59 Comparison between Performance of ICS System with Base and Scenario M

Due to the additional morning loads, Q_{Aux} is higher in the morning for Scenario M. $T_{SolTank}$ is similar for Scenario M and Base case starting at 9 AM through 7 PM. As Scenario M has fewer evening loads than the Base case, it does not show as much of a decrease in $T_{SolTank}$ as the base scenario. This additional energy stored in Scenario M is lost during the night. In Scenario M, the system cannot meet the additional morning loads, and the energy gained during the day is lost at night. Hence, there is a decrease in *Sf* and *n* in Scenario M as compared to base case. Note, $T_{SolTank}$ is higher for Scenario M (25.5^{O}C) than for base case (24.2^{O}C).

5.2.4 Effect of Changing Draw Profile to an Evening Profile (Scenario E)

The Evening[17] profile has the same annual load, but more evening load than the base profile and less morning load than the Morning Centric profile. The results of this Scenario Y are presented in Figure 60.

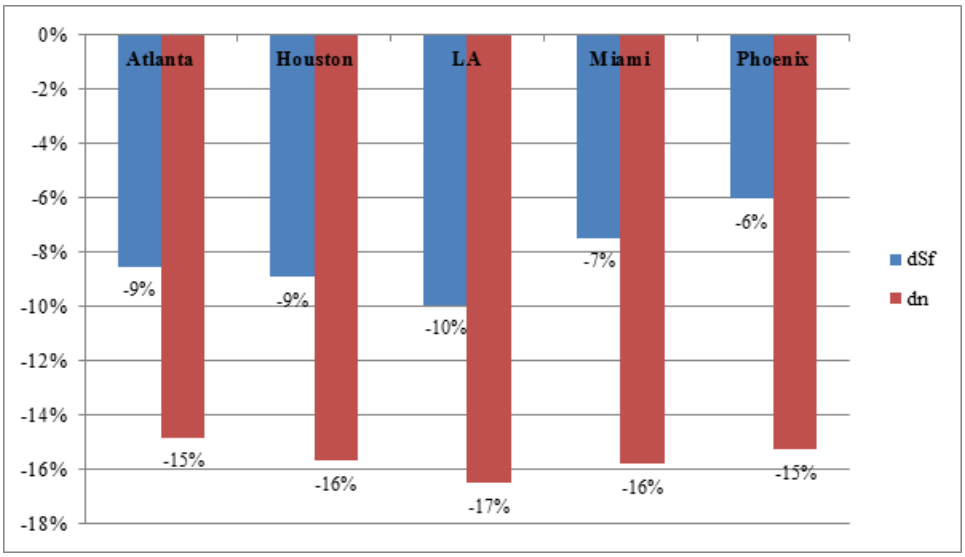

Figure 60 Effect of Changing Draw Profile to Evening Profile, Scenario E

Changing the draw profile to Scenario E has the following effect on the system:

- *Sf* decreases for all locations by 6 – 10 %
- *n* decreases for all locations by 15 – 17 %.

This trend can be explained by studying hourly data for a typical winter day (December, 15) for Los Angeles, CA, presented in Figure 61.

[17] Details of the Yuppie profile are presented in Section 4.3

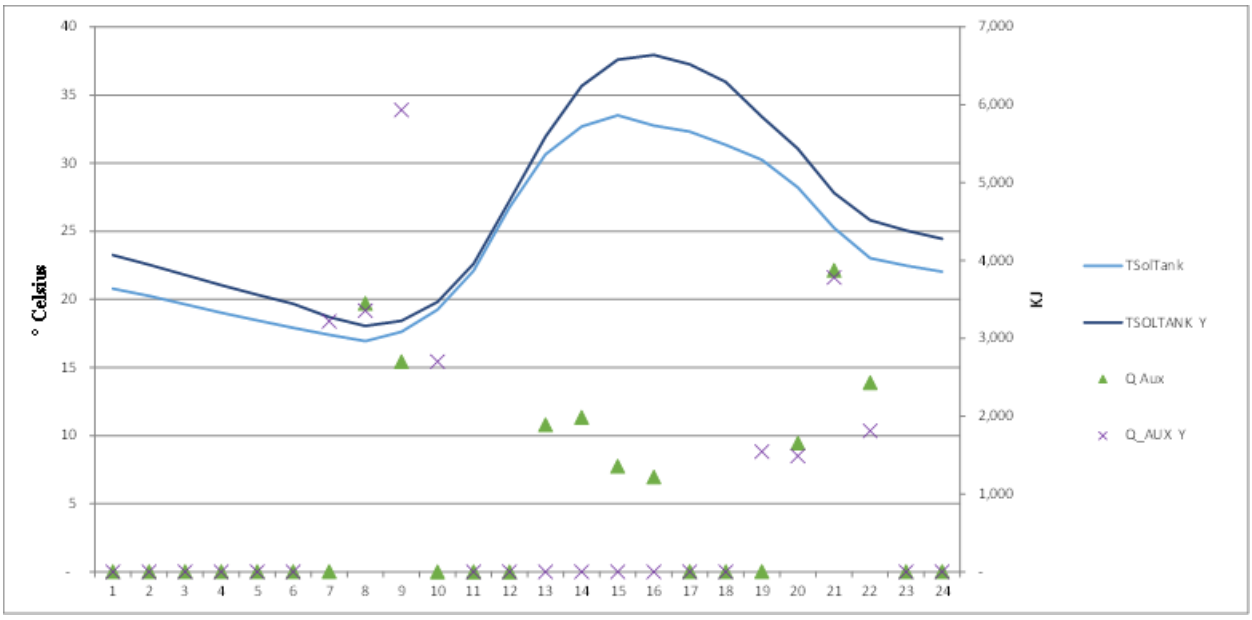

*Daily System Performance, Scenario 2x: *Sf* = 22%, *n* = 18%; Base Scenario *Sf* = 33%, *n* = 27%

Figure 61Comparison between the Performance of an ICS System with Base and Evening Profile

At the start of the day, $T_{solTank}$ is greater for Scenario E by approximately 2 ^{O} C. The ICS system cannot meet the increased morning load with solar energy alone. The system uses approximately twice the auxiliary energy (Q_{Aux}) for the Scenario E in the morning (1 AM through 9 AM). This extra morning load also results in a larger draw from the solar storage tank; this causes the $T_{solTank}$ to decrease to equal Base Scenario. $T_{solTank}$ is the same for both scenarios starting 11 A.M. As the Evening profile does not have the afternoon loads that the base profile does, by 1 P.M, $T_{solTank}$ for the Scenario E is greater than $T_{solTank}$ for the Base Scenario. Due to the decreased load for the afternoon in Scenario E, $T_{solTank}$ for Scenario E is higher than $T_{solTank}$ for the Base Scenario for the rest of the day. The average $T_{solTank}$ for this day is 25.6°C for the Scenario E and 24.2°C for the Base. This increased $T_{SolTank}$ helps the system better meet evening loads, this also causes the system to collect less useful energy and become less efficient. This excess energy stored in Scenario E, in the form of higher $T_{solTank}$, is lost overnight. The inability

of the system to meet increased morning loads, the decrease in system efficiency during day-time is why ICS system in Scenario E shows a decrease in *n* and *Sf*.

5.2.5 Effect of Reducing Mains Temperature (Scenario T_M)

The ICS system was simulated using the nuclear profile; the mains temperature was decreased by 3 °C at all hours of the year (Scenario T_M). Scenario T_M has an increased annual load on the system. This increase in load is different than the increase in load due to Scenario 2x. This is as the total hot water draw is kept constant, but the amount of energy needed from the system is increased. The results of this scenario are presented in Figure 62.

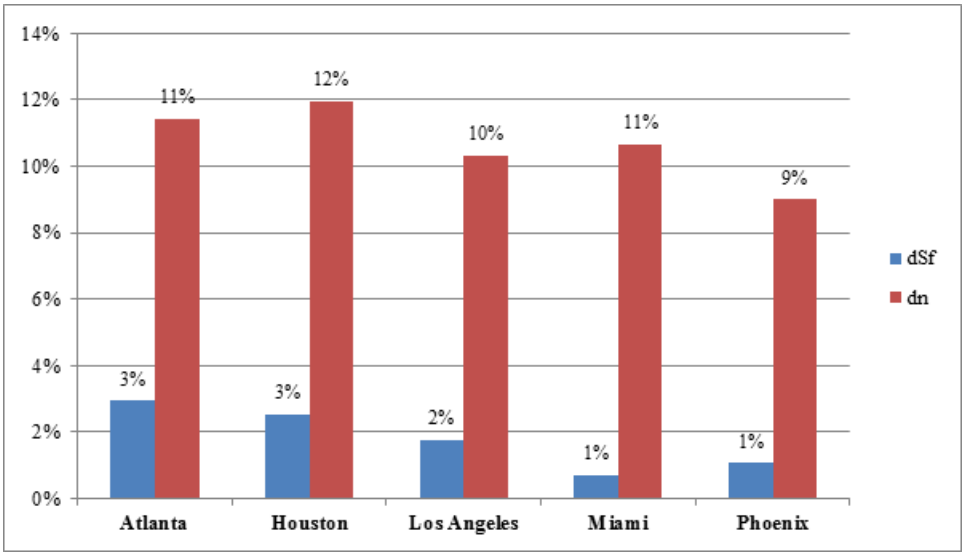

Figure 62 Effect of Reducing Mains Temperature, Scenario TM

We see the following changes in Scenario T_M:

- *n* (System Efficiency*)* increases for all locations by an average of 10 %.
- *Sf* (Solar Fraction) remains almost unchanged. The *Sf* is impacted most for Atlanta, it increases by 3 % (Houston shows an increase of 2.5%; rounded up to 3%).

This trend can be explained by studying hourly data for a typical winter day (December, 15th) in Los Angeles, CA, presented in Figure 63.

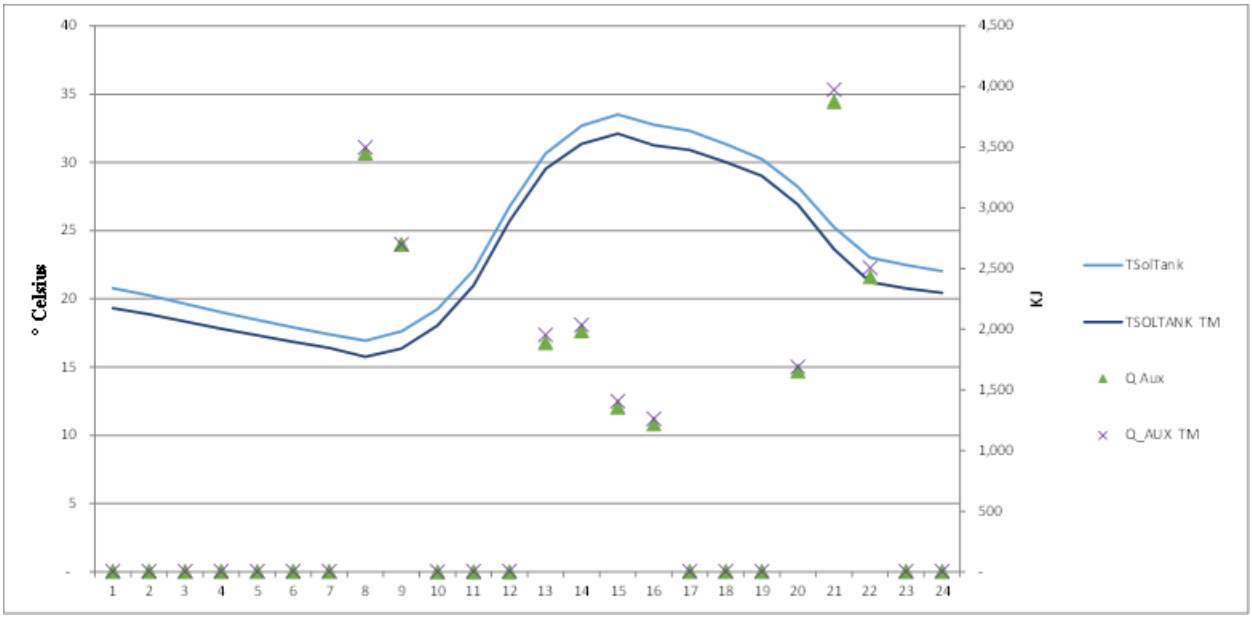

*Daily System Performance, Scenario 2x: *Sf* = 37%, *n* = 33%; Base Scenario *Sf* = 33%, *n* = 27%

Figure 63 Comparison between ICS System with Base Profile and Base Profile with Reduced Mains Temperature

The temperature of the solar tank is 1.3° C lower for Scenario T_M. The reduced $T_{SolTank}$ drives the system to collect more solar energy and hence become more efficient. Average $T_{SolTank}$ is 24.2 °C for the base case and 22.9° C for Scenario T_M. Even though, mains temperature was reduced by 3° C, the difference in $T_{SolTank}$ between the two scenarios is 1.3° C, this is due to the systems increased efficiency. Q_{Aux} is 2 % higher on this day for Scenario T_M. This increase in Q_{Aux} causes the *Sf* to show a 1 – 3 % increase even though system efficiency is improved.

The trend for change in system performance due to Scenario T_M was analyzed for different set of annual total loads (Half load, base load and twice the load). and present the results of these simulations.

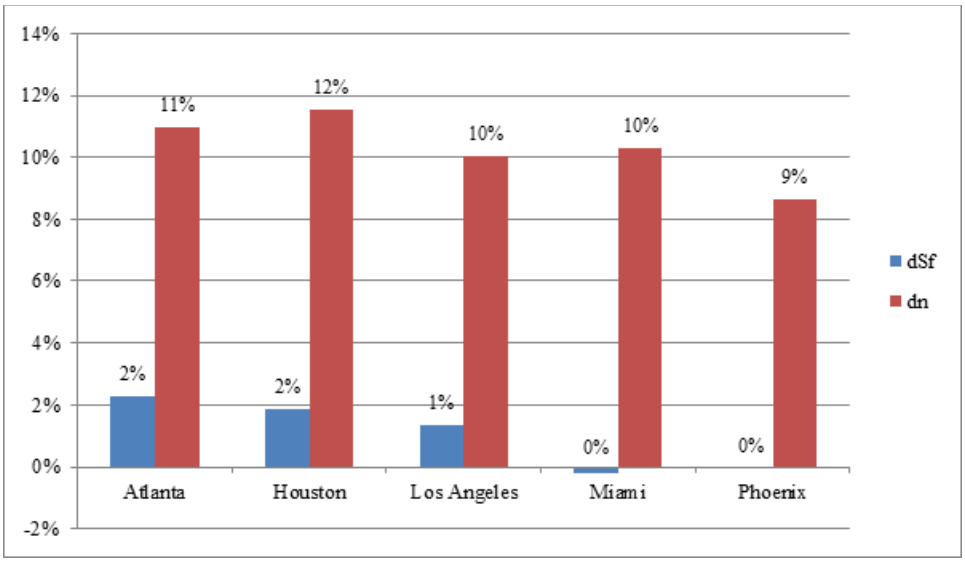

Figure 64 Effect of Reducing Mains Temperature when ICS System is Simulated with Twice the Load, Scenario TM 2x

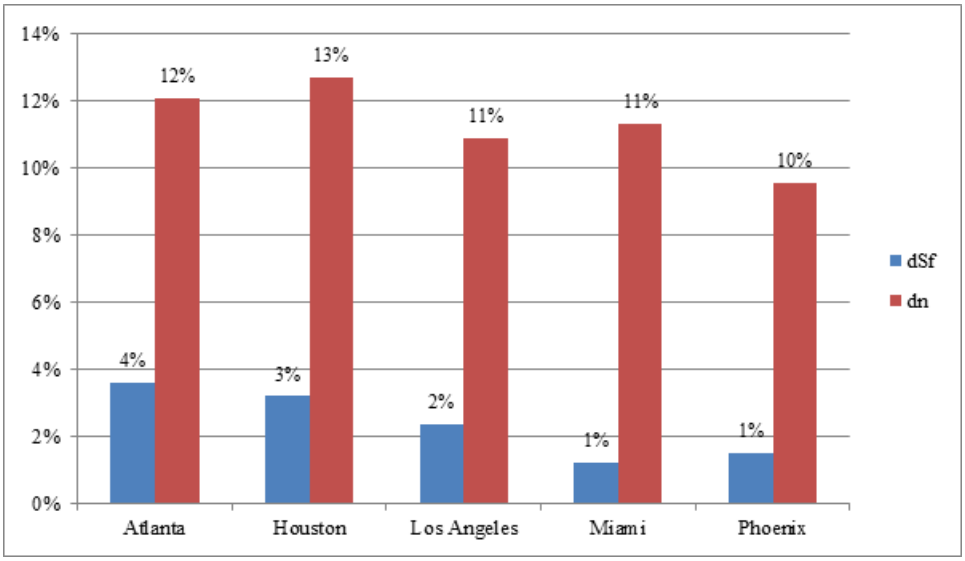

Figure 65 Effect of Reducing Mains Temperature when ICS System is Simulated with Half the Load Scenario TM 0.5x

The change in system performance when mains temperature is reduced for different load levels is very similar to the change in performance from the base load case to Scenario T_M. In each case, *Sf* stays relatively constant, while *n* increases. The increase in *Sf* is slightly higher for Scenario T_M 0.5x than Scenario T_M 2x.

5.2.6 Effect of Day to Day Variation in Load (Scenario V)

The ICS system was simulated by varying the day to day hot water load on the Base profile[18] (Scenario V). These results are presented in Figure 66.

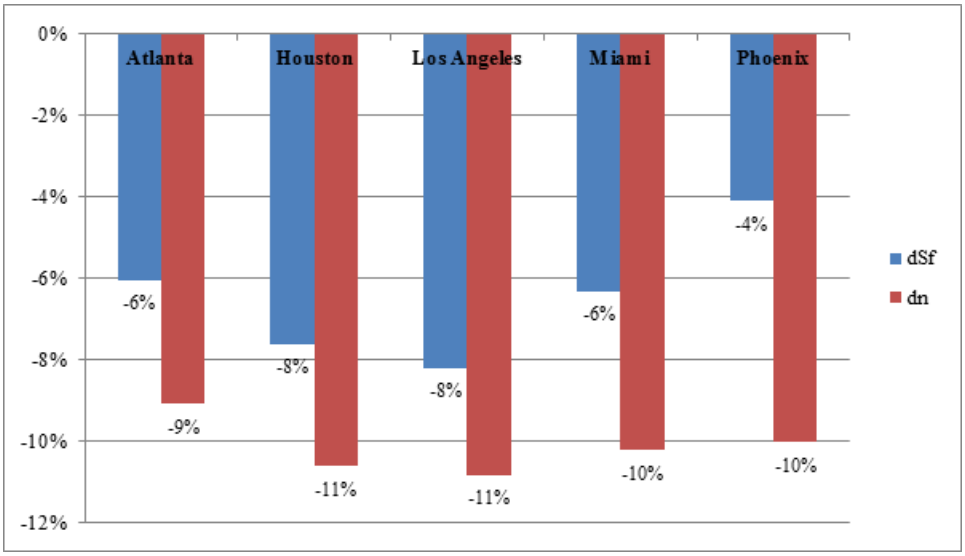

Figure 66 Effect of Introducing Day to Day Variations in Load on the ICS System, Scenario V

We observe the following changes when we switch to Scenario V:

- *Sf* decreases for all locations by approximately 4- 8 %
- *n* decreases for all locations by 9 - 11% on an average.

This decrease in *Sf* and *n* can be explained by understanding system performance under different levels of load. This is represented by the system efficiency curve, which plots system efficiency as a function of load on the system. For an ICS collector, solar fraction decreases by a much greater amount due to increase in load, than it increases for the same unit decrease in load.

[18] This is explained in detail in Section 4.4

As an example, presented in Figure 67 is a comparison of change in *Sf* when the annual load is doubled and when annual load is halved.

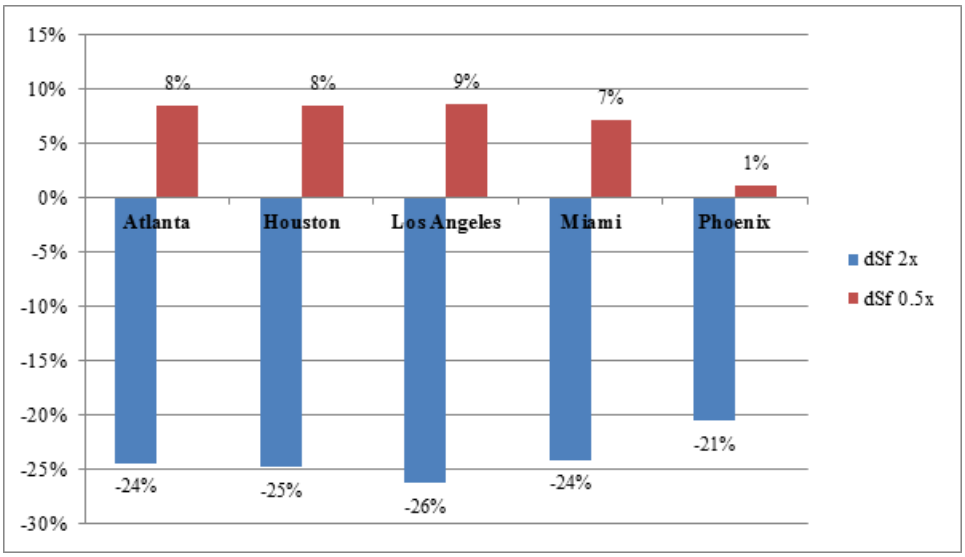

Figure 67 Comparison of Change in *Sf* between System Simulated with Twice and Half Load

A comparison of change in efficiency between the system running at twice and half the annual load is presented in Figure 68.

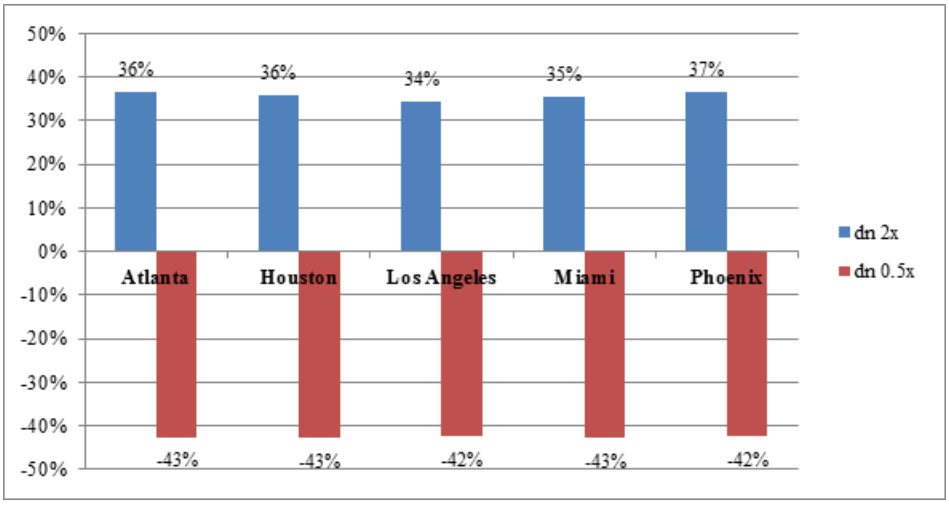

Figure 68 Comparison of Change in *n* between System Simulated with Twice and Half Load

Decrease in *n* is always greater when the system is running at half load than the increase in system efficiency when the system is running at twice the load. The increase in *Sf* when the load is halved is less than the decrease in *Sf* when the load is doubled.

In Scenario V, the system can be thought of running at a reduced load for half the year and an increased load for the other half. Hence the trend in *dSf* and *dn* are a combination of the trends we see at the two different load levels. This can be summarized as:

- Decrease in *dSf* is greater when the load is doubled than the increase when load is halved. Hence when variation in draw is introduced, we see an overall decrease in *Sf*
- Decrease in *dn* is greater when the load is halved, than the increase in *n* when the load is doubled. Hence, we see an overall decrease in *n* when day to day variation is introduced.

5.2.7 Effect of Day to Day Variation in Load on Different Load Profiles

Scenario V was simulated with different draw profiles, Morning and Yuppie. The results of these simulations are presented in Figure 69 and Figure 70.

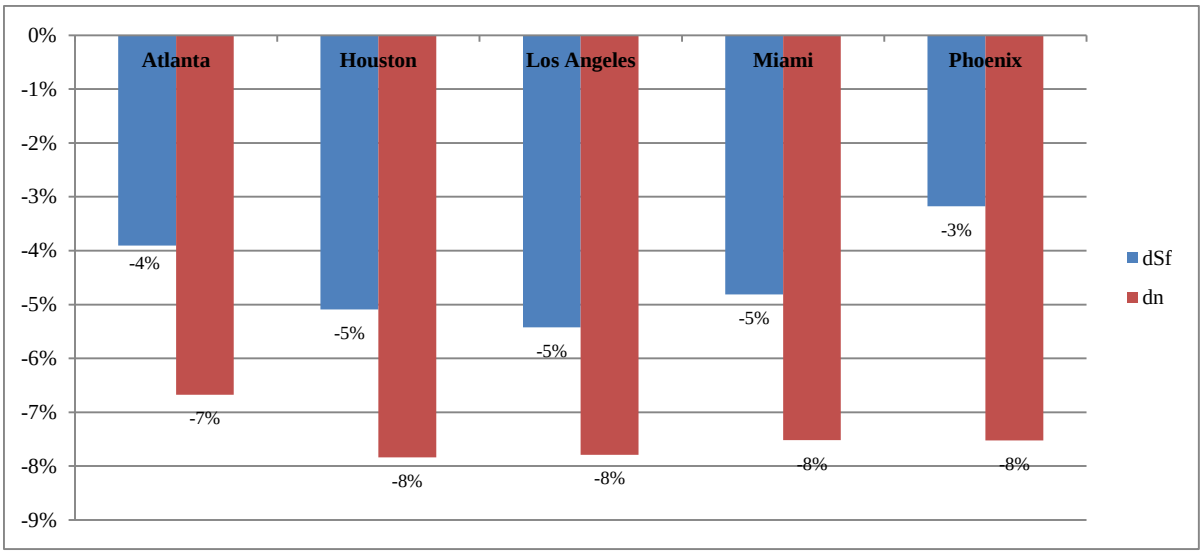

Figure 69 Results of Simulating Scenario V with a Morning Profile

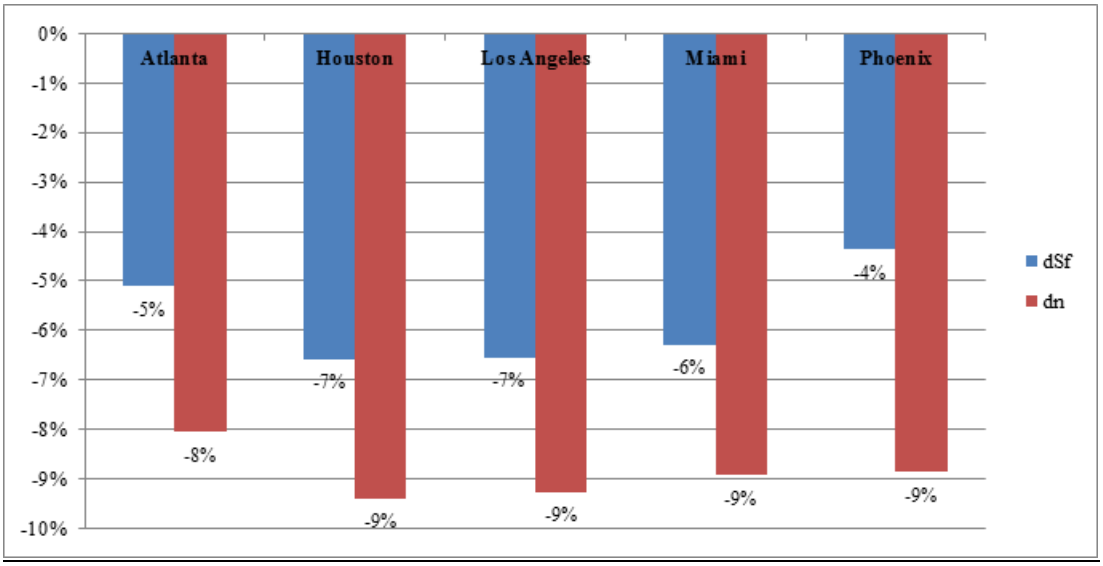

Figure 70 Results of Simulating Scenario V with a Yuppie Profile

The change is system performance when Scenario V is simulated for different load profiles is very similar to the change in performance from the base load case to Scenario V. In each case, *Sf* decreases by 4 – 6% and *n* decreases by 7 – 9 %.

5.2.8 Effect of Using Extreme Profile (Scenario X)

The Extreme[19] profile has the same daily and annual load as the Nuclear profile, all of the load is concentrated in one morning hour (5 AM to 6 AM). The results of this Scenario X are presented in Figure 71.

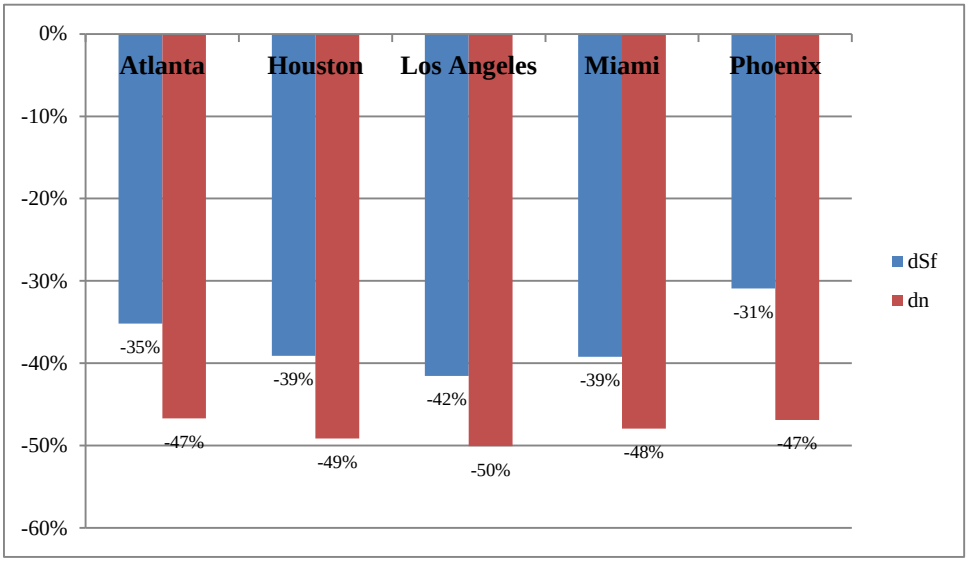

Figure 71 Effect of Changing Draw Profile to Extreme Profile for ICS system, Scenario X

Scenario X has the following effects on annual *n* and *Sf*:

- *Sf* shows significant decrease for all locations, between 31% and 42%.
- *n* shows significant decrease of 47% - 50%

The reason for this significant change is the inability of the system to meet the extreme morning load due to heavy nighttime losses. This can be explained studying hourly data for a typical summer day (June 15th) in Los Angeles, CA. The ICS system struggles to meet hot water demand in the winter for most events in both Base Scenario and Scenario X, system performance

[19] Details of the Extreme profile are presented in Section 4.3

in the winter is similar. However a summer day provides good insight into change in system performance due to Scenario X.

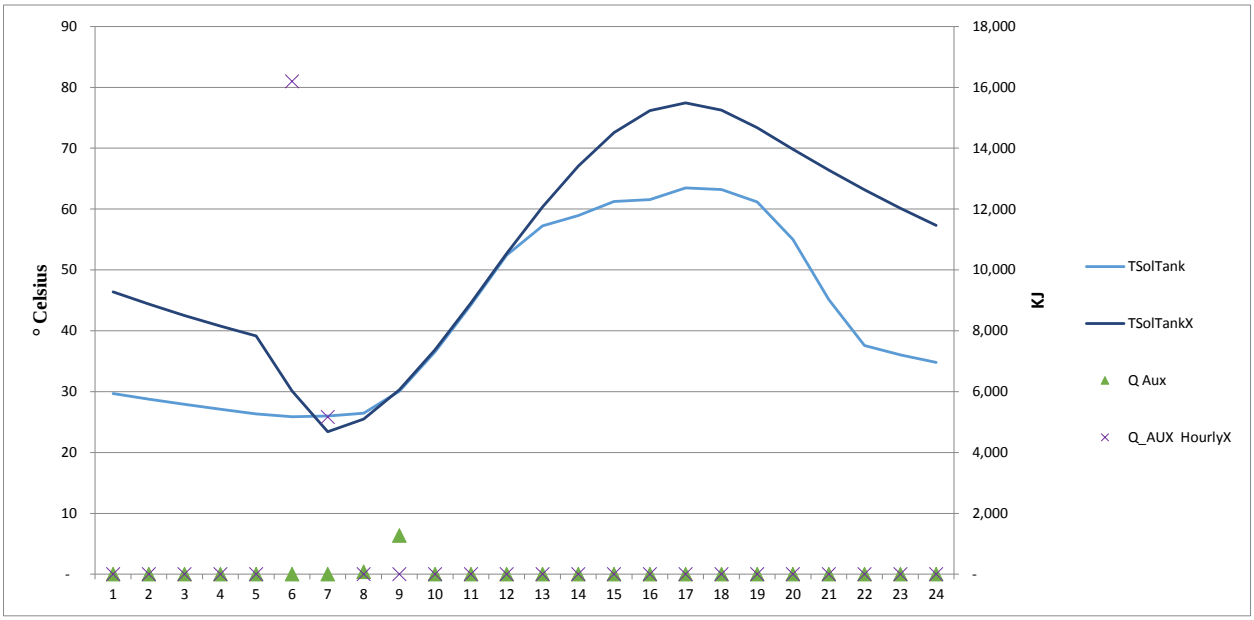

*Daily System Performance, Scenario X: *Sf* = 50%, *n* = 14%; Base Scenario *Sf* = 96%, *n* = 35%

Figure 72 Comparison between ICS System with Nuclear Profile and Scenario X (Los Angeles, CA)

The ICS system meets 96% of the daily load in a summer day in the Base Scenario; the only event in which it needs auxiliary heat is a morning draw. In Scenario X, the ICS system cannot meet the extreme hot water draw in the morning. Even though the system gains a significant amount of energy during the day, it loses a portion of it at night. Thus, being incapable of meeting the complete daily load in the morning. $T_{Sol\ Tank}$ for Scenario X is always higher than Base Scenario for all but one hour of the day. This leads to lower system efficiency under Scenario X.

5.2.9 Effect of Using Hourly Profile (Scenario H)

The Hourly[20] profile has the same daily and annual load as the Nuclear profile, but the draw duration are hourly instead of being in steps of five minutes. The results of this Scenario H are presented in Figure 73.

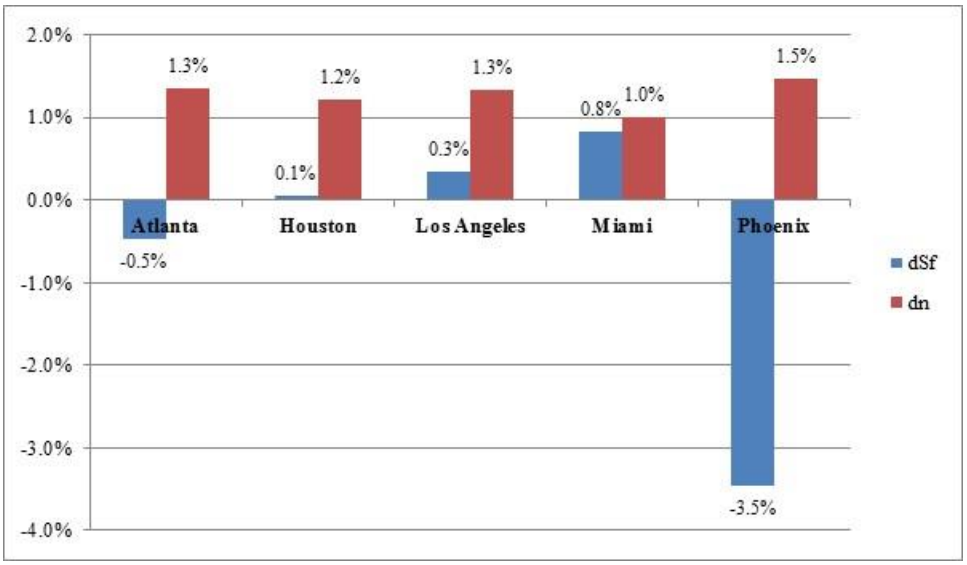

Figure 73 Effect of Changing Draw Profile to Hourly Profile, ICS System (Scenario H)

The system performs almost identically when simulated with both draw profiles. This is due to a well sized storage present in ICS collector. The hourly data for a typical winter day (December 15th) in Los Angeles, CA (Figure 74) also shows almost no difference in system performance for the two profiles.

[20] Details of the Hourly profile are presented in Section 4.3

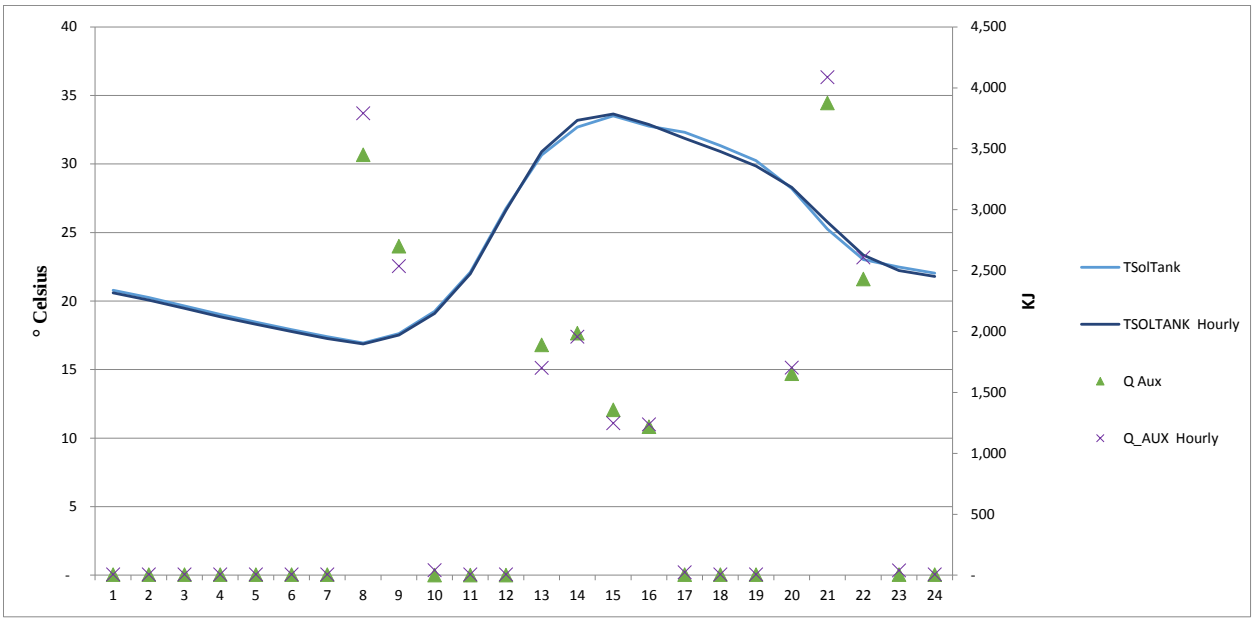

Figure 74 Comparison between ICS System with Nuclear Profile and Scenario H (Los Angeles, CA)

5.3 Comparison of ICS and Glycol Systems

In this section, the difference in performance between ICS and Glycol SDHW systems are presented. This is done for all the variations, the locations that were compared were Atlanta, Houston, Los Angeles, Miami and Phoenix. These locations were chosen as they are common to both the systems analyzed.

5.3.1 Comparison of System with Base Profile

Figure 75 presents a comparison of Glycol and ICS system performance by comparing the *Sf* for Base profile; Figure 76 presents a comparison of *n* for ICS and Glycol systems.

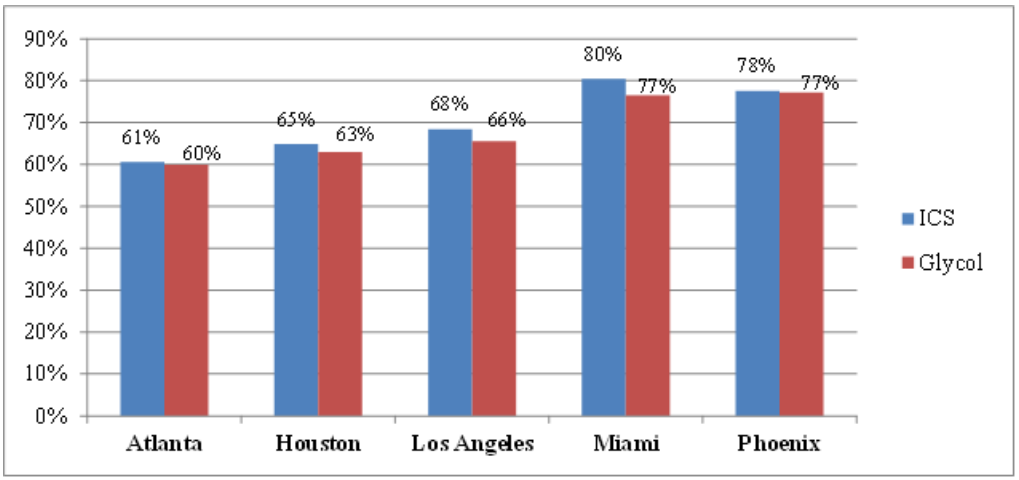

Figure 75 Solar Fraction Comparison between Glycol and ICS Systems

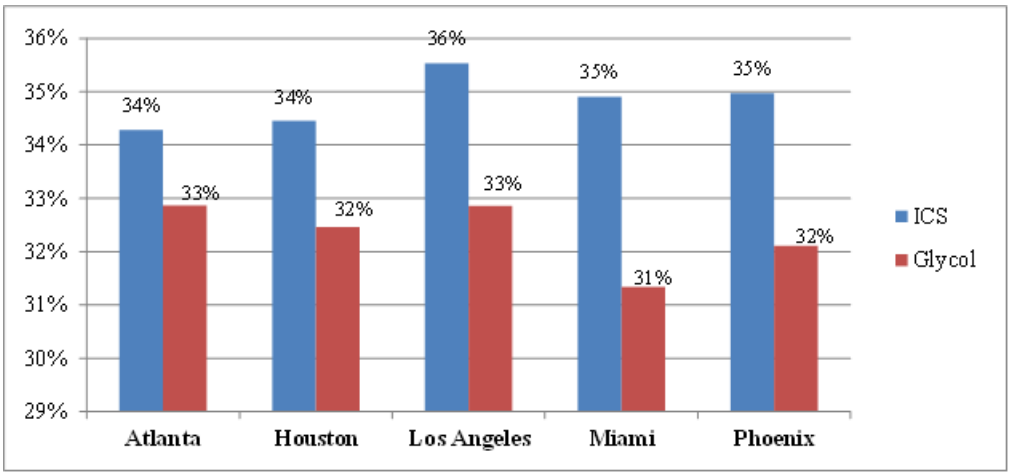

Figure 76 System Efficiency Comparison between Glycol and ICS Systems

The base *Sf* for ICS and Glycol systems are almost equal for all locations; with ICS *Sf* being slightly higher. This is as ICS systems have a higher *n* than Glycol system as ICS systems (as presented in Figure 76). ICS systems have higher *n* than Glycol systems; this is as Glycol system only collect energy when the collector fluid is hotter than the top node of the storage tank. ICS system collect all the energy incident on it. Moreover, ICS systems do not have losses associated with a heat exchanger that Glycol systems have.

5.3.2 Effect of Increasing the Load by a Factor of Two (Scenario 2x)

Shown in Figure 77 and Figure 78 are comparisons of the Glycol and ICS system for Scenario 2x. *Sf* decreases for all locations, both systems; the magnitude of change in *Sf* is greater for the glycol system in all cases. This is explained by the change in *n; n* increases for all locations for both systems, but the magnitude of change in *n* is greater for ICS system.

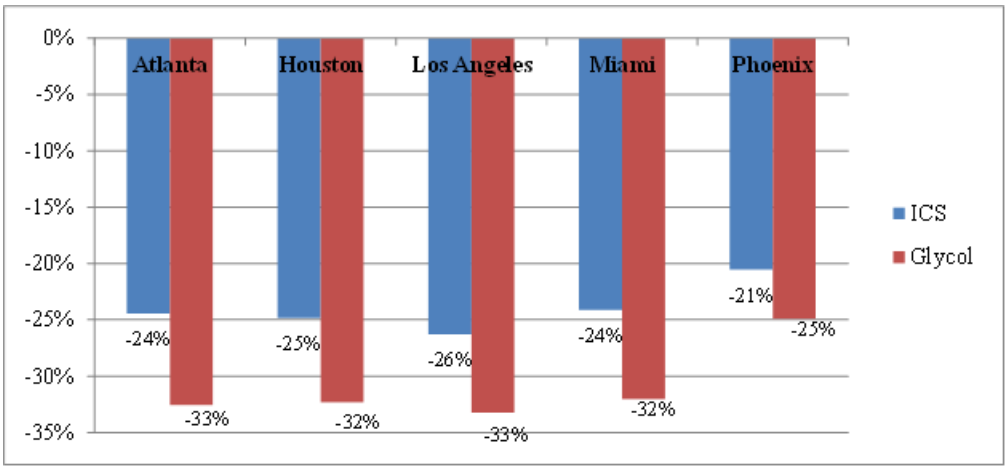

Figure 77 Comparison of Change in *Sf* between ICS and Glycol Systems in Scenario 2x

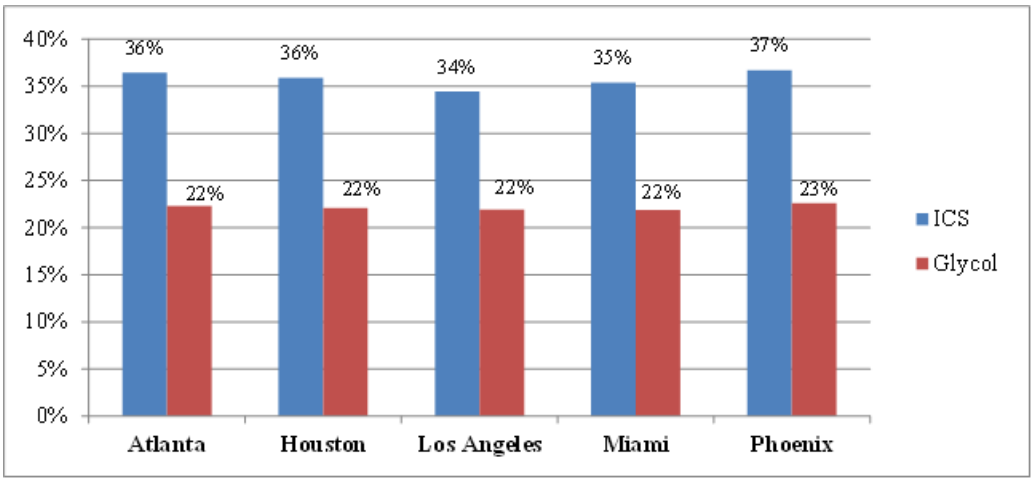

Figure 78 Comparison of Change in *n* between ICS and Glycol Systems in Scenario 2x

The ICS system efficiency is higher than glycol system efficiency as (1) the ICS system has a lower average $T_{SolTank}$[21] and (2) the useful energy collected by the ICS system is driven by the load on the system.

5.3.3 Effect of Reducing Load by Halving Annual Hot Water Draw (Scenario 0.5x)

In Scenario 0.5x, both systems show an increase in *Sf* and a decrease in *n*. These results are presented in Figure 79 and Figure 80.

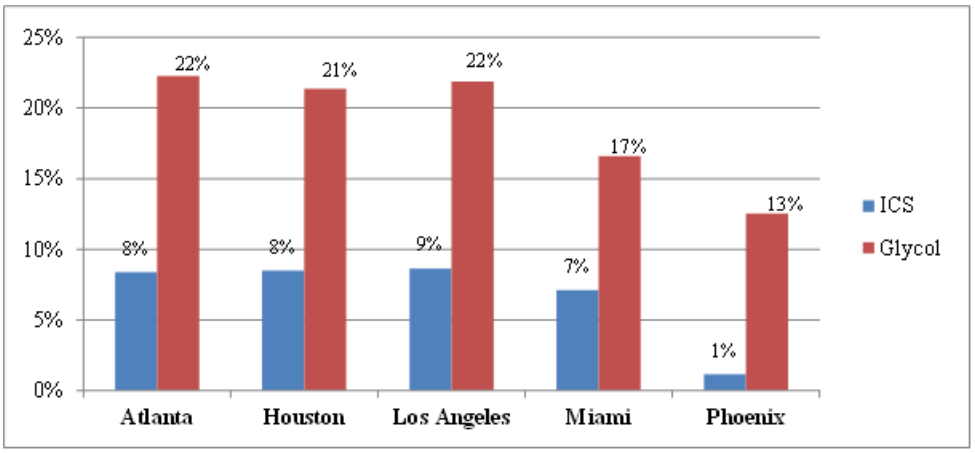

Figure 79 Comparison of Change in *Sf* between ICS and Glycol Systems in Scenario 0.5x

[21] For example, the average $T_{SolTank}$ for the ICS system is 23.9 ^{O}C as compared to 24.4 ^{O}C for the Glycol system in Los Angeles, CA

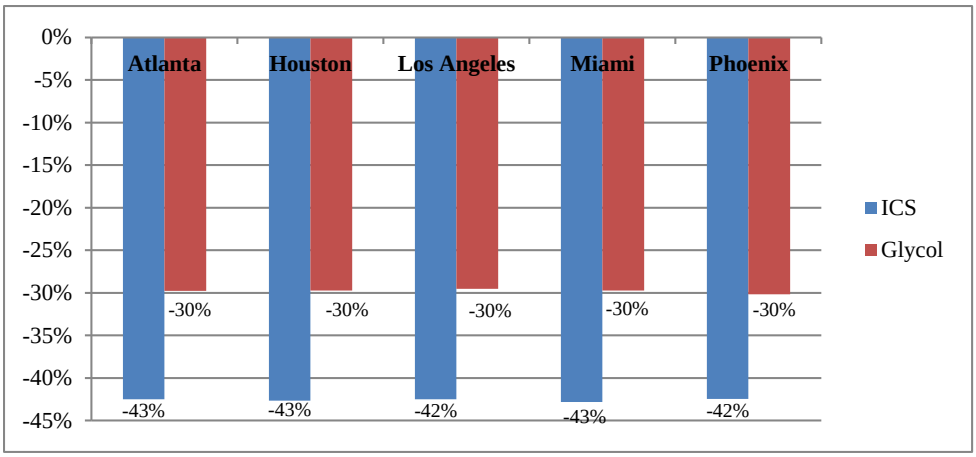

Figure 80 Comparison of Change in *n* between ICS and Glycol Systems in Scenario 0.5x

The glycol system shows a greater increase in *Sf* than the ICS system; this is as the glycol system's decrease in *n* is lesser than the decrease in *n* for the ICS system in Scenario 0.5x. The ICS system shows a greater decrease in *n* because (1) the useful energy collected by the system is driven by the load on the system, and (2) the ICS system loses energy collected at night, the glycol system stores this energy to be used for morning loads.

5.3.4 Effect of Changing Draw Profile to a Morning Centric Profile (Scenario M)

Figure 81 and Figure 82 present a comparison of the change in *Sf* and *n* for ICS and glycol systems. The ICS system shows a greater decrease in *n* and a decrease in *Sf* for Scenario M; the *Sf* in Scenario M shows a slight increase for the glycol system.

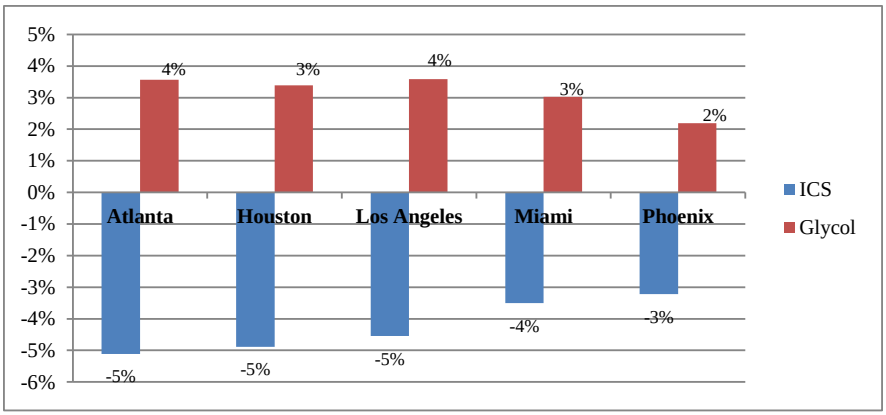

Figure 81 Comparison of Change in *Sf* between ICS and Glycol Systems in Scenario M

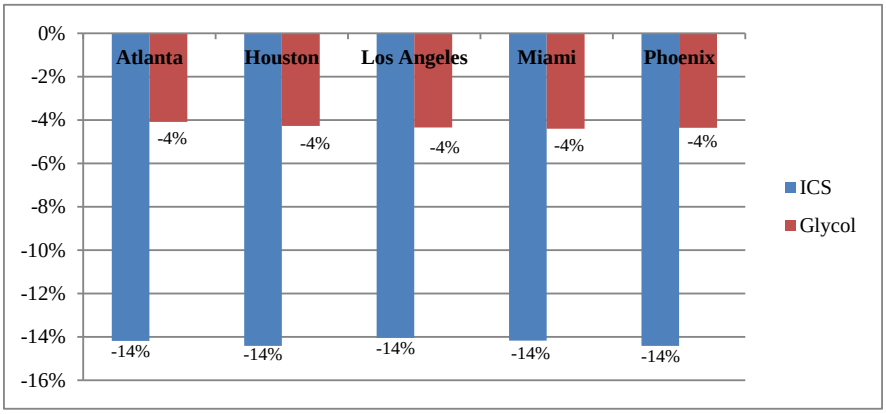

Figure 82 Comparison of Change in *n* between ICS and Glycol Systems in Scenario M

This difference in system performance is due to the glycol system's ability to store collected energy overnight and better meet the increased morning loads in Scenario M.

5.3.5 Effect of Changing Draw Profile to an Evening Profile (Scenario E)

Figure 83 and Figure 84 present a comparison of the change in *Sf* and *n* for ICS and glycol systems. The ICS system shows a decrease in *n* and *Sf* for Scenario E; the glycol system

shows almost no change in *Sf* and a decrease in *n* in Scenario E. The decrease in *n* is smaller for the glycol system than the ICS system.

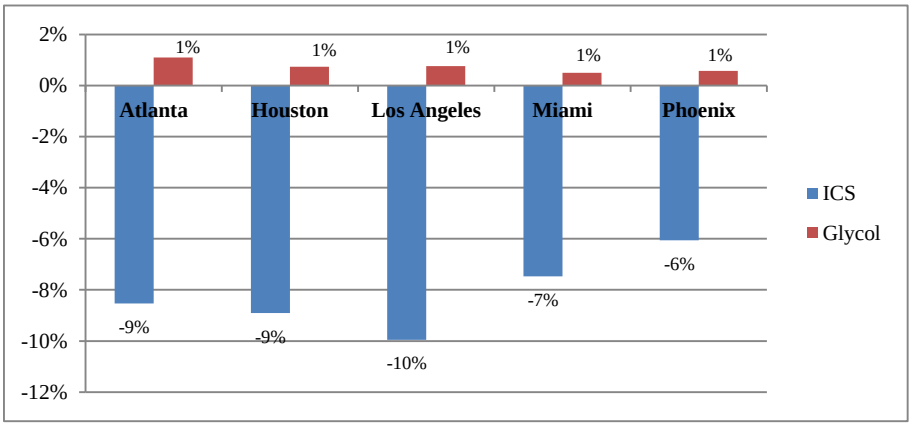

Figure 83 Comparison of Change in *Sf* between ICS and Glycol Systems in Scenario E

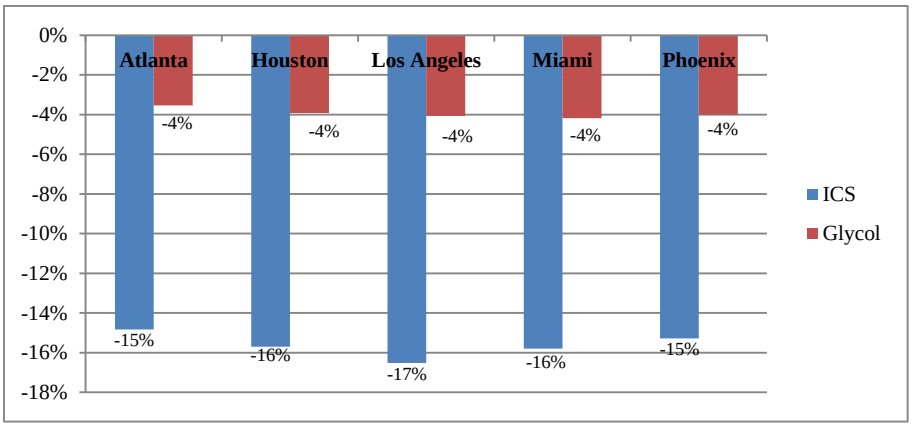

Figure 84 Comparison of Change in *n* between ICS and Glycol Systems in Scenario E

The glycol system shows a smaller change in *Sf* and *n* than the ICS system. This is as the ICS system suffers a loss in efficiency if hot water is not drawn at times when the ICS system is collecting energy; the glycol system can effectively store energy and meet the evening and morning loads in Scenario E.

5.3.6 Effect of Day to Day Variation in Load on Different Load Profiles

Random day to day load variations show a similar trend in both ICS and glycol systems, a decrease in both *Sf* and *n*, as shown in Figure 85 and Figure 86. As discussed in Sections 5.1.7 and 5.2.6, there is a decrease in solar fractions and system efficiencies for both System in Scenario R. Glycols systems show a lower magnitude of change than ICS systems for *Sf* and *n* as their correctly sized storage tank dampens the effect the day to day variations have in Scenario R.

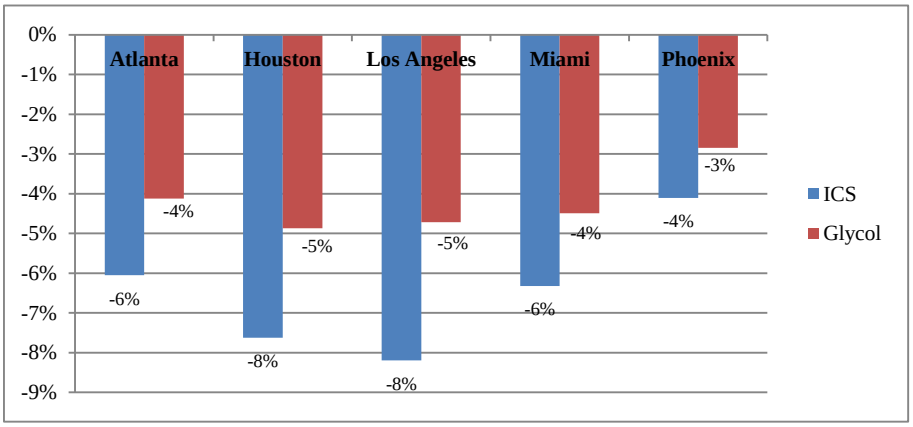

Figure 85 Comparison of Change in *Sf* between ICS and Glycol Systems in Scenario R

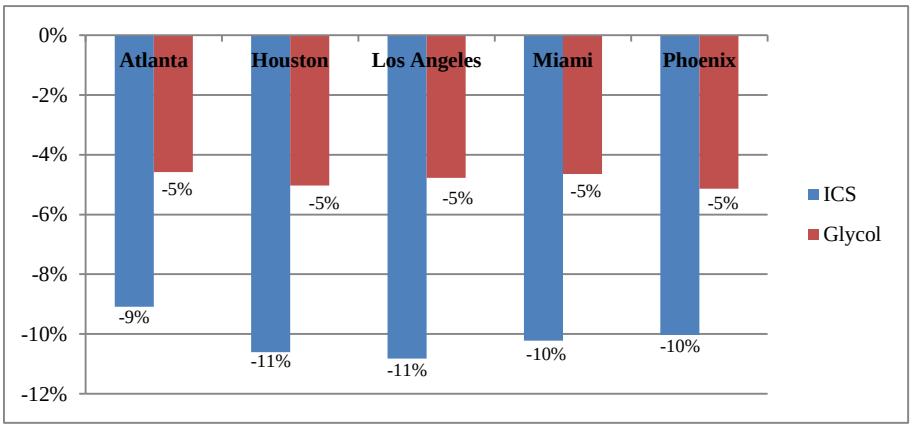

Figure 86 Comparison of Change in *n* between ICS and Glycol Systems in Scenario R

5.3.7 Effect of Using Extreme Profile (Scenario X)

Extreme profile shows very different trend in ICS and glycol systems (Figure 87Figure 88). Glycols systems show almost no change whereas ICS systems show a significant decrease in *Sf* and *n.* This is due to the fact that ICS system are not able to meet heavy morning loads, whereas glycol system can due to their correctly sized storage tank. This has been explained in detail in Sections 5.1.9 and 5.2.8.

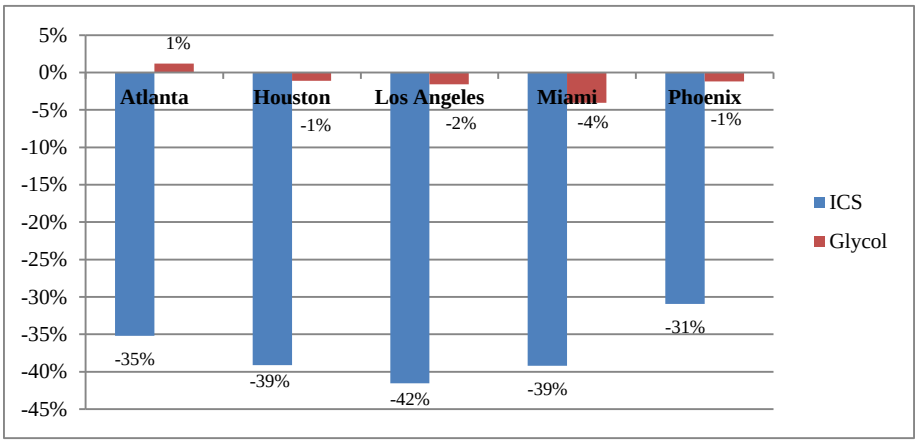

Figure 87 Comparison of Change in *Sf* between ICS and Glycol Systems in Scenario X

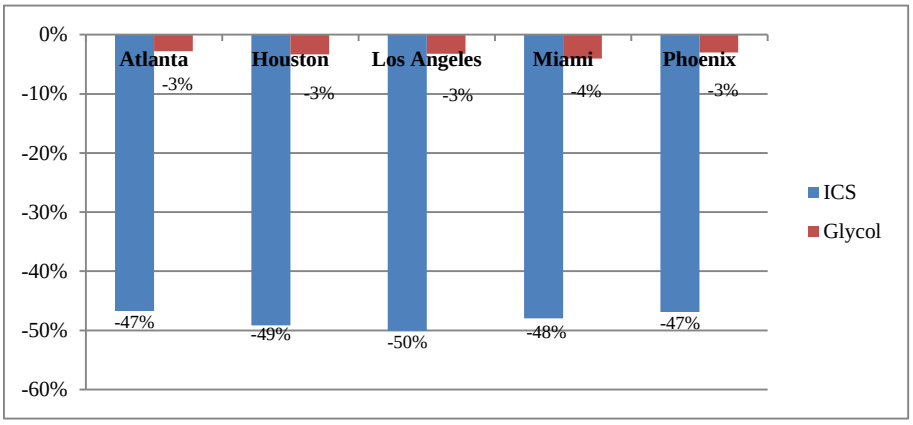

Figure 88 Comparison of Change in *n* between ICS and Glycol Systems in Scenario X

5.3.8 Effect of Using Hourly Profile (Scenario H)

Both ICS and Glycol systems show a similar trend in Scenario H, i.e. almost no change in performance compared to the Base Scenario (Figure 89Figure 90). The results are explained in details in Sections 5.1.10 and 5.2.9.

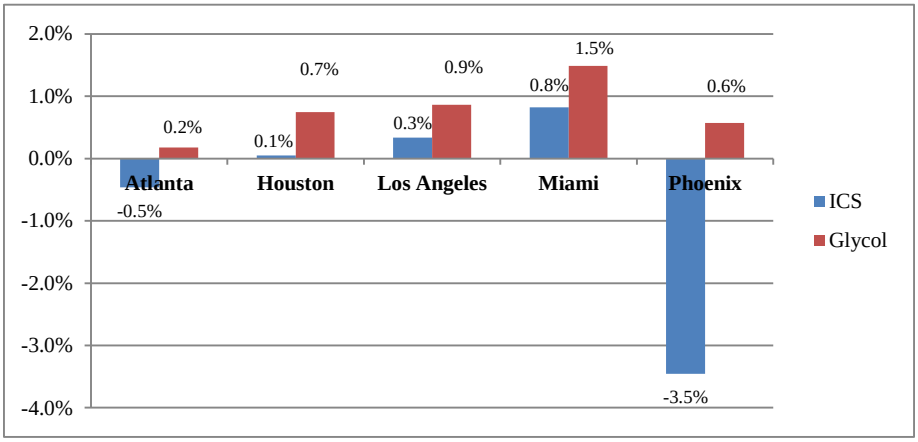

Figure 89 Comparison of Change in *Sf* between ICS and Glycol Systems in Scenario H

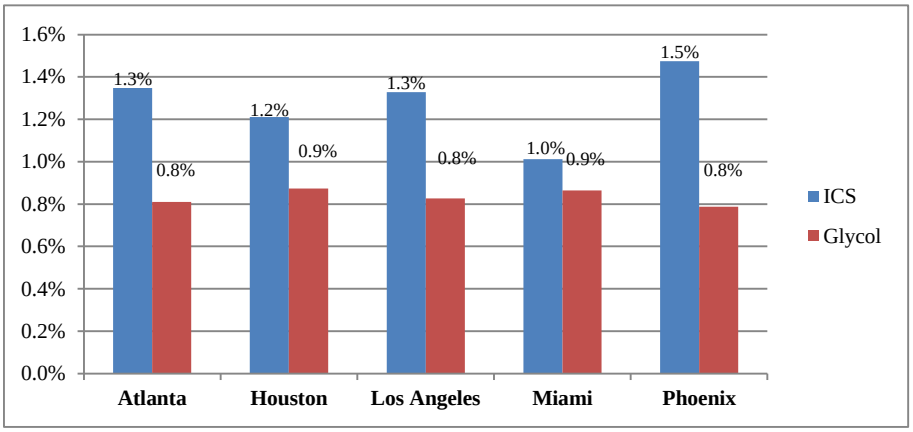

Figure 90 Comparison of Change in *n* between ICS and Glycol Systems in Scenario H

6 Conclusions

Figure 91Figure 92 summarize the scenarios simulated in this study by showing the variation in *Sf* for the glycol and ICS system respectively. The absolute value of the range of *Sf* represents the sensitivity of the system to scenario in consideration.

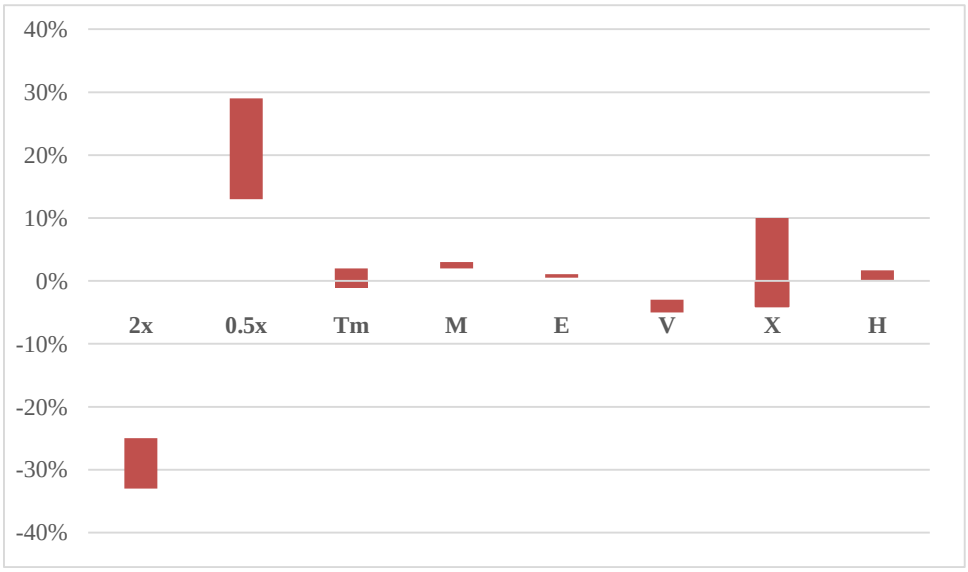

Figure 91 Glycol Systems: Range of Variation of Change in *Sf* per Scenario Simulated

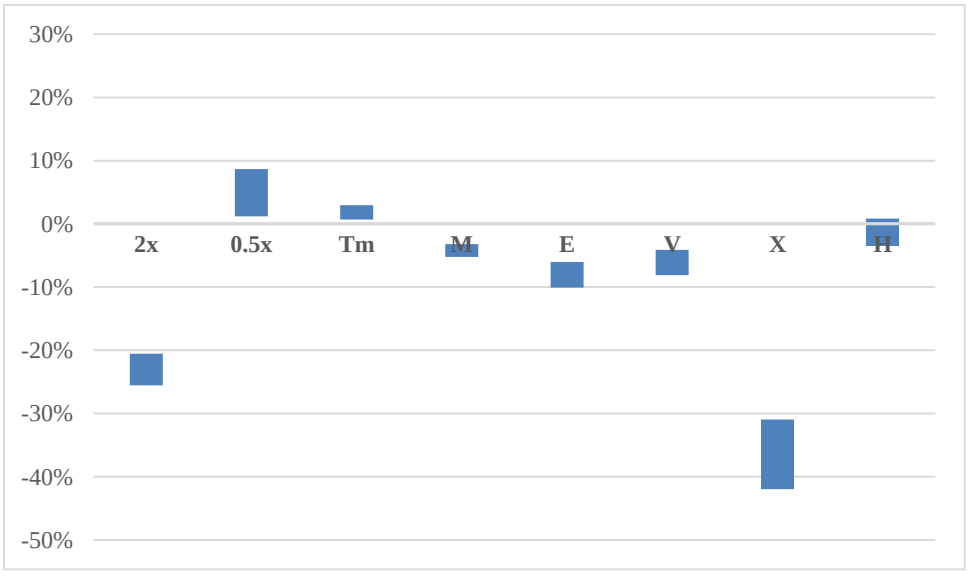

Figure 92 ICS Systems: Range of Variation of Change in Sf per Scenario Simulated

Through the data presented in Figure 91, we can quantify the maximum expected variation in performance of glycol systems for our simulated scenarios; this provides a reasonable estimate for the maximum expected variation in in-situ performance for glycol systems. The maximum expected decrease in *Sf* -25% to -33% (depending on the location) due to a system being applied to twice annual hot water load it has been designed for. Conversely, the system shows an increase in *Sf* of 13% to 29% (depending on location) due to the system being used under half the annual hot water load it has been designed for.

Similarly, through the data presented in Figure 92, we can quantify the maximum expected variation in performance of ICS systems for our simulated scenarios; this provides a reasonable estimate for the maximum expected variation in in-situ performance for ICS systems. The maximum expected decrease in *Sf* is -31% to -42% (depending on the location) due to a system subjected to all morning loads. The ICS system shows a maximum increase in *Sf* of up to 10% when applied to half the designed annual hot water load.

The glycol system shows less variation in performance due to variation in draw profile than the ICS system due to the presence of an appropriately sized and insulated solar storage tank in the glycol system. The solar storage tank helps glycol systems meet the demand for hot water during hours of low sunlight (early morning and late evening). ICS systems show higher sensitivity to profile shape as they cannot meet hot water load during morning and evening times; this morning and evening hot water load is met by the auxiliary heating tank.

6.1 Recommendations for Future Research

This research uses TRNSYS simulation to understand the impact of varying annual load and usage profile patterns on SDHW system performance. A study that meters residential hot

water usage and SDHW system output would provide real world insight into the findings from the simulations conducted for this study.

This analysis can also be expanded to study how varying annual load and use profile effects SDHW systems with different types of collectors (glazed, unglazed etc.), collector orientation, and geographic locations (e.g. all US weather stations) to ascertain if the general trends studied in this research still hold true.

7 Bibliography

(FSEC), P. F. (2004). *A Review of Hot Water Draw Profiles Used in Performance Analysis of Residential Domestic Hot Water Systems.* FSEC.

(FSEC), P. F. (2004). *A Review of Hot Water Draw Profiles Used in Performance Analysis of Residential Domestic Hot Water Systems.* Cocoa, Florida: FSEC.

(NREL), P. D. (2007). *The Technical Potential of Solar Water Heating to Reduce Fossil Fuel Use and Greenhouse Gas Emissions in the United States.* NREL.

Arizona Solar Center. (2001). *Solar Hot Water: A Primer*. Retrieved from Arizaona Solar Center: http://www.azsolarcenter.org/tech-science/solar-for-consumers/solar-hot-water/solar-hot-water-a-primer.html

Barker, C. C. (2007). *Annual System Efficiencies for Solar Water Heating.* Golden, CO: NREL.

Beckman, a. D. (2006). Solar Water Heating: Active and Passive. In a. D. Beckman, *Solar Engineering of Thermal Processes.*

Christensen, J. B. (2006). *Towards Development of an Algorithm for Mains Water Temperature.* Golden, CO: NREL.

D.O.E. (2005). *Department of Energy*. Retrieved from Building Energy Databook, 2005: http://buildingsdatabook.eren.doe.gov/

D.S. Parker, M. A. (2000). Factors Influencing Water Heating Energy Use and Peak Demand in a Large Scale Monitoring Study. *Proceedings of the Symposium on Improved Building Systems in Hot Humid Climates, Texas A&M University.* College Station, TX.

FSEC. (2006). *Solar Water and Pool Heating Manual. Design and Installation & Repair and Maintenance.* Cocoa, FL: FSEC.

J. a. (2005). Cold-Climate Solar Domestic Hot Water Systems Analysis. *2005 DOE Solar Energy Technologies Program Review Meeting.* Denver, CO: NREL (National Renewable Energy Laborotary).

J.Burch and J.Salasovich (NREL), T. H. (2005). An Assessment of Unglazed Solar Domestic Water Heaters. *ISES Solar World Congress.* Orlando, FL.

J.J.Mutch. (1974). *Residential Water heating, Fuel Consumption, Econimics, and Public Policy.* RAND Department.

Jeff W. Thornton, J. D. (2000). Modeling Advances in Low-Cost Integral Collector Storage Solar Domestic Hot Water Systems. *Proceedings of the Solar 2000 Conference Including Proceedings of ASES Annual Conference and Proceedings of the 25th National Passive Solar Conference, 16-21 June 2000.* Madison,WI.

Lowe's. (2009). *Water Heater Selection Guide*. Retrieved from Lowe's: http://www.lowes.com/lowes/lkn?action=howTo&p=BuyGuide/WtrHtrBG.html

NREL. (1996, March). *Energy Efficiency and Renewable Energy Clearing House.* Retrieved from NREL: http://www.nrel.gov/docs/legosti/fy96/17459.pdf

NREL. (2008). *Annual Solar Radiation Map (10km) Static Map (1998 - 2005 Data)*. Retrieved from NREL - Solar: http://www.nrel.gov/gis/images/map_pv_us_annual10km_dec2008.jpg

Parker, C. E. (2009). *Geographical Variation in Potential of Residential Solar Hot Water System Performance in the United States.* Florida Solar Energy Center (FSEC).

Perlman, B. a. (1985). Development of Residential Hot Water Use Patterns . *ASHRAE Transactions Vol. 91 Part 2A*, 657-679.

RETScreen. (2009). *Solar Water Heating Project Model*. Retrieved from RETScreen International: www.retscreen.net/download.php/ang/470/0/swh3.pdf

Salasovich, J. (2001). *Pipe Freezing for Passive Solar Water Heating Systems: A Probabilistic Approach, University of Colorado at Boulder, Boulder, CO Master's Project .* Boulder: University of Colorado.

SRCC. (2009). *Solar Rating & Certification Corporation - Ratings*. Retrieved from Solar Rating & Certification Corporation: Solar Rating & Certification Corporation

Stogsdill, B. B. (1990). Development of Hot Water Use Data Base. *ASHRAE Transactions Vol. 96*, 422-427.

U.S E.I.A. (2010). *Table 1.6. State Level Energy Consumption, Expenditure and Price Estimates, 2010.* Retrieved from U.S. E.I.A: http://www.eia.gov/totalenergy/data/annual/showtext.cfm?t=ptb0106

U.S. E.I.A. (2012, June 27). *How much of our electricity is generated from renewable energy?* Retrieved from U.S. E.I.A: http://www.eia.gov/energy_in_brief/article/renewable_electricity.cfm

U.S. Energy Information Administration (U.S. E.I.A). (2009). *Residential Energy Consumption Survey (2009): Table CE3.1 Household Site End-Use Consumption in the U.S., Totals*

and Averages, 2009. Retrieved from U.S. Energy Information Administration: http://www.eia.gov/consumption/residential/data/2009/index.cfm?view=consumption#end-use

University of Wisconsin. (1975). *About: F-Chart Software: Engineering Software*. Retrieved from F-Chart Software: http://www.fchart.com/about/

W.E.Buckles and S.A.Klein (Solar Energy Laboratory, U. o. (1980). Analysis of Solar Domestic Hot Water Heaters. *Solar Energy Vol. 25*, pp. 417-424.

Whirlpool. (2009). *Whirlpool Water Heaters*. Retrieved from Whirlpool: http://www.whirlpoolwaterheaters.com/products/ByCategory.aspx?id=2

Winter, F. d. (2005). Solar Water Heating with Backup Heating - A Review. *Solar World Congress of ISES.* Orlando, FL: Solar World Congress of ISES.